Deliverable D2.4 – Report on integrated risk assessment tools of relevance to the CRA Toolbox

WP2 – Co-design of the supporting toolbox

Grant Agreement 101093864

Version 1.0 | June 2024

HORIZON-MISS-2021-CLIMA-02-01 - Development of climate change risk assessments in European regions and communities based on a transparent and harmonised Climate Risk Assessment approach

Funded by the European Union

This project has received funding from the European Union's Horizon Europe research and innovation programme under grant agreement No 101093864. Views and opinions expressed are however those of the author(s) only and do not necessarily reflect those of the European Union or the European Climate, Infrastructure and Environment Executive Agency (CINEA). Neither the European Union nor the granting authority can be held responsible for them.

Document Information

Deliverable Title	Report on integrated risk assessment tools of relevance to the CRA Toolbox
Brief Description	This report gives an overview of the main methods available for climate risk assessment, with focus on the hazards identified by the CLIMAAX pilots. Furthermore, it describes the data and methods used in the risk workflows implemented within the CLIMAAX Toolbox.
WP number	WP2
Lead Beneficiary	VU-IVM – Vrije Universiteit Amsterdam
Author(s)	• Maurizio Mazzoleni, Lena Reimann, Jeroen Aerts, Benedetta Sestito (IVM) • Natalia Aleksandrova, Ted Buskop (DELTARES) • Milana Vuckovic (ECMWF) • Suraj Polade, Andrea Vajda (FMI) • Martin Kuban (KAJO) • Andrea Rivosecchi, Davide Serrao, Jeremy Pal, Giuliana Barbato, Giuseppe Giugliano, Alfredo Reder, Guido Rianna, Paola Mercogliano (CMCC) • Dor Fridman, Silvia Artuso (IIASA) • Marta Gabarró Solanas, Víctor González, Erika R. Meléndez-Landaverde (UPC) • Andrea Trucchia, Farzad Ghasemiazma, Giorgio Meschi, Nicola Rebora (CIMA)
Reviewer(s)	Frederiek Sperna Weiland (Deltares), Fredrik Wetterhall (ECMWF)
Deliverable Due Date	30/06/2024
Actual Delivery Date	27/06/2024
Nature of the Deliverable	R – Report
Dissemination Level	PU - Public

Funded by the European Union

This project has received funding from the European Union's Horizon Europe research and innovation programme under grant agreement No 101093864. Views and opinions expressed are however those of the author(s) only and do not necessarily reflect those of the European Union or the European Climate, Infrastructure and Environment Executive Agency (CINEA). Neither the European Union nor the granting authority can be held responsible for them.

Version	Date	Change editors	Changes
0.1	31/05/2023	All authors	First version ready for internal review
0.2	15/06/2023	Frederiek Sperna Weiland, Fredrik Wetterhall	First internal review completed
1.0	27/06/2024	All authors	Revised version ready

Funded by the European Union

This project has received funding from the European Union's Horizon Europe research and innovation programme under grant agreement No 101093864. Views and opinions expressed are however those of the author(s) only and do not necessarily reflect those of the European Union or the European Climate, Infrastructure and Environment Executive Agency (CINEA). Neither the European Union nor the granting authority can be held responsible for them.

Table of Contents

Funded by the European Union

This project has received funding from the European Union's Horizon Europe research and innovation programme under grant agreement No 101093864. Views and opinions expressed are however those of the author(s) only and do not necessarily reflect those of the European Union or the European Climate, Infrastructure and Environment Executive Agency (CINEA). Neither the European Union nor the granting authority can be held responsible for them.

Funded by the European Union

This project has received funding from the European Union's Horizon Europe research and innovation programme under grant agreement No 101093864. Views and opinions expressed are however those of the author(s) only and do not necessarily reflect those of the European Union or the European Climate, Infrastructure and Environment Executive Agency (CINEA). Neither the European Union nor the granting authority can be held responsible for them.

List of figures

Funded by the European Union

This project has received funding from the European Union's Horizon Europe research and innovation programme under grant agreement No 101093864. Views and opinions expressed are however those of the author(s) only and do not necessarily reflect those of the European Union or the European Climate, Infrastructure and Environment Executive Agency (CINEA). Neither the European Union nor the granting authority can be held responsible for them.

List of tables

Funded by the European Union

This project has received funding from the European Union's Horizon Europe research and innovation programme under grant agreement No 101093864. Views and opinions expressed are however those of the author(s) only and do not necessarily reflect those of the European Union or the European Climate, Infrastructure and Environment Executive Agency (CINEA). Neither the European Union nor the granting authority can be held responsible for them.

List of abbreviations and acronyms

Abbreviation / acronym	Description
AR6	Sixth Assessment Report (AR6),
CBA	Cost-benefit analysis
CDI	Combined Drought Indicator
CDS	Copernicus Climate Data Store
CI	Critical infrastructures
CMIP6	Coupled Model Intercomparison Project Phase 6
DEM	Digital Elevation Model
EDO	European Drought Observatory
EM-DAT	Emergency Events Database
ET0	Soil standard evapotranspiration
ETa	Actual crop evapotranspiration
ETc	Crop standard evapotranspiration
ESM	Earth System Models
EURO-CORDEX	Coordinated Downscaling Experiment - European Domain
FAO	Food and Agriculture organization
FAPAR	Fraction of Absorbed Photosynthetically Active Radiation
GAEZ	Global Agro-Ecological Zones data repository
GCM	Global Climate Model
GDP	Gross Domestic Product
GIS	Geographic Information Systems
HEV	Hazard-Exposure-Vulnerability

Funded by the European Union

This project has received funding from the European Union's Horizon Europe research and innovation programme under grant agreement No 101093864. Views and opinions expressed are however those of the author(s) only and do not necessarily reflect those of the European Union or the European Climate, Infrastructure and Environment Executive Agency (CINEA). Neither the European Union nor the granting authority can be held responsible for them.

IAM	Integrated Assessment Models
IPCC	Intergovernmental Panel on Climate Change
Kc	Crop coefficient
LST	Land surface temperature
ML	Machine Learning
NUTS	Nomenclature of territorial units
OSM	OpenStreetMap
PCA	Principal Component Analysis
RCM	Regional Climate model
RCP	Representative Concentration Pathways
SMA	Soil Moisture Anomaly
SMI	Standardized Soil Moisture Index
SPI	Standardized Precipitation Index
SSP	Shared Socioeconomic Pathways
WASP	Weighted Anomaly of the Standardized Precipitation

Funded by the European Union

This project has received funding from the European Union's Horizon Europe research and innovation programme under grant agreement No 101093864. Views and opinions expressed are however those of the author(s) only and do not necessarily reflect those of the European Union or the European Climate, Infrastructure and Environment Executive Agency (CINEA). Neither the European Union nor the granting authority can be held responsible for them.

Executive summary

The objective of Task 2.4 is to contribute with Climate Risk Assessment (CRA) methods to the CLIMAAX Toolbox. The toolbox integrates the components of risk (Hazard, Exposure, Vulnerability) into an integral risk assessment and visualizes risk information to develop regional risk profiles. The CLIMAAX Toolbox is a key component of the CLIMAAX Framework, as described in the Deliverable 1.4.

Though a review of past research studies, this deliverable underlines the critical role of CRA in guiding informed decision-making and implementing sustainable adaptation strategies. This report identifies and describes existing CRA methods, including risk indexing, damage assessment, assets and population exposure, integrated assessment models, cost-benefit analysis, scenario analysis, and multi-risk methods. After consultation with the CLIMAAX project partners and pilot regions, the CLIMAAX Toolbox applies three CRA methods: risk indexing, damage analysis, and assets and population exposure. These methods are available in the toolbox to estimate current and future impacts for nine climate hazards: river flood, coastal flood, extreme precipitation, drought, heatwave, wildfire, windstorm, heavy snow, blizzard.

The CLIMAAX Toolbox contains 14 workflows that estimate risks for the nine climate hazards. In CLIMAAX, a risk workflow is a 'stepwise' data processing scheme to calculate risk, making use of both large scale and local datasets of hazard, exposure, and vulnerability. The workflows allow for the risk assessment of historical and future climate change conditions (e.g. using Representative Concentration Pathways of 2.6, 4.5 and/or 8.5). The risk workflows are designed such that pilots, local communities, regional authorities, and any other user can develop their own hazard and risk maps by using either local data or by downloading pre-calculated maps.

This report further discusses the advantages and disadvantages of the different climate risk assessment methods and the influence of uncertainty in risk assessment.

Funded by
the European Union

This project has received funding from the European Union's Horizon Europe research and innovation programme under grant agreement No 101093864. Views and opinions expressed are however those of the author(s) only and do not necessarily reflect those of the European Union or the European Climate, Infrastructure and Environment Executive Agency (CINEA). Neither the European Union nor the granting authority can be held responsible for them.

1 Introduction

1.1 Purpose of the document

Climate change is a pressing challenge that has led to significant impacts on ecosystems, economies, and social inequalities (Savelli et al., 2023). As climate change related hazards such as droughts and floods are increasing in intensity or frequency, understanding, and assessing climate-related risks and their impact on society have become of pivotal importance. Therefore, CRAs are used to evaluate the potential impacts of climate change on various economic sectors and to identify vulnerable hotspots to prioritize adaptation and mitigation actions (Jurgilevich et al., 2017).

In addition to large (national-) scale CRAs, regional- to local-scale CRAs are important due to the different physical and socioeconomic characteristics of the climate-impacted regions. For example, coastal cities experience increased risks caused by sea-level rise, but may not be exposed to the same hazards as inland cities, which could be more prone to drought and wildfires. Furthermore, cities have different climate risks as characterised by differences in exposure and vulnerability than rural areas (Egbinola et al., 2017). Moreover, using large-scale assessment of climate risk for local scale assessment could lead to misleading results due to the exclusion of local characteristics such as structural flood protection, or local critical infrastructure. A robust CRA at the local and regional level is thus crucial to inform adaptation interventions, and to contribute to the resilience of local populations (Adger et al., 2018).

1.2 Objectives

Through a review of past research studies, this deliverable underlines the critical role of CRA in guiding informed decision-making and implementing sustainable adaptation strategies. This is done by achieving three complementary objectives:

1 Introduce to the different users the CLIMAAX framework and toolbox, their links, the existing CRA tools and platform, and define the criteria for the selection of the CRA method to be implemented within the CLIMAAX toolbox (Section 2).
2 Present a review of current approaches used to assess risk related to different types of hazards, such as river floods, coastal floods, drought, wildfire, heatwaves, snow, blizzards, and windstorms (Section 3).
3 Leveraging the insights and lessons extracted from the review of the current risk assessment methods, this report includes on overview of the pre-defined CRA workflows implemented within the CLIMAAX toolbox (Section 4).

The CLIMAAX toolbox integrates state-of-the-art climate risk data for use at the regional to local scales. The toolbox allows regions and local communities to integrate risk data (Hazard, Exposure, Vulnerability) into an integral CRA and visualise risk information to contribute to the prioritisation of regional risk profiles.

Funded by the European Union

This project has received funding from the European Union's Horizon Europe research and innovation programme under grant agreement No 101093864. Views and opinions expressed are however those of the author(s) only and do not necessarily reflect those of the European Union or the European Climate, Infrastructure and Environment Executive Agency (CINEA). Neither the European Union nor the granting authority can be held responsible for them.

1.3 Relation to other project work

This deliverable is part of the Task 2.4 of the WP2 – Co-design of the supporting toolbox. As such, this deliverable is highly linked with the datasets of hazard, exposure, and vulnerability developed and collected in the other tasks of WP2. Moreover, there is a strong link between this work and WP1 and WP3. The knowledge, and results from WP1 informed WP2 on the different CRA methods, while WP2 developed the CLIMAAX toolbox that represent a pillar for the CRA framework of WP1. Similarly, WP3 informed WP2 on the pilot's needs with respect to hazard, exposure, vulnerability, and risk information. All will be employed by the regions / Third Parties in WP5 and further extensions and improvements of the workflows will be conducted in WP6.

Funded by
the European Union

This project has received funding from the European Union's Horizon Europe research and innovation programme under grant agreement No 101093864. Views and opinions expressed are however those of the author(s) only and do not necessarily reflect those of the European Union or the European Climate, Infrastructure and Environment Executive Agency (CINEA). Neither the European Union nor the granting authority can be held responsible for them.

2 The CLIMAAX Toolbox

This section aims at introducing the CLIMAAX toolbox, existing data platforms and tools, and the criteria used to select the risk assessment methods within the CLIMAAX toolbox.

2.1 Purpose and link with the CLIMAAX framework

The CLIMAAX toolbox is a key component of the CLIMAAX Framework. The framework aims at empowering regions to conduct inclusive and harmonised CRAs. The CLIMAAX framework consists of a five-step assessment cycle of “Scoping”, “Risk Exploration”, “Risk Analysis”, “Key Risk Assessment, and “Monitoring & Evaluation” (more details are included in the Deliverable 1.4 “Climate risk assessment framework”). In this context, the purpose of the CLIMAAX toolbox is to guide, support, quantify, and contextualise the risk estimated in the Risk Analysis step. It is worth noting that before applying the CLIMAAX toolbox, the user will need to carry out the Risk Identification step to identify hazards and risks that are most apparent or of significant concern to key stakeholders and the wider public.

The CLIMAAX toolbox provides the user with a flexible tool for performing CRA using both local and European large-scale data. The toolbox allows the risk assessment for a variety of different hazards following specific “risk workflows”. In CLIMAAX, a risk workflow is defined as a 'stepwise' data processing scheme to estimate risk as a combination of hazard, exposure, and vulnerability information. Each workflow is applied to one specific hazard, designed for historical and future hazard, exposure, and vulnerability.

The CLIMAAX toolbox allows the user to implement different risk workflows using multiple datasets of hazard, exposure, and vulnerability historical information. Moreover, the toolbox allows to estimate future risk based on the availability of datasets of future hazard, exposure, and vulnerability. For example, several risk workflows use the EURO-CORDEX data to assess projected precipitation for Representative Concentration Pathways (RCP), such as 2.6, 4.5 and 8.5. In addition, one of the risk workflows considers a range of socioeconomic scenarios such as the Shared Socioeconomic Pathways (SSPs) until the end of the 21st century. More information can be found in section 4 of this deliverable and in the Deliverables D2.2 (Report on Hazard tools of relevance to the CRA Toolbox) and D2.3 (Report and database on pan European vulnerability and exposure projections). Deliverable 1.4 (Climate risk assessment framework) provides guidelines to the different users on how to select relevant future scenarios. As the CLIMAAX project progresses, the implementation of the risk analysis workflows will be extended and further harmonized.

2.2 Existing risk data platforms and tools

Data platforms for CRA as a combination of hazard, exposure, and vulnerability are already publicly available. These databases can be used for both the retrieval of useful information for CRA but also for validating existing risk assessments. However, these databases often offer pre-computed risk data that are not validated at the country level and do not accommodate user-defined inputs and needs. In addition, there are many open-source tools providing climate risk to allow the user an easy-

Funded by the European Union

This project has received funding from the European Union's Horizon Europe research and innovation programme under grant agreement No 101093864. Views and opinions expressed are however those of the author(s) only and do not necessarily reflect those of the European Union or the European Climate, Infrastructure and Environment Executive Agency (CINEA). Neither the European Union nor the granting authority can be held responsible for them.

to-access view at the country or regional level. However, they also do not easily allow the integration of other data sets to be used as inputs.

One of the main platforms for CRA is the Risk Data Hub of the European Commission Disaster Risk Management Knowledge Centre's[1]. The Risk Data Hub provides an easy-to-use mapping tool that visualizes pre-calculated risks for a range of hazards, exposed assets, and a generic (i.e. hazard-independent) vulnerability indicator at NUTS0 up to NUTS3 levels. However, the Risk Data Hub does not yet allow for the integration of the user's own data or risk assessment procedures. Furthermore, risk assessments based on geospatial raster data as well as the integration of vulnerability into the assessment are currently not possible.

The Copernicus Climate Data Store (CDS) contains climate model project data and reanalysis, as well as a large range of spatial and temporal information for several hazards, such as floods, wildfire, heatwaves at the European and global scales[2]. The CDS provides elaborate documentation on how to use the toolbox, as well as open-access code and data access through an API. However, the CDS primarily focuses on the provision of hazard data rather than risk assessment procedures and does not guide how to select or process these data for a risk assessment.

The Emergency Events Database (EM-DAT; CRED, 2019)[3] is a global database managed by the Centre for Research on the Epidemiology of Disasters that records information on the occurrence and impacts of mass disasters worldwide. In particular, the dataset includes events with at least 10 fatalities, 100 people affected, a declaration of a state of emergency, or a call for international assistance. The database has been operational since 1988, contains over 26,000 records of disasters, and serves as a significant resource for humanitarian action, disaster preparedness, and risk reduction strategies. Concerning floods, the Dartmouth Flood Observatory maintains a global active archive of large flood events, including information on location, time, affected area, and estimated damages (Kettner et al., 2021).

The Aqueduct Atlas is developed by the World Resources Institute (WRI) to assess water risk worldwide (Reig et al., 2013; Ward et al., 2020)[4]. In particular, the atlas provides data on water stress, water risks to agriculture and food security, and coastal and riverine flood risks, for current and future projections for different climate change scenarios (RCP4.5, RCP8.5) and socioeconomic pathways (SSP2, SSP3). The Aqueduct tools and data are freely available online, allowing users to conduct their water risk assessments and analyses (see an example in Figure 1).

Climate-ADAPT[5] is a European Climate Adaptation Platform maintained by the European Environmental Agency, aiming to support decision-making concerning climate change adaptation.

[1] https://drmkc.jrc.ec.europa.eu/risk-data-hub#/dashboardrisk

[2] https://cds.climate.copernicus.eu/#!/home

[3] https://www.emdat.be/

[4] https://www.wri.org/aqueduct

[5] https://climate-adapt.eea.europa.eu/#t-database

Funded by the European Union

This project has received funding from the European Union's Horizon Europe research and innovation programme under grant agreement No 101093864. Views and opinions expressed are however those of the author(s) only and do not necessarily reflect those of the European Union or the European Climate, Infrastructure and Environment Executive Agency (CINEA). Neither the European Union nor the granting authority can be held responsible for them.

This is achieved by data and information sharing linked to climate change impacts and adaptation options. Similar to the Risk Data Hub, it provides guidelines, handbooks and CRA step-by-step instructions for national-level policy makers and coordinators developing adaptation plans. The platform allows for the visualization of different hazards and social vulnerabilities relevant to urban adaptation. However, the platform is not designed to assist in analysing data in general as it focusses in mainly on providing a framework for climate adaptation.

In addition to the publicly available data sources, there are also tools for assessing climate risk. The open-source impact model CLIMADA was developed for probabilistic CRAs based on damage calculations (Aznar-Siguan & Bresch, 2019). The model includes several hazards, such as tropical cyclones and wildfires, and it allows for integrating custom code and data for risk assessment. However, customizing the model requires technical expertise and training. Moreover, CLIMADA is not designed to assess risks posed to exposed populations or assets.

The CLIMAAX toolbox draws upon the existing toolboxes by adopting risk assessment procedures, data, and guidelines, and collates these pieces of information in one open-access, consistent, and customizable toolbox across Europe.

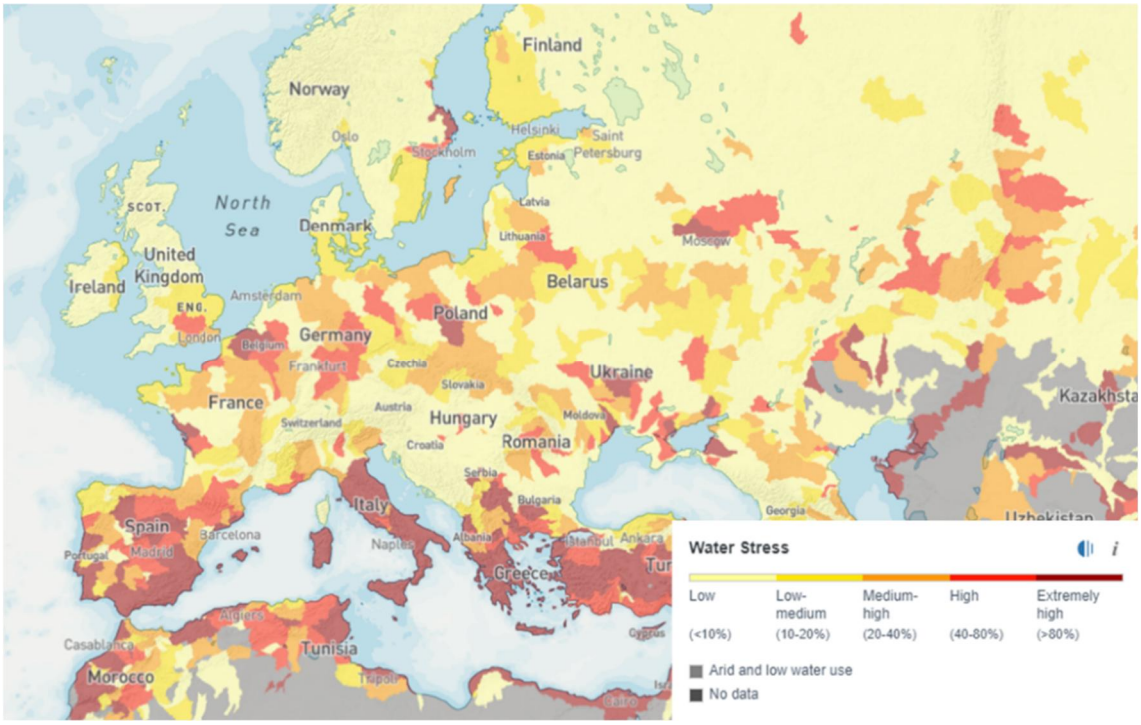

Figure 1. Water stress measures the ratio of total water demand to available renewable surface and groundwater supplies. Water demand includes domestic, industrial, irrigation, and livestock uses (Aqueduct)

Funded by the European Union

This project has received funding from the European Union's Horizon Europe research and innovation programme under grant agreement No 101093864. Views and opinions expressed are however those of the author(s) only and do not necessarily reflect those of the European Union or the European Climate, Infrastructure and Environment Executive Agency (CINEA). Neither the European Union nor the granting authority can be held responsible for them.

2.3 Selection criteria for the risk assessment within the CLIMAAX toolbox

The CLIMAAX toolbox considers nine different hazards: flood, drought, extreme precipitation, heatwave, windstorm, wildfire, heavy snow, blizzards, and multi-risk (combined extreme precipitation and temperature). This selection is the result of the consultation with the five CLIMAAX pilot regions (in collaboration with WP3). For these hazards, a review was performed to identify existing CRA methods, via the following sources:

- Scientific research with a sufficient number of citations
- Official EU reports
- Existing CRA frameworks implemented in the CLIMAAX pilots.

Once the different CRA methods were identified, we considered the following criteria for the selection of CRA methods for the CLIMAAX toolbox:

- Feasible to be implemented within the CLIMAAX toolbox
- Understandable and comprehensive also for users that are not trained in the technical or conceptual construction of risk assessment tools.

We did not consider:

- CRA and tools (see section 2.2) with major gaps that hamper their application at the regional to local scale. For example, some CRA are based on large-scale dataset that neglect local infrastructures (e.g. levee system) that could significantly affect risk assessment.
- CRA methods that included modelling activities, e.g. hydraulic modelling for flood propagation or impact assessment model. Including simulation models within the framework could have led to significant technical challenges due to computational time at large-scale, data limitation for model calibration, and technical issues in the implementation of the models within the toolbox software environment.

This resulted in the selection of three main risk assessment methods (see section 3) for a total of 14 risk workflows.

Funded by the European Union

This project has received funding from the European Union's Horizon Europe research and innovation programme under grant agreement No 101093864. Views and opinions expressed are however those of the author(s) only and do not necessarily reflect those of the European Union or the European Climate, Infrastructure and Environment Executive Agency (CINEA). Neither the European Union nor the granting authority can be held responsible for them.

3 Background of the selected risk assessment methods

This section provides an overview of previous studies focused on the different methods used for CRA within the CLIMAAX toolbox. The Intergovernmental Panel on Climate Change (IPCC), defines risk as is 'the potential for adverse consequences for human or ecological systems, recognising the diversity of values and objectives associated with such systems' (Reisinger et al., 2020). In particular, risk is expressed the dynamic interaction between hazard, vulnerability, and exposure of human and natural systems (Pachauri et al., 2014), highlighting the need for a consistent multi-disciplinary approach for CRA. In this context, IPCC defines the risk assessment drivers as:

Hazard: The potential occurrence of a natural or human-induced physical event or trend that may cause loss of life, injury, or other health impacts, as well as damage and loss to property, infrastructure, livelihoods, service provision, ecosystems, and environmental resources.

Exposure: The presence of people, livelihoods, species or ecosystems, environmental functions, services, and resources, infrastructure, or economic, social, or cultural assets in places and settings that could be adversely affected.

Vulnerability: The propensity or predisposition to be adversely affected. Vulnerability encompasses a variety of concepts and elements including sensitivity or susceptibility to harm and lack of capacity to cope and adapt. Vulnerability can be classified in social vulnerability (i.e. the societal characteristics that make a community (un-) prepared to face a hazard while it is manifesting, and to cope with its consequences and recover after it occurred) and physical vulnerability (i.e. the characteristics that make the of exposed elements assets (buildings, infrastructure, etc) more or less sensitive).

In the context of climate change, risks can arise from potential impacts of climate change as well as human responses to climate change. For this reason, in the Sixth Assessment Report (AR6) this risk framework accounting for 3 drivers was recently extended with a fourth risk driver: Response, which can include the influence of both adaptation and mitigation responses on risk and responses (Ara Begum et al., 2022).

3.1 Risk indexing method

Over the past decades, several methods have been developed for comprehensive climate and disaster risk assessments that combines hazard, exposure and vulnerability drivers (see e.g. Adger et al., 2018 and Jurgilevich et al., 2017 for recent reviews of the literature). Here, we analyse studies that has employed the Hazard-Exposure-Vulnerability (HEV) framework to assess climate risks.

Multiplicative Approach: One of the most common methods for assessing climate risk using the HEV framework is the multiplicative approach, where risk is calculated as the product of hazard, exposure, and vulnerability (Cardona et al., 2012; Oppenheimer et al., 2015). This approach assumes that all three components contribute equally to the overall risk and are independent of each other.

Multiple studies have employed this multiplicative approach to assess various climate-related risks, such as flood, drought, and wildfire. As an illustration, a selection of examples are hereby referenced.

Funded by the European Union

This project has received funding from the European Union's Horizon Europe research and innovation programme under grant agreement No 101093864. Views and opinions expressed are however those of the author(s) only and do not necessarily reflect those of the European Union or the European Climate, Infrastructure and Environment Executive Agency (CINEA). Neither the European Union nor the granting authority can be held responsible for them.

Dawson et al. (2018) used a multiplicative risk equation to quantify climate risks to urban infrastructure, combining hazard, exposure, and vulnerability components. The European Environment Agency (2024) presented a structured risk assessment for Europe, using a multiplicative approach to combine hazard, exposure, and vulnerability factors. Winsemius et al. (2013) developed a global river flood risk assessment using a multiplicative approach to combine hazard, exposure, and vulnerability components. Muis et al. (2015) developed a probabilistic method for assessing future trends in national-scale flood risk, integrating recent advances in global-scale flood hazard modelling with exposure data based on land use change. Koks et al. (2015) applied a multiplicative risk model to assess flood risks, integrating hazard, exposure, and social vulnerability components. Chuvieco et al. (2023) reviewed different methods for wildfire risk assessment, including the determination of fire ignition and propagation (hazard), the spatial extent to which fire overlaps with valued assets (exposure), and the potential losses and resilience to those losses (vulnerability).

These existing methods assessed risk focusing on hazard, exposure, and vulnerability. However, some risk frameworks contain response/coping capacity as a fourth component, to emphasise its importance (Marin-Ferrer et al., 2017). Frameworks that contain this fourth component are the INFORM risk framework (Figure 1) and the AR6 (H. Lee et al., 2023). The INFORM framework's methodology is set up to determine which regions or countries are at risk from natural hazards (e.g. floods), to assess which factors have led to this risk, and to analyse the temporal pattern underlying climate risk. This way, the risk is quantified and helps determine if the region or country needs (international) assistance (Marin-Ferrer et al., 2017).

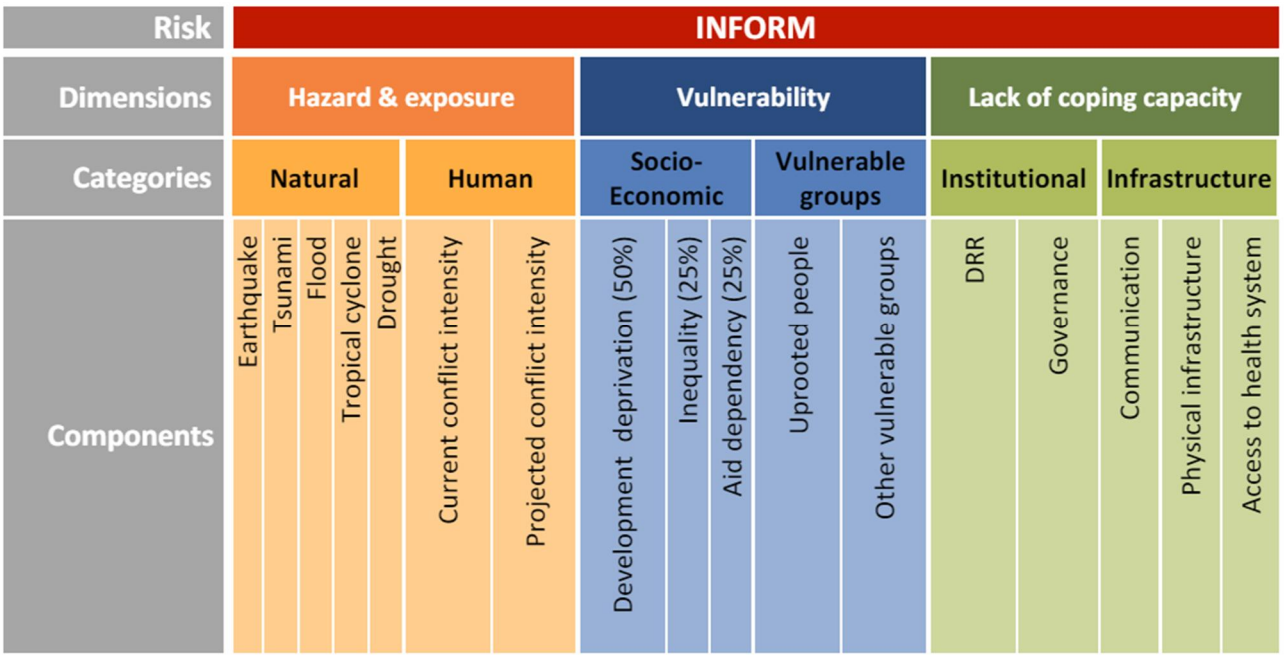

Figure 2. The INFORM risk framework (Marin-Ferrer et al., 2017)

Funded by the European Union

This project has received funding from the European Union's Horizon Europe research and innovation programme under grant agreement No 101093864. Views and opinions expressed are however those of the author(s) only and do not necessarily reflect those of the European Union or the European Climate, Infrastructure and Environment Executive Agency (CINEA). Neither the European Union nor the granting authority can be held responsible for them.

While the main advantage of the multiplicative approach is its simplicity, this approach has been criticized for assuming independence between hazard, exposure, and vulnerability. Additionally, methods that consider equal weighting of the risk components may not reflect the relative importance of each factor in contributing to the overall risk.

To address these limitations, many studies have assessed risk as a weighted average between hazard, exposure, and vulnerability. For example, Dilley (2005) and Carrão et al. (2016) assessed multi-risk by overlaying weighted hazard, exposure, and a set of vulnerability indicators. Similarly, Garschagen et al. (2021) developed a multi-hazard risk assessment framework that combined hazard, exposure, and vulnerability using a weighted approach. Those methods were shown to be more flexible in incorporating the relative importance of each risk component. However, the determination of the weights can be subjective, may vary depending on the context and needs to be assessed using information from relevant stakeholders.

Fuzzy Logic Approach: This approach was proposed to address the subjective choice of the weight coefficients in the multiplicative approach. Here, the risk components are represented as fuzzy sets, and the risk is calculated using fuzzy arithmetic operations considering risk values as classes rather than numerical values (Kelly et al., 2023). In this approach, membership functions for different categories (e.g. low, medium, high risk) are introduced to assess how much a value belongs to a certain category (or fuzzy set), assigning a value between 0 (not a member) and 1 (full member) to represent the degree of membership. In this way, numerical values can be converted into fuzzy number that provides a set of values indicating the weight between 0 and 1 to different memberships. In the example of Figure 3, a risk value of about 83 corresponds to a high flood risk category. Aitkenhead et al. (2023) applied a fuzzy logic approach to minimise the subjectivity in drought risk assessment, thus improving the efficiency of risk assessment as a tool for spatial decision-making (see Figure 3). The fuzzy logic approach has the advantage of accounting for the uncertainty and subjectivity in CRA, leading to a possibilistic risk representation.

The advantage of fuzzy logic approaches is the ability to handle uncertainty and imprecise data by allowing for partial membership in sets and using linguistic variables. Moreover, this approach uses linguistic variables and rules that are similar to human reasoning, making the models more interpretable and easier to understand for decision-maker.

However, the implementation of this approach can be more complex and may require specialised expertise. For example, fuzzy logic approaches heavily rely on expert knowledge for the assessments of membership functions and fuzzy rules, introducing potential biases and inconsistencies. Moreover, the outputs of fuzzy logic systems can be difficult to validate and compare with other risk assessment methods. Finally, as the number of input variables and fuzzy memberships increases, the computational complexity of the fuzzy logic method can increase, especially for large-scale climate risk assessments. Because of these reasons, this approach is not applied withing the CLIMAAX toolbox.

Funded by the European Union

This project has received funding from the European Union's Horizon Europe research and innovation programme under grant agreement No 101093864. Views and opinions expressed are however those of the author(s) only and do not necessarily reflect those of the European Union or the European Climate, Infrastructure and Environment Executive Agency (CINEA). Neither the European Union nor the granting authority can be held responsible for them.

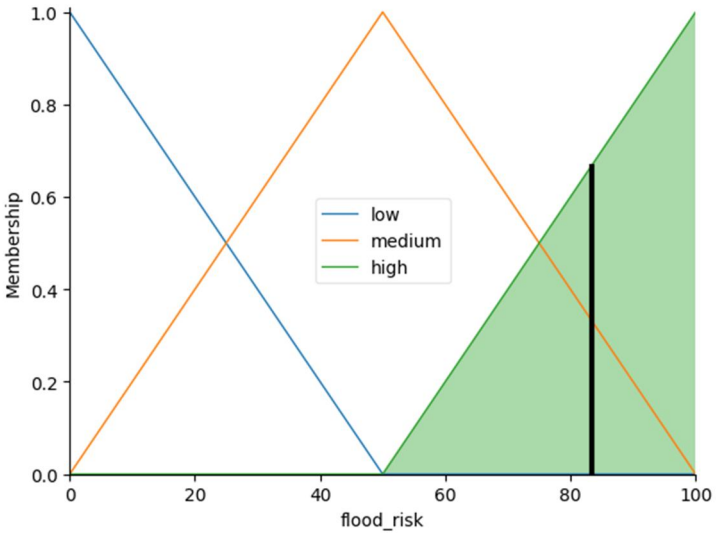

Figure 3. Examples of fuzzy membership for flood risk6.

Bayesian Network Approach: In this approach, risk is assessed as a probabilistic relationship between hazard, exposure, and vulnerability, represented as nodes in a Bayesian network. The conditional probabilities between the risk components are estimated based on available data or expert knowledge. The risk is then calculated as the joint probability of the three components. For example, Joo et al. (2019) developed a flood risk assessment method to derive the integrated weights for the risk components and indicators using Bayesian networks. Similarly, Wetzel et al. (2022) developed an alpha-level Bayesian Network based on the impact chain and applied it to an exemplary what-if scenario to simulate changes in risk if certain risk drivers change. The Bayesian network approach can capture the complex interdependencies between the HEV components and can handle uncertainty more effectively than deterministic methods. However, the development of the network structure and the estimation of the conditional probabilities can be challenging, especially when data is limited.

Bayesian networks can be applied to a wide range of climate-related hazards (e.g. floods, droughts, and wildfires), and can be tailored to different spatial and temporal scales. The assessment of the individual risk components (hazard, exposure, and vulnerability) can provide valuable insights for targeted adaptation and risk reduction strategies. On the other hand, the Bayesian approach does not account for the complex interactions that can occur between hazard, exposure, and vulnerability (Di Baldassarre et al., 2013; Mazzoleni et al., 2021). Moreover, extensive data availability is often needed for assessing risk with this approach, which may be difficult in developing countries or at finer spatial scales. In some cases, the calculation of the weights in the risk assessment can be subjective and depend on the stakeholders involved. Because of these reasons, this approach is not applied withing the CLIMAAX toolbox.

[6] https://benny.istan.to/blog/2023510-wcrrnfsscbiyg6899xs2lgdij2db4k

Funded by the European Union

This project has received funding from the European Union's Horizon Europe research and innovation programme under grant agreement No 101093864. Views and opinions expressed are however those of the author(s) only and do not necessarily reflect those of the European Union or the European Climate, Infrastructure and Environment Executive Agency (CINEA). Neither the European Union nor the granting authority can be held responsible for them.

3.2 Damage assessment

Damage assessment provides a quantitative understanding of the potential impacts of a climate-related hazards expressed as extent of damages. On the other hand, the risk indexing method estimate the likelihood and severity of future harm or loss by evaluating potential threats and vulnerabilities. Damage assessment has become increasingly used to assess how changes in the frequency and severity of a hazard due to climate change can exacerbate economic damage to regions and sectors. The damage is calculated by combining hazard maps with exposure and vulnerability data employing economic damage functions. Damage functions relate the magnitude of a climate-related hazard, such as flood depth, wind speed, or temperature, to the resulting economic or human impacts. These functions are typically derived from empirical data on past disaster events. One of the first applications of damage function assessment is described in Heneka & Ruck (2008) and Hinkel et al. (2014) with a focus on windstorm damage to buildings and coastal flood damage, respectively. While those studies focused on specific hazards, Prahl et al. (2016) unified the concept of damage function across different hazards such as coastal flooding, wind storms, and heatwaves. Below, we will describe the application of the damage assessment methodology to different hazards.

Flood damage assessment

Flood damage assessment has been widely applied, with a number of damage functions developed for different regions and asset types (Figure 3). Huizinga et al. (2017) developed a global database of flood depth-damage functions for various land use and building types to account for factors like construction materials, flood mitigation measures, and socioeconomic conditions. These functions relate hazard to the percentage of asset value that is damaged, allowing for the estimation of direct economic losses. Hazard information is based on water depth information for a given return period, i.e., the likelihood of an event to occur (de Moel et al., 2014).

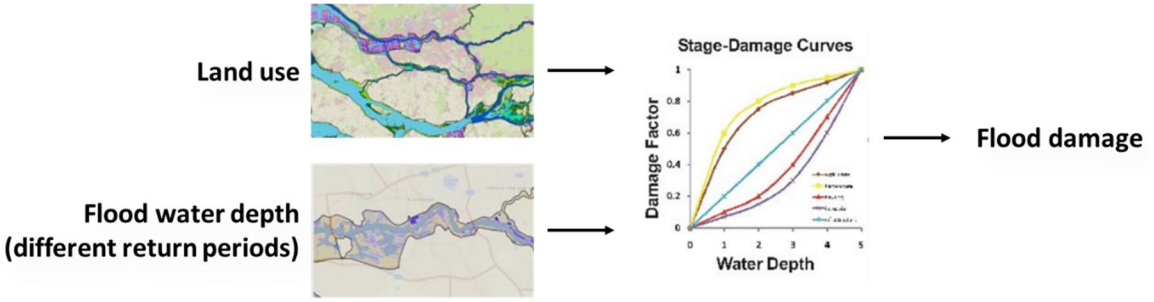

Figure 4. Schematic representation of the flood damage assessment method

The hazard is then linked with the exposure (land use) and vulnerability (damage curve) to assess flood damage. In particular, for each grid cell flood depth is combined with exposure data on land use- or building types by using stage-damage curves. These stage-damage curves show for each flood water level how much damage can occur (as a percentage of the maximum damage).

A comprehensive review of the methods used to construct stage–damage function curves for residential, commercial, agricultural, and industrial categories is reported in Romali et al. (2015).

Funded by
the European Union

This project has received funding from the European Union's Horizon Europe research and innovation programme under grant agreement No 101093864. Views and opinions expressed are however those of the author(s) only and do not necessarily reflect those of the European Union or the European Climate, Infrastructure and Environment Executive Agency (CINEA). Neither the European Union nor the granting authority can be held responsible for them.

Englhardt et al. (2019) developed an approach for large-scale flood damage assessments using damage curves exploiting buildings' characteristics as object-based information to represent exposure and vulnerability to flooding. Similarly, Wouters et al. (2021) advanced current flood damage assessments by extracting individual building characteristics and estimating damage based on the buildings' vulnerability. Endendijk et al. (2023) used a survey dataset of experienced damages and the implementation of flood damage mitigation measures on the household level, collected after the flood event in the Netherlands in 2021, to build depth-damage curves for flood damage assessment.

Coastal flood damage assessment has received significant attention, particularly in the context of sea-level rise and the increasing frequency of extreme storm surges. Hinkel et al. (2014), for example, developed a set of depth-damage functions for various land use types in coastal regions, similar to the aforementioned approaches used for river floods. The workflow implemented within the CLIMAAX toolbox for coastal floods is based on this study. The approach proposed in Hinkel et al. (2014) also accounted for a wide range of uncertainties in socioeconomic development, sea-level rise, population data, and adaptation strategies. Boettle et al. (2016) expanded on this work, proposing a unified approach accounting for the nonlinear relationship between sea-level rise and flood intensity. Moreover, the proposed damage function incorporates the potential construction of flood defence used to reduce vulnerability over time. Prahl et al. (2018) provided a dataset of macroscale damage and protection cost curves for the 600 largest European coastal cities. Parodi et al. (2020) coupled an ensemble of hydrodynamic models with a direct impact model to analyse the influence of wave height, storm surge level, sea level rise, topography, and socio-economic changes on coastal flood damage. Duo et al. (2020) presented a coastal flood impact application based on a multi-damage model exploiting flood-damage curves for residential, commercial, industrial and transport building categories.

Drought damage assessment

Damage assessment for drought can be more challenging than for other hazards, due to the large scale and longer duration of droughts. Nonetheless, several damage functions have been developed for drought-related impacts on agriculture, water resources, and other sectors. For example, Wei et al. (2023) developed a growth-stage-based drought vulnerability for soybeans combining a crop growth model and damage assessment curves. Similarly, Cui et al. (2019) used S-shaped soybean damage curves to assess the soybean drought losses at four growth periods, while Monteleone et al. (2022) developed maize drought vulnerability curves for the Po River Basin (Italy) to represent the relationship between crop water stress and maize yield losses. Naumann et al. (2015) proposed a power-law damage function linking drought severity and related damages in two economic sectors, i.e., cereal crop production and hydropower generation for 21 European countries. Based on this approach, the CLIMAAX workflow on agricultural drought is defined by FAO as an insufficient amount of soil moisture to satisfy crops evapotranspiration needs. The damage assessment hence focuses on quantifying the reduction in yield for 14 rainfed crops. Thus, this workflow provides a simple tool to estimate the damage, or "lost-opportunity cost'", of preserving rainfed agricultural systems rather than investing in efficient irrigation systems. Quantifying this cost is becoming a pressing issue across Europe. One hand, semi-arid regions will be increasingly prone to water shortages and forced to reduce allocations to irrigation to satisfy other public needs (Fader et al.,

Funded by the European Union

This project has received funding from the European Union's Horizon Europe research and innovation programme under grant agreement No 101093864. Views and opinions expressed are however those of the author(s) only and do not necessarily reflect those of the European Union or the European Climate, Infrastructure and Environment Executive Agency (CINEA). Neither the European Union nor the granting authority can be held responsible for them.

2016). On the other, historically wet regions might be forced to invest in the large-scale expansion of their irrigation systems, as the decreasing water availability may soon hinder the potential of rainfed systems to satisfy growing production demands (Grusson et al., 2021; Peltonen-Sainio et al., 2021).

Windstorm damage assessment

Concerning windstorm damage assessment, Koks & Haer (2020) developed a wind damage model that links storm footprint with economic damage based on the type of building. This approach built the foundation of the risk workflow for windstorm in the CLIMAAX toolbox. A similar approach was proposed also by Welker et al. (2021). Heneka & Ruck (2008), developed damage functions for assessing wind-induced damage to residential buildings, relating wind speed to the percentage of building value lost. Prahl et al. (2016) built on the method from Heneka & Ruck (2008) to propose a unified approach to windstorm damage assessment accounting for the spatial distribution of wind speeds and the heterogeneity of the exposed building, allowing for a more comprehensive risk assessment at different spatial scales. Gardiner et al. (2008) designed a modelling based approach for the wind damage assessment to forest. This unified approach enables the transfer of methodology between hazards and a consistent treatment of uncertainty.

Wildfire damage assessment

Damage functions for wildfires typically relate fire intensity, as measured by variables like flame length or fire line intensity, to the percentage of damaged assets or structures. One example is the work by Lüthi et al. (2021), who used the risk modelling platform CLIMADA for assessing the economic impacts of wildfires using intensity-damage curves in a globally consistent and spatially explicit approach (see Figure 5). Recently, El Meouche et al. (2020) developed a probabilistic fire risk framework modelling the fire hazard and the vulnerability of potential assets using fire-damage curves. One of the key challenges in wildfire damage assessment is the need to account for the complex interactions between fire behaviour, fuel loads, and human activities.

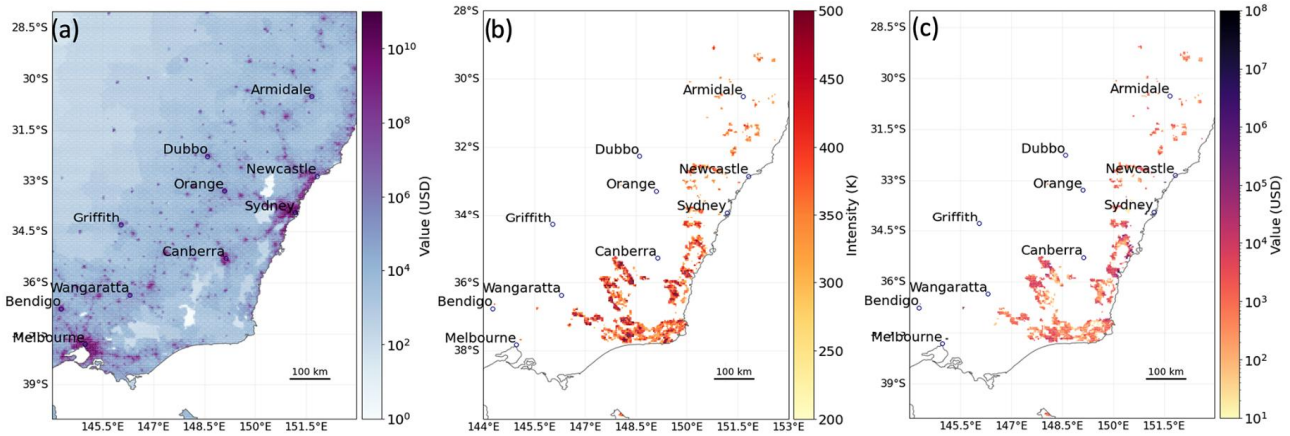

Figure 5. Maps of south-eastern on Wildfire risk in Australia showing (a) the spatial distribution of exposed asset values generated using LitPop (Eberenz et al., 2020), (b) the wildfires active between 29 December 2019 and 6 January 2020, and (c) the resulting damage per grid point as estimated by CLIMADA (Lüthi et al., 2021).

Funded by the European Union

This project has received funding from the European Union's Horizon Europe research and innovation programme under grant agreement No 101093864. Views and opinions expressed are however those of the author(s) only and do not necessarily reflect those of the European Union or the European Climate, Infrastructure and Environment Executive Agency (CINEA). Neither the European Union nor the granting authority can be held responsible for them.

Heatwave damage assessment

With respect to heatwave damage assessment, Mora et al. (2017) developed a global database linking temperature-mortality relationships, based on empirical data from past heatwave events. These functions were used to quantify the current and projected occurrence of deadly heatwaves worldwide to inform the development of early warning systems and adaptation strategies. As previously mentioned, Prahl et al. (2016) proposed a unified approach to design heatwave damage curves that could be transferred also to other hazards like coastal flooding and wind storms. Their damage functions relate apparent temperature (a measure of heat stress) to mortality. A main challenge in heatwave damage assessment is the complex interactions between environmental, human physiology, and socioeconomic conditions (e.g. age, health status, and access to cooling resources) when designing damage curves.

Snow damage assessment

Snow damage assessment is performed using a similar approach to the ones aforementioned. For example, Ortner et al. (2023) developed a novel risk assessment approach for calculating spatial avalanche risk by combining large-scale hazard mapping with damage curves based on exposure information. Similarly, Zubkov et al. (2024) implemented a snow damage model consisting of a numerical weather prediction-based snow accumulation model for forest canopies and a mechanistic critical snow load mode. An important aspect difficult to be addressed in these models is the complex interactions between snow accumulation, wind, and other environmental factors, as well as the potential for secondary impacts like power outages and disruptions of other critical infrastructures.

The use of damage functions in CRA helps to quantify the potential impacts of different climate-related hazards across different regions and sectors (de Brito et al., 2024). Moreover, damage assessment can support decision-making in developing informed-based risk mitigation strategies, adaptation measures, and disaster response plans. However, this approach is inevitably affected by some limitations (de Brito et al., 2024). For example, the sparse availability and quality of empirical loss data can be a significant constraint, particularly in developing countries and regions with limited historical records. Moreover, as previously mentioned, damage functions do not account for the complex interactions between hazard, exposure, and vulnerability and dynamics between changing climate conditions, evolving socioeconomic factors, and the implementation of adaptation measures. Damage functions that rely on historical data may not adequately capture the effects of changing climate conditions or evolving socioeconomic factors. Addressing these challenges will be crucial for improving damage assessment and supporting climate adaptation and resilience-building efforts, particularly in the face of the growing impacts of climate change.

3.3 Exposed assets and population

Climate risk can also be assessed by evaluating the susceptibility of infrastructure, populations, and ecosystems to hazards based on their exposure. For example, Eberenz et al. (2020) developed a global dataset of asset exposure to climate risk by disaggregating national-level asset values to a high-resolution grid using a combination of nightlight intensity and population data (Figure 6).

Funded by the European Union

This project has received funding from the European Union's Horizon Europe research and innovation programme under grant agreement No 101093864. Views and opinions expressed are however those of the author(s) only and do not necessarily reflect those of the European Union or the European Climate, Infrastructure and Environment Executive Agency (CINEA). Neither the European Union nor the granting authority can be held responsible for them.

Flood exposed assets and population

Recent studies have integrated advanced modelling frameworks to assess flood risks by considering exposed populations and assets. For instance, Shu et al. (2023) used the First Street Foundation Flood Model to integrate data on flood extent and exposure to assess property-level economic impacts in the U.S. Hirabayashi et al. (2013) assessed flood risk by overlaying the projected fluvial flood changes estimated from CMIP6 with the population dataset Gridded Population of the World (CIESIN, 2016). These models help in understanding how flood risks are evolving due to climate change and population growth.

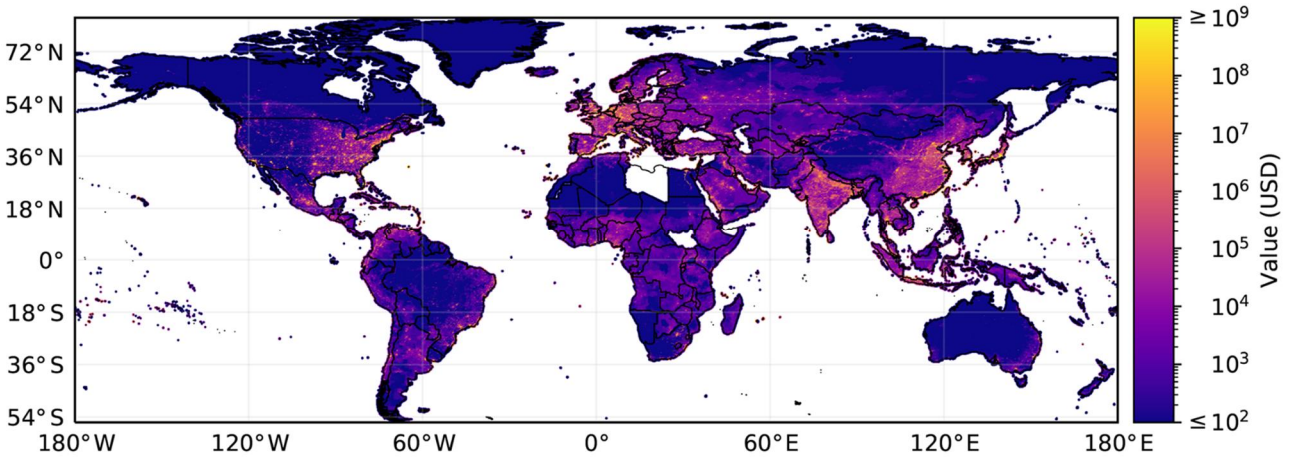

Figure 6. Global gridded asset exposure values scaled to a resolution of 600 arcsec (Eberenz et al., 2020)

Drought exposed assets and population

Concerning droughts, Das et al. (2023) assessed the population exposure to drought under different climate change and population scenarios using statistical indices as a proxy of drought hazard. Moreover, they explored the contribution of individual exposure (climate, population, and interaction) in future climate change scenarios. Similarly, Spinoni et al. (2021) assessed the exposure of population, forests, croplands and pastures to meteorological droughts (i.e. precipitation deficit) worldwide in the 21st century. The exposure to drought hazard (assessed using the Standardized Precipitation Index) is presented for five Shared Socioeconomic Pathways (SSP1-SSP5) at four Global Warming Levels (1.5°C to 4°C). Alonso et al. (2019) identified the agricultural areas most vulnerable to drought by using a principal component analysis (PCA) based on the indicators characterizing the exposure (e.g. vegetation indices and soil characterization variables), sensitivity and adaptive capacity of the agricultural system. Gu et al. (2020) quantified the future changes in global drought exposure by comparing projected drought conditions (using the Standardized Precipitation Evapotranspiration Index) and corresponding socioeconomic exposures for additional 1.5 and 2.0-degree warming trajectories under three RCPs (2.6, 4.5 and 8.5).

Windstorm exposed assets and population

Current studies on windstorms, wildfires, and heatwaves frequently include models that map the exposure of assets and populations to these events. Batke et al. (2014) generated hurricane exposure vulnerability site score at a meso-climate level with a resolution of 50m×50m. This was

Funded by the European Union

This project has received funding from the European Union's Horizon Europe research and innovation programme under grant agreement No 101093864. Views and opinions expressed are however those of the author(s) only and do not necessarily reflect those of the European Union or the European Climate, Infrastructure and Environment Executive Agency (CINEA). Neither the European Union nor the granting authority can be held responsible for them.

achieved by combining a wind pressure model, historical hurricane data, and an exposure model that can incorporate simple wind dynamics within a digital elevation model (DEM). Jung & Schindler (2024) developed a new exposure atlas for European winter storms by combining representative storm hazard and storm exposure indices for forested areas, built-up areas, and population. In particular, the wind hazard was assessed by modelling wind speed for the 27 most extreme winter storm events from 1993 to 2022 based on ERA5. The Storm exposition index was assessed by combining the normalized storm exposure indices for population, forested area, and built-up area following the approach schematized in Figure 7. The research by Gonçalves et al. (2024) focuses on assessing wildfire exposure and social vulnerability for local communities, at the level of villages or small human settlements, emphasizing the importance of considering local conditions for effective risk reduction strategies. Salis et al. (2021) employed an advanced simulation modelling approach using the minimum travel time fire spread algorithm for characterizing wildfire exposure and risk transmission on the island of Sardinia, Italy. Land-use data is used to determine the wild wildfire transmission.

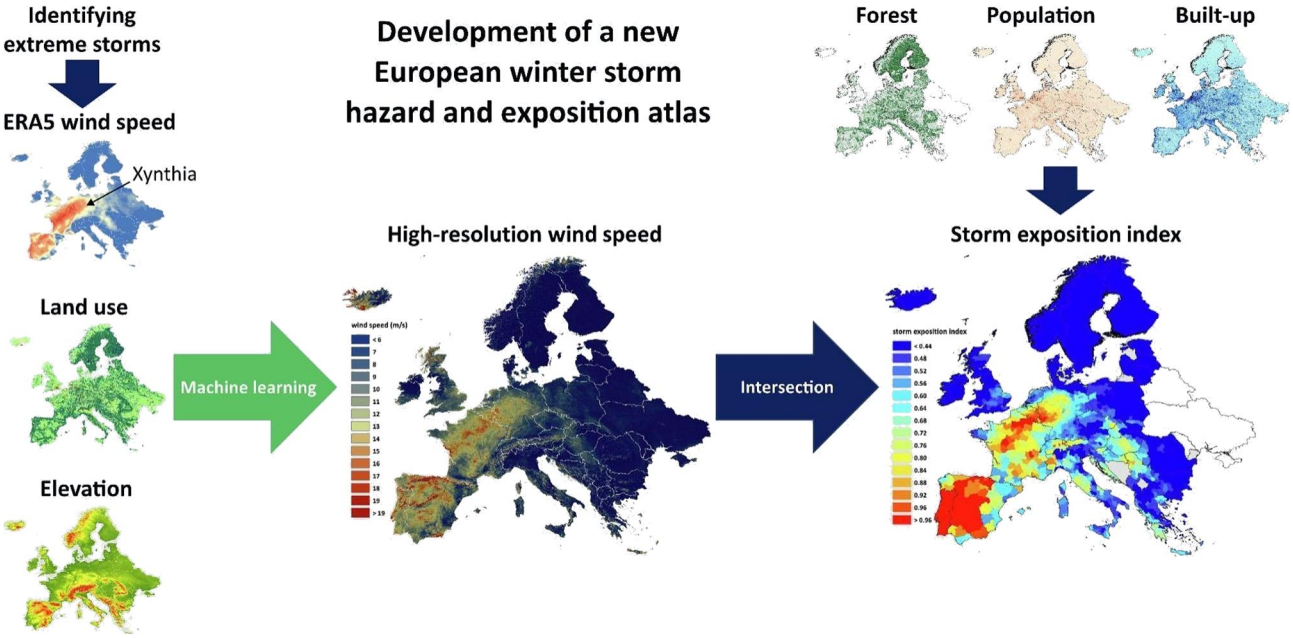

Figure 7. Methodology used to assess the European winter storm exposure atlas (Jung & Schindler, 2024)

Heatwave exposed assets and population

Heatwave risk assessments are particularly focused on vulnerable populations, such as the elderly and those without access to air conditioning. This information on population characteristics is crucial for public health planning and response strategies. Nishant et al. (2022) estimated changes in future exposure to heatwaves over Australia by combining future projections of heatwaves from the regional climate model NARCliM1.5 with projections of the Australian population in its capital cities. Similarly, Chambers (2020) performed a global study of heatwave exposure by exploiting global gridded climate reanalysis from ERA5 for the years 1980-2018, population, and demographic data, this work analyses trends in the change in exposure of vulnerable populations to heatwaves, providing global and per-country aggregate statistics. Using a similar approach, Ullah et al. (2022)

Funded by the European Union

This project has received funding from the European Union's Horizon Europe research and innovation programme under grant agreement No 101093864. Views and opinions expressed are however those of the author(s) only and do not necessarily reflect those of the European Union or the European Climate, Infrastructure and Environment Executive Agency (CINEA). Neither the European Union nor the granting authority can be held responsible for them.

and Mishra et al. (2017) found that the compounding effects of projected heatwaves and socio-economic trends will exacerbate the population exposed to heatwaves in South Asia.

Snow exposed assets and population

For heavy snow events, risk assessments typically focus on the impact on transportation networks and critical infrastructure (Petrova, 2011). A number of numerical models have been used to better predict where snow will cause road closures or accidents (Hong & Yun, 2024; Usman et al., 2011), helping to manage snow removal and emergency responses effectively.

3.4 Other methods

Several additional approaches are used for the assessment of climate risk but are not included in the CLIMAAX toolbox based on the selection criteria described in section 2.3.

Integrated Assessment Models (IAMs) are computer models that integrate both physical and social science aspects to assess the impacts of climate change on various sectors such as agriculture, energy, and health. IAMs are a trade-off between detail and simplification of environmental (focus of earth system models; ESM) and socio-economic conditions. IAMs are pivotal in understanding complex environmental problems and aiding decision-making processes (Wilson et al., 2021). Here, we discuss the application of IAMs in CRA, specifically examining the latest research associated with the natural hazards included in the CLIMAAX toolbox.

Cost-benefit analysis (CBA) has emerged as a powerful tool for assessing the economic impacts of climate-related hazards and evaluating the potential benefits of adaptation measures, using, for example, numerical models. It is worth noting that this approach does not focus directly on assessing risk, but rather on adaptation measures. CBA has been widely used for CRA in recent years, as it allows decision-makers to quantify the trade-offs between the costs of implementing risk reduction strategies and the potential damages that can be avoided.

Scenario analysis allows a user to explore how different potential future climate pathways could impact society and their consequent decision-making (Riddell et al., 2019). This approach was first proposed in the 1980s to forecast future energy demand and supply and develop robust strategic plans that are more flexible accounting for plausible future states (Riddell et al., 2019). For CRA, several scenarios of changes in global temperatures, precipitation, and socioeconomic pathways, among others, are considered based on projected greenhouse gas emissions.

Multi-risk assessment is crucial for understanding and mitigating the impacts of compound and consecutive natural hazards. This approach considers the interplay between different hazards and their potential interactions, which can lead to cascading impacts and risk (de Brito et al., 2024; Zscheischler et al., 2018). A number of qualitative and quantitative approaches have been proposed in the past years for multi-risk assessment methods (Gill & Malamud, 2016). Among the qualitative approaches, anecdotical approaches have been proposed to assess the relationship between primary and secondary hazards (Dilley, 2005). On the other hand, quantitative methods are used to assess the occurrence of potential cascading hazards by modelling the cause-effect chain and deriving the occurrence probability distribution (Tilloy et al., 2019). Among them, we can find impact-chain models, weighted overlay approach, and Bayesian network models.

Funded by the European Union

This project has received funding from the European Union's Horizon Europe research and innovation programme under grant agreement No 101093864. Views and opinions expressed are however those of the author(s) only and do not necessarily reflect those of the European Union or the European Climate, Infrastructure and Environment Executive Agency (CINEA). Neither the European Union nor the granting authority can be held responsible for them.

4 Risk assessment workflows within the CLIMAAX Toolbox

This section describes the methods and implementation of the different risk workflows of the CLIMAAX toolbox. The workflows are implemented by different CLIMAAX partners, and the selection of the CRA method for a given hazard reflects the expertise of the specific responsible and interest of the CLIMAAX pilot regions identified in collaboration with WP3. As a result, 14 different workflows are implemented within the CLIMAAX toolbox. For all workflows, we designed a similar structure to provide the users with a homogenous implementation of the workflows.

The first step that the user must perform for assessing their own customized CRA, as described in the CLIMAAX framework, is to select the type of hazard they would like to focus on. They can select between flood, windstorm, heatwave, wildfire, drought, extreme precipitation, and snow and blizzards, and multi-risk (focus on extreme precipitation and temperature). Once the hazard is identified, the user can read the guideline to the specific risk workflow and follow one of the proposed methodologies. In fact, it is worth noting that some hazards (e.g. drought) have different workflows depending on the CRA implemented (as described in section 3). Each workflow is divided in hazard and risk assessment (Figure 8). First, following the instructions in the toolbox, the user can either assess the hazard using pre-calculated European and/or large-scale datasets or by use local data to assess hazard following the method described in the hazard assessment section (specific for a given hazard type). It is worth noting that some workflows (e.g. the one for costal flood) have multiple methods for assessing the hazard. Second, the user can calculate the risk, also in this case by using either European or large-scale data of exposure and vulnerability or using local data. Exposure and vulnerability data can refer to historical conditions or future scenarios (see D2.3 for more detail on exposure and vulnerability data available at pan-European scale).

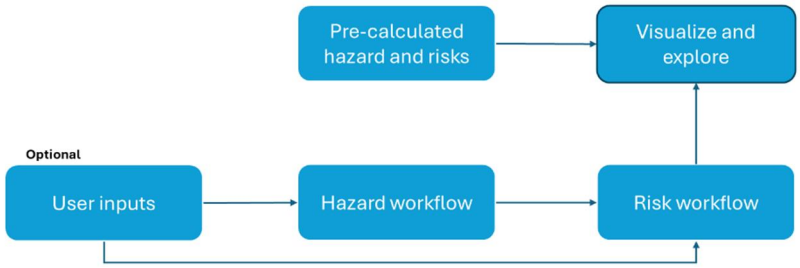

Figure 8. Steps for the CRA assessment and visualization within the CLIMAAX toolbox for a given hazard

A summary of the different risk workflows implemented within the toolbox are reported in Table 1 and Table 2. For each workflow, the table indicates the types of hazards, risk assessment methods, and hazard, exposure, and vulnerability data, and reference period (i.e., historical or future or both) included in the toolbox. More information about the data used are reported in the following sections and in the Deliverables D2.2 and D2.3. In the following subsections, each workflow is described by first introducing the main risk approach and components to define risk, such as hazard, exposure, and vulnerability. Finally, the output of the toolbox based on the specific risk workflow are visualized. It is worth noting that the data reported in Table 2 are representative of the examples reported in the CLIMAAX toolbox. A user can decide to use their own local data for the CRA assessment.

Funded by the European Union

This project has received funding from the European Union's Horizon Europe research and innovation programme under grant agreement No 101093864. Views and opinions expressed are however those of the author(s) only and do not necessarily reflect those of the European Union or the European Climate, Infrastructure and Environment Executive Agency (CINEA). Neither the European Union nor the granting authority can be held responsible for them.

Table 1. Summary of the risk workflow characteristics implemented in the CLIMAAX toolbox

Hazard type		Risk assessment	Hazard data	Exposure and vulnerability	Risk output
Flood	River flood	Damage assessment	River flood depth and extent maps	Land use, vulnerability damage curves	Map of flood depth and damage
	Flood damage and population exposures	Damage assessment and exposure	Flood depth maps	Open street map, Buildings damage and population exposure	Map of flood damage; population exposed and displaced; exposed critical infrastructures
	Coastal flood	Damage assessment	Coastal flood depth and extent maps	Land use, vulnerability damage curves	Map of flood depth and damage
Extreme precipitation		Risk index method	Precipitation intensity for a given return period, impact rainfall thresholds	Critical infrastructures and population density	Impact rainfall thresholds; Shift in magnitude and frequency
Drought	Drought risk	Risk index method	Drought hazard index calculated based on monthly precipitation timeseries	Multiple exposure and vulnerability indices (social and economic)	Map of relative drought risk
	Agricultural drought	Damage assessment	Crop yield reduction	Total crop production and aggregated crops revenue	Map revenue loss
	Drought exposure	Exposed population	Combined Drought Indicator	Population density	Exposed population
Heatwave		Risk index method	Maximum Land Surface Temperature	Population density	Heatwave risk level
Wildfire	Wildfire risk	Risk index method	Fire susceptibility	Population, Economy, Ecology	Road, Population, Ecological and Economic risks
	Wildfire exposure	Exposed population	Fire Weather Index	Population density	Exposed population
Windstorm		Damage assessment	Footprint of maximum wind gusts	Land use, vulnerability damage curves	Wind damage map
Heavy snow		Exposed population	Annual probability of occurrence	Population density	Exposed population
Blizzards		Exposed population	Annual probability of occurrence	Population density	Exposed population
Multi-hazard		Risk index method	Precipitation and temperature thresholds as proxy of floods and heatwaves	Airports and sensitivity and adaptive-capacity indicators	Risk maps of extreme temperature and precipitation

Funded by the European Union

This project has received funding from the European Union's Horizon Europe research and innovation programme under grant agreement No 101093864. Views and opinions expressed are however those of the author(s) only and do not necessarily reflect those of the European Union or the European Climate, Infrastructure and Environment Executive Agency (CINEA). Neither the European Union nor the granting authority can be held responsible for them.

Table 2. Summary of the climate data used for historical and future scenarios within the risk workflow examples of the CLIMAAX toolbox

Hazard type		Time horizon(s)	Future scenarios	Datasets	Lead CLIMAAX partner
Flood	River flood	1980, 2030, 2050, and 2080	RCPs 4.5 and 8.5	JRC and Aqueduct	DELT
	Flood damage and population exposures	1980, 2030, 2050, and 2080. Population in 1975, 1990, 2000, 2015 or the population projection of either 2025 or 2030.	RCPs 4.5 and 8.5	JRC, Aqueduct, and GHSL	CMCC
	Coastal flood	Historical (ca. 2018) and 2050	RCP 8.5	Flood maps based on GTSM	DELT
Extreme precipitation		Historical (e.g. 1976-2005) and future periods (e.g. 2041-2070)	RCP 8.5	EURO-CORDEX	UPC
Drought	Drought risk	Historical (e.g. 1979-2019) and future periods (e.g. 2015-2100)	SSP1-RCP2.6 SSP3-RCP7.0 SSP5-RCP8.5	ISIMIP	IIASA
	Agricultural drought	Historical and future periods (e.g. up to 2050)	RCP2.6, RCP4.5 and RCP8.5	EURO-CORDEX	CMCC
	Drought exposure	Historical (e.g 2012 -2023)	-	JRC	ECMWF
Heatwave		Historical (1971-2000) and three future periods (2011-2040, 2041-2070 and 2071-2100)	RCPs 4.5 and 8.5	EURO-CORDEX	KAJO
Wildfire	Wildfire risk	Two past (1961–1990 and 1991–2010) and five future (2011–2020, 2021–2040, 2041–2060, 2061–2080 and 2081–2100) periods.	RCPs 4.5 and 8.5	ECLIPS2.0 and EFFIS datasets	CIMA
	Wildfire exposure	Historical (e.g. 1981-2005) and future periods (e.g. 2021-2098)	RCP2.6, RCP4.5 and RCP8.5	Fire danger indicators	CMCC
Windstorm		Historical (e.g. 1979-2021)		Winter windstorm indicators	DELT
Heavy snow		Historical (e.g. 1940 to present) and three future periods (2011-2040, 2041-2070 and 2071-2100).	RCP2.6, RCP4.5 and RCP8.5	ERA5 EURO-CORDEX	FMI
Blizzards		Historical (e.g. 1940 to present) and three future periods (2011-2040, 2041-2070 and 2071-2100).	RCP2.6, RCP4.5 and RCP8.5	ERA5 EURO-CORDEX	FMI
Multi-hazard		Historical (e.g. 1961 to 2019) and three future periods (2011-2100)	RCP2.6, RCP4.5 and RCP8.5	UERRA MESCAN-SURFEX; EURO-CORDEX	CMCC

Funded by the European Union

This project has received funding from the European Union's Horizon Europe research and innovation programme under grant agreement No 101093864. Views and opinions expressed are however those of the author(s) only and do not necessarily reflect those of the European Union or the European Climate, Infrastructure and Environment Executive Agency (CINEA). Neither the European Union nor the granting authority can be held responsible for them.

4.1 Flood

4.1.1 River flood damage

Risk method

In this workflow the risk is assessed by combining maps of potential river flood extent with exposure and vulnerability data in the form of economic damage functions. The economic damage is mapped based on the flood depth maps, land use maps, damage curves, and country-specific economic parameters that approximate the economic value of different land use types (calculated based on the country's GDP). The resulting data and maps can help the user in assessing potential hotspots of economic damage due to river flooding for different return periods of high river flows (i.e., 1 in X years extreme event for river flooding). It is worth noting that the flood hazard maps used in this workflow do not account for the presence of river flood defences, such as levee systems, that may already be in place, and are mainly representative for flooding in larger river neglecting flooding for smaller water bodies in full. It is important to always check the result against existing local knowledge of the infrastructure. It is also recommended to consider using alternative (local) sources for flood maps where local processes are better represented.

Hazard data

Two main datasets are used to assess river flood hazard. On the one hand, high-resolution flood maps developed by the Joint Research Centre (Baugh et al., 2024), openly available via the Joint Research Centre Data Catalogue, are used to represent river flood extent and inundation depth maps for various return periods under the present-day climate (no climate scenarios are available). The flood maps come at a resolution of 3 arc-seconds (30-75m in Europe depending on latitude) and a range of return periods (10, 20, 50, 100, 200, and 500 years) based on hydrodynamic simulations forced with past hydrological events.

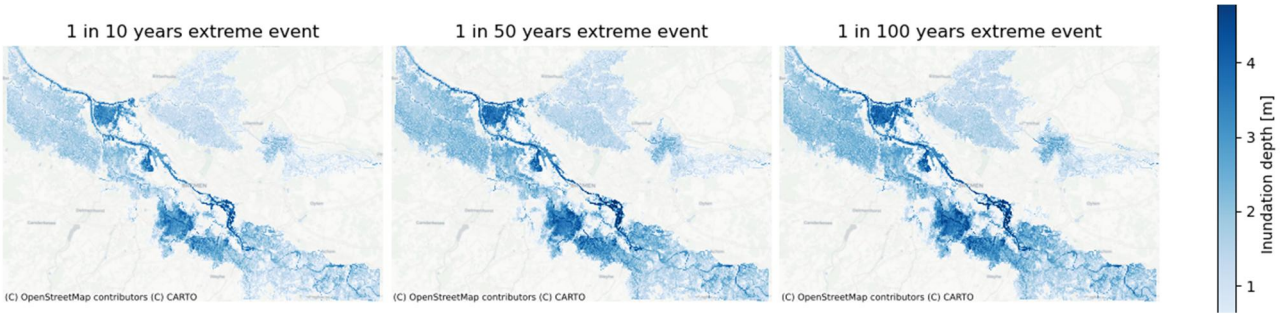

Figure 9. River flood maps for different return periods for the area of Bremen, Germany, retrieved from the JRC dataset of European flood maps (Baugh et al., 2024).

On the other hand, coarse-resolution flood map datasets from Aqueduct Floods Tool (Ward et al., 2020), openly available via the World Resources Institute website, are used to assess the likely impact of climate change on the river flood hazard based on flood simulations. This dataset includes flood maps for extreme flood events under the baseline climate (ca. 1980) and in future climates (2030, 2050, 2080 for RCP4.5 and RCP8.5 climate scenarios) with global coverage and spatial resolution of 30 arc-seconds (300-750 m depending on latitude in Europe).

Funded by the European Union

This project has received funding from the European Union's Horizon Europe research and innovation programme under grant agreement No 101093864. Views and opinions expressed are however those of the author(s) only and do not necessarily reflect those of the European Union or the European Climate, Infrastructure and Environment Executive Agency (CINEA). Neither the European Union nor the granting authority can be held responsible for them.

Exposure and vulnerability data

The land-use information for a specific year is used as a proxy for exposure. In this workflow we use LUISA land cover information (100m^2 spatial resolution) available at European level for 2018[7]. The land use encompasses various types of urban areas, natural land, agricultural fields, infrastructure and waterbodies. Damage curves for infrastructure, expressed as relative damage percentage, are then used as proxy for flood vulnerability (Huizinga et al., 2017). The curves allow to determine, for a given land-use category, what fraction ('damage factor') of the economic value is at risk given a particular flood depth. To assess the potential total damage under a given scenario, monetary value is assigned per land use category, expressed as the potential loss in €/m². This value is scaled based on the country's GDP (an advanced user can further refine the monetary value by adjusting the inputs).

Risk visualization

The outputs of this workflow are:

- River flood inundation maps for the area of interest corresponding to extreme events with different return periods based on European high-resolution dataset (Figure 9).
- Comparison of flood depth maps between the future and historical climates under two climate scenarios (RCP4.5 and RCP8.5) for different return periods derived from a coarse-resolution global dataset.
- Flood damage maps, expressed in terms of economic damage, for extreme events with different return periods based on available flood maps for the historical climate. (Figure 10). Aggregated data on damage within each land use category is also an output from this workflow.

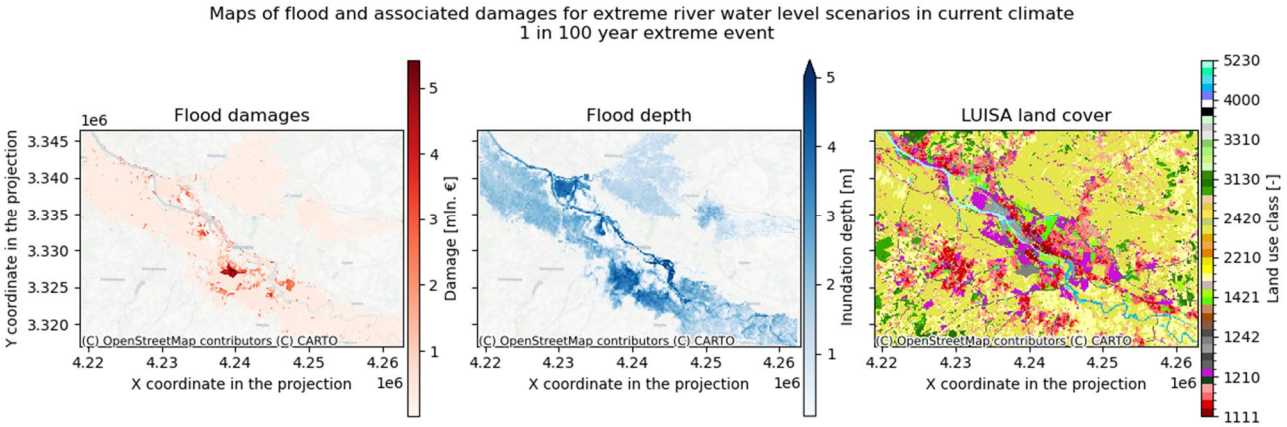

Figure 10. River flood damages for extreme river flow scenarios under historical climate derived based on the JRC's European flood maps (Baugh et al., 2024).

4.1.2 Flood building damage and population exposure

Risk method

This workflow assesses buildings damage and population exposure by combining potential flood data, population, and building data. For building damage, the flood depth maps are used with

[7] https://data.jrc.ec.europa.eu/collection/luisa

Funded by the European Union

This project has received funding from the European Union's Horizon Europe research and innovation programme under grant agreement No 101093864. Views and opinions expressed are however those of the author(s) only and do not necessarily reflect those of the European Union or the European Climate, Infrastructure and Environment Executive Agency (CINEA). Neither the European Union nor the granting authority can be held responsible for them.

building type data, damage curves and EU level economic parameters, to assess the total damage caused. For population exposure, flood depth and population density rasters are used directly to assess population exposed. The resulting data and maps help the user in observing differences in building damage and exposure (e.g. population displacement) depending on flood return period, as well as observe potential hotspots. When using this workflow, it is important to remember that the method does not consider flood defences that may be present for the assessment of the flood hazard. However, in the toolbox the user can add specified local flood maps which could be more tailored to local conditions (e.g. accounting for the presence of local hydraulic structures) and higher resolution to assess local damage.

Hazard data

Similarly to the river flood workflow (section 4.1.1), this workflow uses the "River flood hazard maps for Europe and the Mediterranean Basin region" dataset, created by the Copernicus Emergency Management Service (Baugh et al., 2024), and available via Joint Research Centre. The dataset maps flood water depths over return periods 10, 20, 50, 100, 200, and 500, at a resolution of 3 arc seconds, covering longitude -24.54° to 67.26°, and latitude 27.81° to 71.13° (see Figure 11). However, as mentioned before, the user can also add local flood extent and water depth maps.

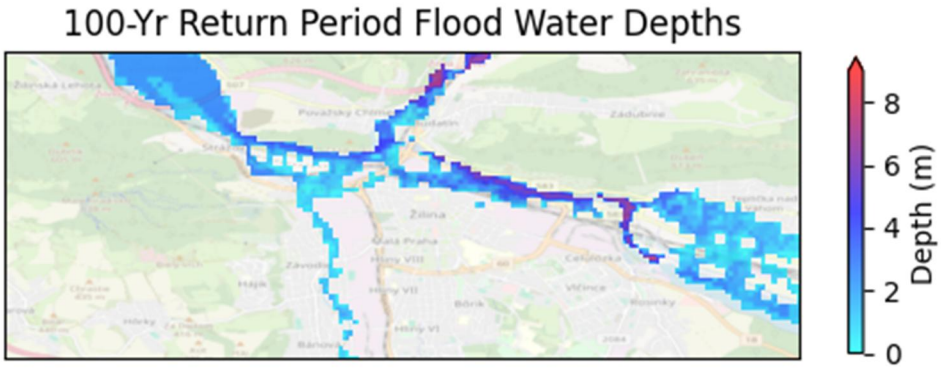

Figure 11. Example flood water depths for 100-year return period in the area of Žilina, Slovakia, retrieved from the JRC dataset of European flood maps (Baugh et al., 2024).

Exposure and vulnerability data

Open Street Map (OSM) is used to collect building information, both geometry and classification, while the GHS-POP dataset (Schiavina et al., 2023), published by the European Commission's Joint research Centre is used for mapping the population estimates or projections, with a resolution of 3 arc seconds. The damage assessment follows the same procedure and data of the river flood damage workflow in section 4.1.1. In addition, the workflow allows for selecting the population estimate in 5-year intervals between 1975 and 2020, or the population projection of either 2025 or 2030 (Figure 12).

Funded by the European Union

This project has received funding from the European Union's Horizon Europe research and innovation programme under grant agreement No 101093864. Views and opinions expressed are however those of the author(s) only and do not necessarily reflect those of the European Union or the European Climate, Infrastructure and Environment Executive Agency (CINEA). Neither the European Union nor the granting authority can be held responsible for them.

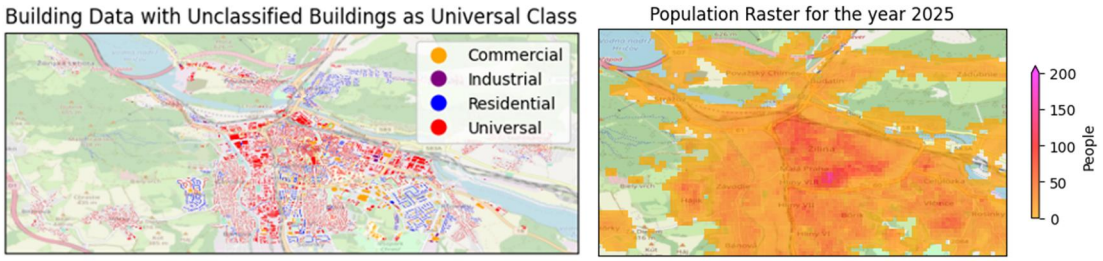

Figure 12. Example building class map (left), and population estimate for 2025 (right) for the area of Žilina, Slovakia.

Risk visualization

This workflow generates similar flood damage assessment than the one in section 4.1.1 but it adds a number of details with respect to different exposure classes. For a specific area, the outputs are:

- Flood depth maps for a specific return period.
- Population raster for a specific date.
- Damage curves by class type.
- Map of building type and class.
- Building water exposure maps.
- Building damage maps and estimated annual building damage graph.
- Critical infrastructure map with flooded area.
- Population exposed maps and estimate annual exposed population graph.
- Population displaced maps and estimate annual displaced population graph.

Ultimately, expected annual damage and expected annual exposed population are outputted in the workflow (Figure 13 and Figure 14), as well as critical infrastructure exposure (Figure 15), and population displaced, which is a subset of population exposed constrained by a higher minimum flood water depth (Figure 16).

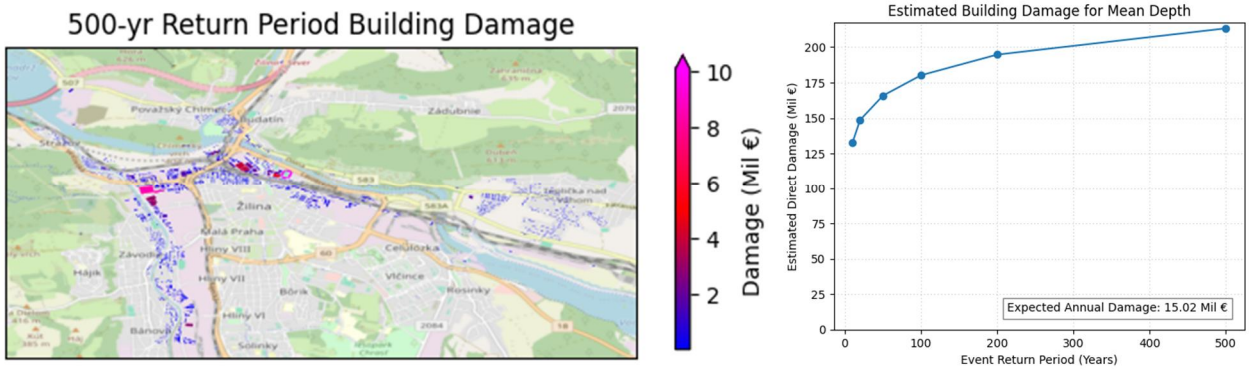

Figure 13. Example outputs, building damage map (left), and building damage graph (right).

Funded by the European Union

This project has received funding from the European Union's Horizon Europe research and innovation programme under grant agreement No 101093864. Views and opinions expressed are however those of the author(s) only and do not necessarily reflect those of the European Union or the European Climate, Infrastructure and Environment Executive Agency (CINEA). Neither the European Union nor the granting authority can be held responsible for them.

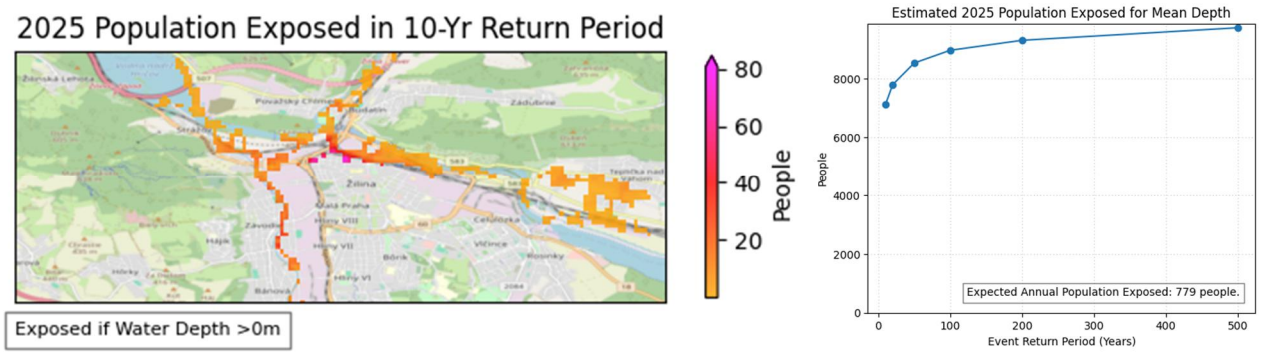

Figure 14. Example outputs, population exposed map (left), and population exposed graph (right).

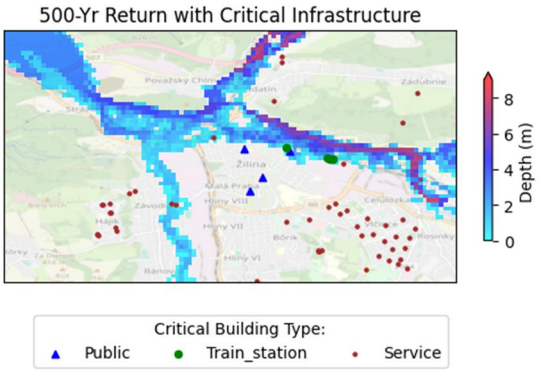

Figure 15. Example output for critical infrastructure exposed to a 500-year return period.

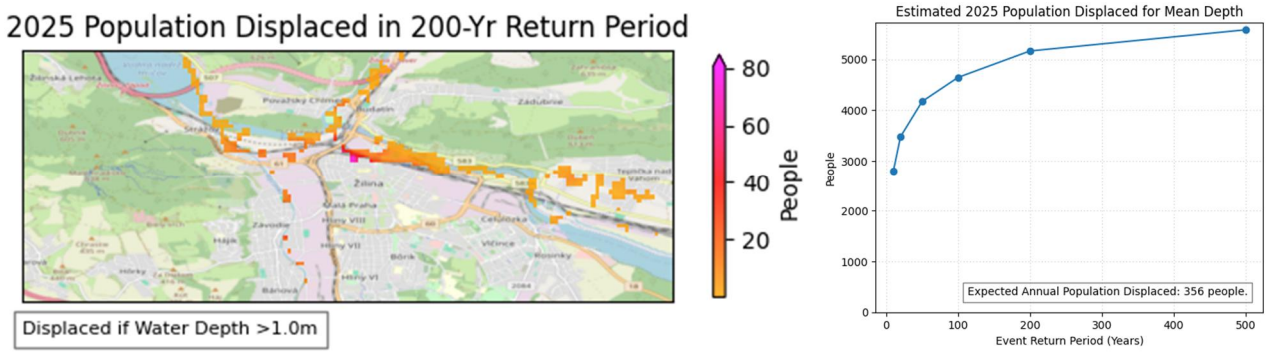

Figure 16. Example outputs, population displaced map (left), population displaced graph (right).

4.1.3 Coastal flood

Risk method

This workflow estimates the potential impacts of coastal flooding caused by extreme sea water levels. The flood risk is calculated by combining maps of potential coastal flood extent with exposure and vulnerability data in the form of economic damage functions for infrastructure. Similarly to the risk workflow for river flooding, flood damage is expressed in economic terms and is calculated by applying damage curves to the coastal flood inundation depth maps. The flood damage is mapped by combining flood depth maps, land use maps, damage curves, and information on the approximate economic value of different land use types. This method does not account for

Funded by the European Union

This project has received funding from the European Union's Horizon Europe research and innovation programme under grant agreement No 101093864. Views and opinions expressed are however those of the author(s) only and do not necessarily reflect those of the European Union or the European Climate, Infrastructure and Environment Executive Agency (CINEA). Neither the European Union nor the granting authority can be held responsible for them.

coastal flood defences that might be in place but maps out damages in the absence of coastal defences.

In addition to the risk assessment based on flood maps, this workflow includes guidance on retrieving extreme water levels and the expected sea level rise in future scenarios for the area of interest to estimate the increase in water levels in the future.

Hazard data

Coastal flooding is caused by extreme coastal water levels, elevated during sea storms (storm surges). Under climate change, the coastal water levels are expected to further increase with sea level rise.

In this workflow we make use of two different types of hazard data:

- Coastal water level statistics. These are derived from the global dataset of tides and surges by Muis et al. (2020) and provide information on the coastal water level extremes. To account for the effect of climate change, also the relative sea level rise is considered based on the IPCC AR6 dataset available through the NASA Sea Level Projection Tool[8].

- Coastal flooding inundation maps. In this workflow, we use the dataset of Global Flood Maps (see Figure 17) openly available via the Microsoft Planetary Computer[9]. This dataset is based on a bathtub inundation model (the model includes flood attenuation and roughness), a global digital elevation dataset (MERIT) and coastal water levels from Muis et al. (2020).

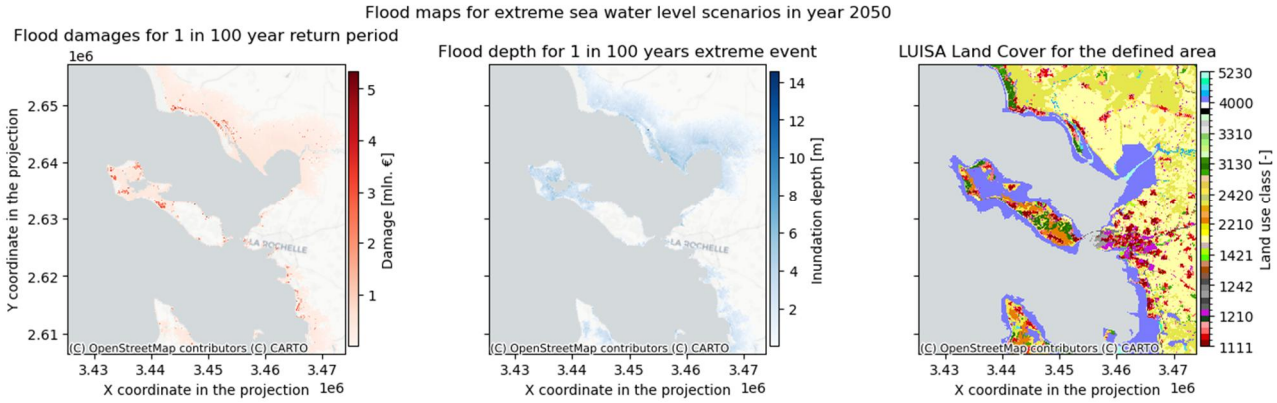

Figure 17. Estimated flood damage map, flood hazard map (middle), and LUISA land cover (right) for the area of La Rochelle, France.

In the damage calculations for the risk assessment only the Global Flood Maps map dataset is used. Flood maps are available for extreme sea storms with different statistical occurrence (e.g. once in 5 years, once in 100 years etc). The dataset has a relatively high spatial resolution of 3 arc-seconds (30-75 m in Europe depending on the latitude) which enables a more detailed calculation of damages. In this dataset, global flood maps are available for two scenarios: present-day climate (ca.

[8] https://sealevel.nasa.gov/ipcc-ar6-sea-level-projection-tool

[9] https://planetarycomputer.microsoft.com/dataset/deltares-floods

Funded by the European Union

This project has received funding from the European Union's Horizon Europe research and innovation programme under grant agreement No 101093864. Views and opinions expressed are however those of the author(s) only and do not necessarily reflect those of the European Union or the European Climate, Infrastructure and Environment Executive Agency (CINEA). Neither the European Union nor the granting authority can be held responsible for them.

2018) and the year 2050 under RCP8.5 climate scenario. The difference between the two scenarios is mainly in the sea level rise values (this dataset does not account for changes to storm surge heights as a consequence of climate change). Although only one scenario for the future climate is available, this is most likely sufficient for an assessment up to 2050, because the difference in projected sea level rise in different scenarios up to 2050 is minor (up to several centimeters).

However, it is important to note that the global flood map dataset carries significant uncertainty especially because it does not fully account for flood defences (it only accounts for the larger-scale topography). It is important to assess the suitability of this dataset against local knowledge and use alternative (more accurate) local flood maps if possible.

Exposure and vulnerability data

The LUISA dataset (see Figure 17) and damage curves that were used in the river flood risk workflow are also used in the coastal flood workflow to assess exposure and vulnerability to coastal flooding.

Risk visualization

The resulting data and maps from this risk workflow will help the identification of potential hotspots of economic damage due to coastal flooding for different return periods of extreme sea levels. For each climate, present-day climate (ca. 2018) and 2050 (RCP8.5 scenario), different return periods of the extreme conditions are considered. The outputs of this workflow are:

- Flood depth and extent maps for the area of interest.
- Flood damage maps, expressed in economic value, per scenario and return period (example in Figure 16).

4.2 Extreme precipitation

Risk method

The extreme precipitation workflow has been constructed to guide users, communities, and regions in understanding how their current critical impact-based rainfall thresholds will be affected by climate change for specific locations or entire regions. Thus, risk is assessed as a function of precipitation intensity, associated with a critical impact-based rainfall threshold, and its potential magnitude and frequency variations due to climate change. It is worth noting that this workflow does not account for the rainfall-runoff transformation and flood propagation in the flood prone area like the flood workflows in section 4.1.

In this workflow, a critical impact rainfall threshold is defined as the precipitation necessary to trigger unsustainable or unacceptable impacts. However, this concept is closely related to the “risk-tolerance level” that can vary by region. For this reason, the risk workflow description in the CLIMAAX toolbox includes a detailed description of how to identify critical impact-based threshold based on the local case.

By combining the information from precipitation intensity (magnitude and duration), return period (frequency) and local vulnerability, it is possible to develop impact-based rainfall thresholds leading to extreme precipitation risk. These thresholds are defined as the precipitation required within a specific timeframe to trigger various tolerable or unacceptable impacts, such as urban flooding in

Funded by the European Union

This project has received funding from the European Union's Horizon Europe research and innovation programme under grant agreement No 101093864. Views and opinions expressed are however those of the author(s) only and do not necessarily reflect those of the European Union or the European Climate, Infrastructure and Environment Executive Agency (CINEA). Neither the European Union nor the granting authority can be held responsible for them.

vulnerable areas or sites (e.g., low-lying). Such rainfall thresholds are commonly used in the design of civil works like road drainage systems, flood protection infrastructure and serve as decision support values for early warning systems helping link local potential risk and their consequences to specific rainfall intensity values (Meléndez-Landaverde & Sempere-Torres, 2022). As identifying the current local critical impact-based rainfall thresholds is indispensable for using the extreme precipitation workflow, a step-by-step guide on developing and identifying these is included in the workflow.

Hazard data

EURO-CORDEX climate projections for precipitation flux at a 12km spatial resolution have been employed for hazard assessment. As an example within the workflow, the 30-years timeframes 1976-2005 and 2041-2070 periods are used to represent historical simulations and future climate projections, respectively. As a first step, the temporal series of annual maximum precipitation from the EURO-CORDEX dataset based on a single combination of global climate model (GCM, ICHEC EC EARTH), regional climate models (RCM, RACMO22E by KNMI), and RCP (8.5) are extracted. Then, a probability distribution function is defined to fit the annual maximum precipitation series. In this risk workflow, we used a General Extreme Value (GEV) distribution. After that, the expected intensities for each duration (3, 6 and 12 hours based on non-biased corrected EURO-CORDEX datasets) and defined return periods (2, 5, 10, 25, 50, 100, 200 and 500) are calculated. Once the expected precipitation for two different 30-year periods is calculated, the precipitation changes (%) relative to a defined period (either historical or future projection) can be visualised. This will allow the user to identify a possible positive or negative precipitation change in the region relative to a climate baseline simulation. As an example, within the CLIMAAX toolbox we have calculated the expected intensity and changes in precipitation for specific durations, return periods, GCM and RCM model pairs, and RPCs at the European scale.

It is worth noting that the hazard data are assessed for a single GCM, RCM, RCP, and timeframes period (30 years in this example) combination. However, the user can select a different combination and follow the same steps previously described. However, as the EURO-CORDEX datasets are downloaded for all Europe the hazard assessment may take some hours to be carried out.

Exposure and vulnerability data

Critical thresholds include exposure and vulnerability as closely related to the “risk-tolerance level”, defined as the maximum amount of loss, impact, or frequency that areas, communities, and regions are prepared to handle due to extreme precipitation. Consequently, these naturally vary across communities and sectors (e.g., transportation or agriculture) as risk is not absolute but a social construct that depends on the local context, the coping capacity, and risk perception. Local knowledge of users and local stakeholders, authorities, and responders can support assessing the acceptable levels of risk for the community and provide vulnerability details on local vulnerabilities.

Risk visualization

The objective of the extreme precipitation is to explore how the current critical impact-based rainfall thresholds will vary in terms of frequency and magnitude. Therefore, the output is conditioned to the two types of risk analysis presented in this workflow, for a specific location within an area of interest

Funded by the European Union

This project has received funding from the European Union's Horizon Europe research and innovation programme under grant agreement No 101093864. Views and opinions expressed are however those of the author(s) only and do not necessarily reflect those of the European Union or the European Climate, Infrastructure and Environment Executive Agency (CINEA). Neither the European Union nor the granting authority can be held responsible for them.

(site-specific risk assessment) or an entire analysis area (regional risk assessment). For a specific site, the changes in magnitude (%) and return period values (frequency) can be directly printed. Change in return period represents the new frequency compared to the current magnitude. Figure 18.a shows the new return period (or frequency) of 100 mm/24 hours in 2070. On the other hand, change in magnitude represents the relative percent change between the current magnitude (baseline) and a year within the climate projections (e.g., 2070) if the current frequency remains fixed. Figure 18.b, shows the magnitude shift for 100mm/24h threshold with fixed frequency in 2041-2070.

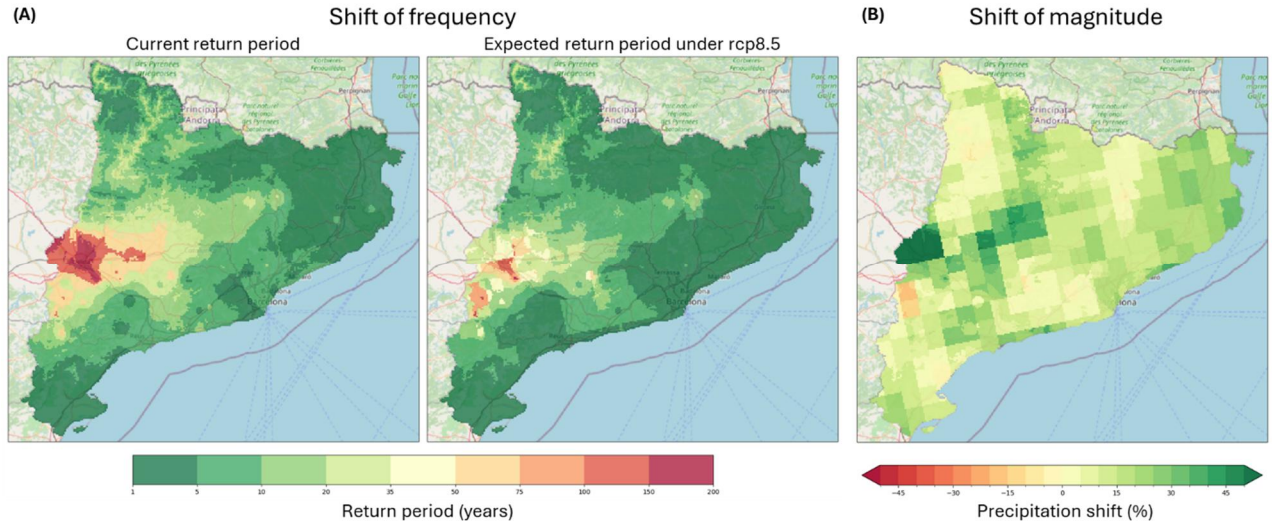

Figure 18. Shifts of frequency (A) and magnitude (B) for 100mm/24h threshold defined by the Catalonia Meteorological Service for low risk

By clearly defining impact and critical rainfall thresholds based on their tolerance levels, communities and sectors can proactively develop metrics for CRA, design appropriate adaptation measures, enhance their overall resilience, and understand how impacts can vary under the influence of climate change scenarios.

4.3 Drought

Drought can be defined as a prolonged period of abnormally low rainfall, leading to a shortage of water over a specific region for a given period. Droughts are characterized by a deficit between water supply and demand, and can have important consequences for society, ecosystems, and agriculture. Understanding the different types of droughts and their complex dynamics is essential for implementing sustainable mitigation and adaptation strategies. Droughts are often classified into four main types different by their severity, impacts, and time scales:

Meteorological drought: Often caused by short-term or prolonged precipitation deficiency. Climate variability, including phenomena such as El Niño and La Niña, can influence meteorological droughts. Impacts of meteorological droughts highly depend on timing and seasonality.

Funded by the European Union

This project has received funding from the European Union's Horizon Europe research and innovation programme under grant agreement No 101093864. Views and opinions expressed are however those of the author(s) only and do not necessarily reflect those of the European Union or the European Climate, Infrastructure and Environment Executive Agency (CINEA). Neither the European Union nor the granting authority can be held responsible for them.

Agricultural drought: A medium-term phenomenon, characterized by reduced soil moisture content and is caused by a prolonged period of meteorological drought. The lack of soil moisture can have a significant impact on crop growth.

Hydrological drought: Characterized by lower streamflow, reduced water level in water bodies, and may also affect groundwater storage.

Socioeconomic drought: encompasses the broader impacts of water scarcity on society

In the CLIMAAX toolbox we mainly focus on meteorological and agricultural drought.

4.3.1 Drought risk

Risk method

A number of approaches have been proposed in the last years for assessing drought risk, and its components (Hagenlocher et al., 2019). Here, we follow the framework proposed by Carrão et al. (2016) to reproduce drought risk maps at NUTS2 spatial resolution for both historical and future projections. Risk is assessed as the product between the hazards, exposure, and vulnerability indicators. This is done by normalizing regional risk values against the minimum and maximum values at European level or among a selection of regions to obtain a normalized.

Hazard data

Drought hazard for a given region is estimated as the probability of exceedance the median of regional (e.g., EU level) severe precipitation deficits for a historical reference period (e.g. 1979-2019) or for a future projection period (e.g. 2015-2100). The GSWP3 and W5E5 global meteorological forcing data processed for ISIMIP3a, sets on a 0.5°x0.5°C global grid and at daily time steps are used for the historical period of 1979-2019. For the future projections, we used the ISIMIP3b bias-adjusted atmospheric climate input data, available for 5 CMIP6 global climate models (GFDL-ESM4, IPSL-CM6A-LR, MPI-ESM1-2-HR, MRI-ESM2-0, UKESM1-0-LL), and three SSP-RCPs combinations (SSP126, SSP370, SSP585). Based on this precipitation data we calculated the Weighted Anomaly of the Standardized Precipitation (WASP) index to define the severity of precipitation deficit as proxy of drought hazard. The WASP-index considers the annual seasonality of the precipitation cycle and is computed by summing weighted standardized monthly precipitation anomalies.

Exposure and vulnerability data

Drought exposure is assessed by quantifying the relative exposure of a region from a multidimensional set of indicators. This approach uses a non-compensatory model to account for the spatial distribution of a potential impact for crops and livestock, competition on water (e.g., for industrial uses represented by the water stress indicator), and human direct need (e.g., for drinking purposes). The different indicators of drought exposure used in this workflow are:

- Historical harvested land represents the exposure of agricultural activity to drought[10]
- Cropland landcover under different Shared Socio Economic Pathways (SSPs) (Zhang et al., 2023)

[10] https://mapspam.info/

Funded by the European Union

This project has received funding from the European Union's Horizon Europe research and innovation programme under grant agreement No 101093864. Views and opinions expressed are however those of the author(s) only and do not necessarily reflect those of the European Union or the European Climate, Infrastructure and Environment Executive Agency (CINEA). Neither the European Union nor the granting authority can be held responsible for them.

- Historical livestock density[11]
- Historical and future water stress indicator as proxy for competition on water[12].
- Historical and future population counts[13]

The selection of the proxy indicators for drought vulnerability follows the criteria defined by Naumann et al. (2014). Vulnerability to drought combines aggregated proxy indicators representing the economic, social, and infrastructural factors of social vulnerability at each geographic location. First, indicators for each factor are combined using the same approach as for drought exposure. In the second step, individual factors are arithmetically aggregated (using the simple mean) into a composite model of drought vulnerability. Vulnerability indicators used in this workflow can be classified as:

- Historical and future Gross domestic product per capita (Wang & Sun, 2022)
- Historical and future population counts living in rural areas.

Risk visualization

The main output from this workflow are maps of the relative drought hazard and drought risk of European NUTS3 regions within a selected country and a focal NUTS2 area. Drought risk maps refer to both historical conditions and future scenarios.

Moreover, the changes in drought hazard and relative drought risk between different NUTS3 regions can be compared between different scenarios and timeframes. In fact, the relative drought risk in each NUTS3 under different scenario can be benchmarked against the risk of neighbouring areas.

The pre-processed data at European NUTS3 level is available for the following scenarios:

- Historical (1979-2019)
- SSP1-RCP2.6 near future (2015-2050)
- SSP1-RCP2.6 far future (2050-2100)
- SSP3-RCP7.0 near future (2015-2050)
- SSP3-RCP2.0 far future (2050-2100)

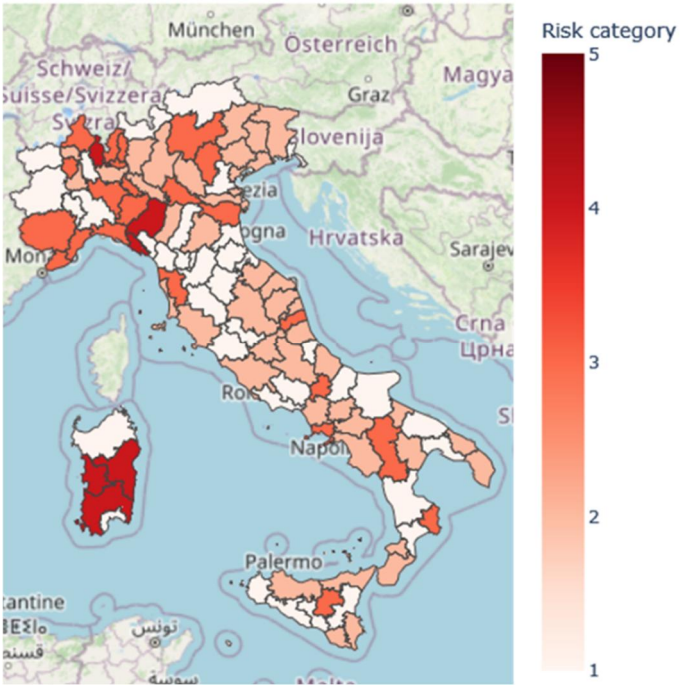

Figure 19. Example of current drought risk in Italy

SSP5-RCP8.5 near future (2015-2050)

- SSP5-RCP8.5 far future (2050-2100)

[11] https://www.fao.org/livestock-systems/global-distributions/en/

[12] https://www.wri.org/data/aqueduct-global-maps-40-data

[13] https://ec.europa.eu/eurostat/

Funded by the European Union

This project has received funding from the European Union's Horizon Europe research and innovation programme under grant agreement No 101093864. Views and opinions expressed are however those of the author(s) only and do not necessarily reflect those of the European Union or the European Climate, Infrastructure and Environment Executive Agency (CINEA). Neither the European Union nor the granting authority can be held responsible for them.

4.3.2 Agricultural drought damage

Risk method

This risk workflow provides a simple tool to quantify potential revenue crop yields losses caused by precipitation deficit, i.e. meteorological drought. The hazard component of the assessment is represented by the potential yield losses deriving from water scarcity, defined as the deficit in crop evapotranspiration potential, in the absence of irrigation. The total crop production and the aggregated crops revenue are used to quantify the exposure of the agricultural sector in economic terms. Finally, the current distribution of irrigation systems is used to map vulnerability. Risk is then assessed as the product between the yield loss and the revenue per grid-cell. Thus, using this tool communities will get a spatial quantification of potential revenue losses from reduced crop production (see Figure 20), and will also be able to identify the most vulnerable areas to precipitation deficits.

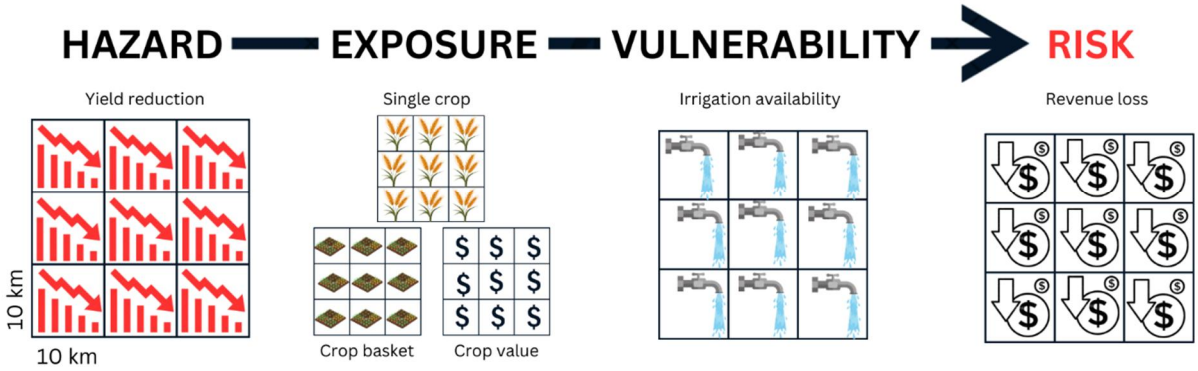

Figure 20. Schematization of the method used to calculate agricultural drought risk.

Hazard data

Hazard is calculated as the potential loss in yield for a given crop in the absence of an artificial irrigation system compensating for precipitation scarcity. This is particularly relevant for semi-arid regions which are increasingly prone to prolonged drought periods making artificial irrigation unfeasible. At the same time, the workflow is a valuable tool for historically wet regions that have not yet invested in large-scale irrigation systems but might experience significant reductions in precipitation rates with climate change. The first step for the hazard assessment is the calculation of the soil standard evapotranspiration (ET0) using the Penman-Monteith equation described by FAO (Allen et al., 1998), representing the climate-driven evapotranspiration demand for a given crop. ET0 is calculated combining daily rainfall intensity, relative humidity, wind speed, surface downward solar radiation, maximum and minimum air temperature data extracted from one combination of global and regional climate models from EURO-CORDEX for the historical period, as well as the RCP2.6, RCP4.5 and RCP8.5 global warming scenarios. The default model combination is MPI-M-MPI-ESM-LR (global) and SMHI-RCA4 (regional), but to compare the results the workflow indicates the other four combinations of global and regional climate model allowing to download all the necessary climate variables for all the future scenarios. The standard evapotranspiration is then

Funded by the European Union

This project has received funding from the European Union's Horizon Europe research and innovation programme under grant agreement No 101093864. Views and opinions expressed are however those of the author(s) only and do not necessarily reflect those of the European Union or the European Climate, Infrastructure and Environment Executive Agency (CINEA). Neither the European Union nor the granting authority can be held responsible for them.

combined with a series of crop-specific information condensed in a crop coefficient (Kc; Chapagain & Hoekstra, 2004) to derive the crop standard evapotranspiration (ETc), representing the maximum evapotranspiration potential for a given crop. From ETc, it is possible to derive the actual crop evapotranspiration (ETa) using precipitation data to estimate the local water availability for the plant. Finally, using the equations from the FAO I&D 33 paper (Doorenbos & Kassam, 1979), is then possible to relate the ratio between the rainfed and the maximum evapotranspiration potential to the crop yield loss (%) in rainfed-only conditions. The hazard assessment can currently be performed for the 14 crops parameterised in the crop table.

Exposure and vulnerability data

Drought exposure is assessed using two different datasets. First, we used the crop production [ton] for 42 crops in 2010 from the MapSPAM repository (International Food Policy Research Institute, 2019). Data is available as global .tif rasters at 5 arc-min resolution for different combinations of human inputs and irrigation mode. Second, we used the crop aggregated value [US$] and irrigation availability for 2010 from the FAO-IIASA Global Agro-Ecological Zones data repository (GAEZ). Data is available as global .tif rasters at 11 km resolution showing the aggregated crops value in 2010 international dollars (GK$), having the same purchasing power of US dollars (USD). On the other hand, vulnerability is expressed as cropland full-irrigation availability. This information is also sourced from GAEZ and is available at the same resolution as the aggregated value data. The dataset shows the percentage of cropland in each grid-cell equipped with full-irrigation systems.

Risk visualization

The tool is designed to work considering different future time periods and emission scenarios, allowing the user to understand the implications of different levels of global warming. The main outcome of this workflow is a map of the reduced revenue (Euro/grid-cell) due to absence of irrigation and precipitation deficit (Figure 21).

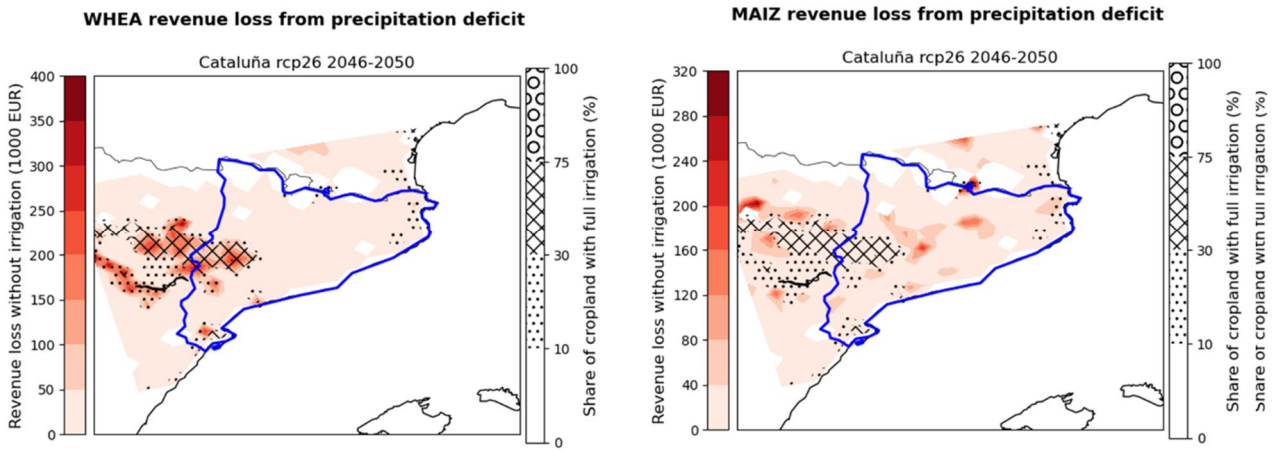

Figure 21. Revenue loss without irrigation for wheat (left) and maize (right)

Funded by the European Union

This project has received funding from the European Union's Horizon Europe research and innovation programme under grant agreement No 101093864. Views and opinions expressed are however those of the author(s) only and do not necessarily reflect those of the European Union or the European Climate, Infrastructure and Environment Executive Agency (CINEA). Neither the European Union nor the granting authority can be held responsible for them.

4.3.3 Drought population exposure

Risk method

This workflow assesses drought risk as combination of hazard and exposure data, by overlaying the drought hazard data, expressed through Combined Drought Indicator (Sepulcre-Canto et al., 2012), and population data.

Hazard data

The Combined Drought Indicator (CDI) that is implemented in the European Drought Observatory (EDO) is used to identify areas affected by agricultural drought, and areas with the potential to be affected. In the current version of the toolbox we use the CDI provided by Copernicus. CDI can be downloaded from the Copernicus server[14] and is derived by combining three drought indicators produced operationally in the EDO framework - namely the:

S*tandardized Precipitation Index (SPI):* The SPI indicator measures precipitation anomalies at a given location, based on a comparison of observed total precipitation amounts for an accumulation period of interest (e.g. 1, 3, 12, 48 months), with the long-term historic rainfall record for that period (Edwards & McKee, 1997; McKee et al., n.d.).

Soil Moisture Anomaly (SMA): The SMA indicator is derived from anomalies of estimated daily soil moisture (or soil water) content - represented as Standardized Soil Moisture Index (SMI) - which is produced by the JRC's LISFLOOD hydrological model, and which has been shown to be effective for drought detection purposes (Laguardia & Niemeyer, 2008).

FAPAR Anomaly: The FAPAR Anomaly indicator is computed as deviations of the biophysical variable Fraction of Absorbed Photosynthetically Active Radiation (FAPAR), composited for 10- day intervals, from long-term mean values. Satellite-measured FAPAR represents the fraction of incident solar radiation that is absorbed by land vegetation for photosynthesis and is effective for detecting and assessing drought impacts on vegetation canopies (Gobron et al., 2005).

It is worth noting that this risk workflow, and in particular the CDI dataset, does not consider future scenarios of climate change. However, the use of the CDI provides a number of advantages, despite future scenarios are not included. For of all, the CDI's classification scheme includes several warning levels (Watch, Warning, and Alert), which can help policymakers and stakeholders in developing more informed drought management and mitigation plans. Moreover, providing forecasted CDI information up to 3 months, this dataset helps in proactive drought management by early intervention and planning, identifying areas that could be potentially affected by drought.

Exposure and vulnerability data

Exposure is assessed by overlaying the European population density map at 30 arcsec resolution using the Global Human Settlement Population dataset (Pesaresi et al., 2013).

[14] https://drought.emergency.copernicus.eu/tumbo/gdo/map/?id=2112

Funded by the European Union

This project has received funding from the European Union's Horizon Europe research and innovation programme under grant agreement No 101093864. Views and opinions expressed are however those of the author(s) only and do not necessarily reflect those of the European Union or the European Climate, Infrastructure and Environment Executive Agency (CINEA). Neither the European Union nor the granting authority can be held responsible for them.

Risk visualization

The main outcome of this workflow is a map overlapping the number of affected populations with CDI (Figure 22). In particular, areas are classified according to three primary CDI drought classes as:

- Watch: Precipitation is less than normal. SPI-3 <-1 or SPI-1 < -2
- Warning: - indicating that soil moisture is in deficit. SMA <-1 and (SPI-3 < -1 or SPI-1 < -2)
- Alert: Vegetation shows signs of stress. DFAPAR < -1 and (SPI-3 < -1 or SPI-1 < -2)

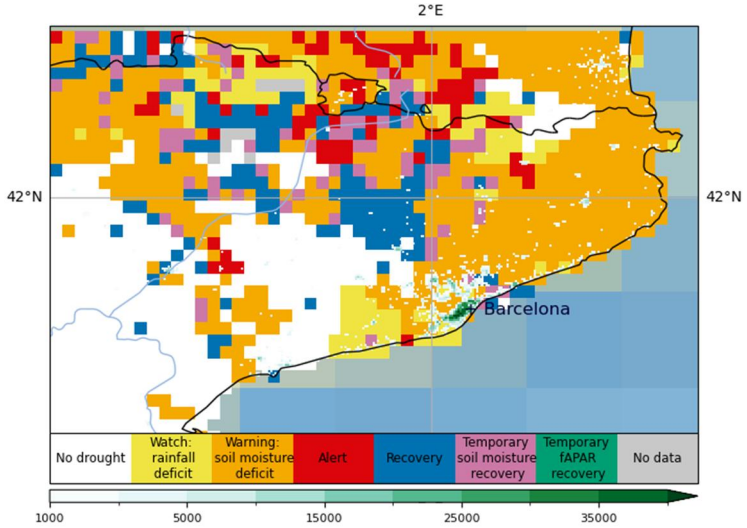

Figure 22. Combined Drought indicator and population number in the Catalonia pilot

4.4 Heatwave

Risk method

Multiple methodologies can be used to define a heatwave. But in general, a heatwave is determined using thresholds for air temperature and its persistency (duration in the number of days). The most common definition of a heatwave is the occurrence of multiple consecutive days with the maximum air temperature over a certain threshold. In some methodologies thresholds are also defined for the minimum air temperature.

The heatwave workflow focuses on estimating the frequency of heatwave events for the present and the future climate based on the EURO-CORDEX climate scenarios data. The workflow aids the user in understanding the effect of climate change on the occurrence of heatwaves under different climate change scenarios (RCPs) within a user-defined region in Europe. This data is obtained for different temporal resolutions (months or years). Changes to heatwave duration (total number of days) are also analysed.

The risk to the vulnerable population due to heat can be analysed using the land surface temperature (heat exposed areas) data in combination with the information on the distribution of the vulnerable population groups (distribution of vulnerable population). In this workflow we demonstrate such analysis using high-resolution satellite-derived (measured) data of land surface temperature. The exposure and vulnerability data are classified in 5 classes and then combined using the risk matrix

Funded by the European Union

This project has received funding from the European Union's Horizon Europe research and innovation programme under grant agreement No 101093864. Views and opinions expressed are however those of the author(s) only and do not necessarily reflect those of the European Union or the European Climate, Infrastructure and Environment Executive Agency (CINEA). Neither the European Union nor the granting authority can be held responsible for them.

reported in Table 2. Vulnerable population data are classified to 5 equal interval classes, and heat exposed areas are classified based on the temperature.

Hazard data cannot be included in the risk matrix due coarse resolution. However, based on the hazard data of the heatwave occurrence in the future you will get the information if the heatwave risk will be more severe in the future for your selected area.

Hazard data

In this workflow, the user can assess heatwave hazard following the EuroHeat, PESETA IV and Xclim projects methodology. Because of the different requirements for the heatwave definitions from the CLIMAAX pilot regions we needed to implement multiple methodologies for the heatwave estimation. The pilots have different requirements for the maximum temperature thresholds, usage of minimal temperature, threshold for time duration etc. The heatwave estimation is defined based on the 3 methodologies (Euro Heat, Peseta IV and XCLIM). Each of these methodologies uses different criteria for the heat wave estimation.

- The Euro Heat defined the heatwave as a period ≥ 2 consecutive days in which the maximum temperature is above the daily threshold calculated for a 30-year-long reference period. The threshold is defined as a period where the maximum and the minimum daily temperature are over the 90th percentile of the monthly distribution for at least two days.
- The PesetaIV methodology defines a heatwave as a period of ≥ 3 consecutive days in which the maximum temperature is above the daily threshold calculated for a 30-year-long reference period. The threshold is defined as the 90th percentile of daily maximum temperature, centred on a 31-day window. The user has also the possibility of the changing the threshold for the consecutive days and maximum temperature.
- The XCLIM methodology defined the heatwave based on the temperature (in degree Celsius) and consecutive day thresholds which needs to be assessed specifically for each region by the local health authorities or used ones recommended in the toolbox.

For the heatwave risk assessment of this workflow, the Landsat8 Land surface temperature (LST) for the summer months of June, July, and August is used as a proxy of heatwave hazard for overheated areas. Once LST is either calculated within the CLIMAAX toolbox (e.g. by using Landsat 8 imagery) or downloaded from the RSlab webportal for years 2013-2021 # https://rslab.gr/Landsat_LST.html, it is then possible to calculate the highest temperature value for each pixel. The resulting raster is finally reclassified into 5 classes of temperature, i.e. from the low hazard value (T<20 degree Celsius) to the highest value (T>50 degree Celsius), see Table 3 and Figure 23. Landsat 8 land surface temperature data can be used to assess the 5 temperature classes.

Exposure and vulnerability data

Density of vulnerable population groups (people over 65 years, and under 5 years old from local data) is used as proxy of heatwave vulnerability. Below, we apply the risk workflow to the CLIMAAX Zilina pilot. The local data for densely populated (or sensitive) places can be used to enhance the spatial accuracy and identification of the most vulnerable places. However, these data need to be prepared by the local authorities (following the recommendations from the heatwave toolbox).

Funded by the European Union

This project has received funding from the European Union's Horizon Europe research and innovation programme under grant agreement No 101093864. Views and opinions expressed are however those of the author(s) only and do not necessarily reflect those of the European Union or the European Climate, Infrastructure and Environment Executive Agency (CINEA). Neither the European Union nor the granting authority can be held responsible for them.

Table 3. Risk matrix for the heatwave workflow with vulnerable population classified into 5 equal groups

Exposure	Vulnerability				
	Class 1	Class 2	Class 3	Class 4	Class 5
Class 5: (T>50C)	5	10	15	20	25
Class 4: (40C<T<50C)	4	8	12	16	20
Class 3: (30C<T<40C)	3	6	9	12	15
Class 2: (20C<T<30C)	2	4	6	8	10
Class 1: (T<20C)	1	2	3	4	5

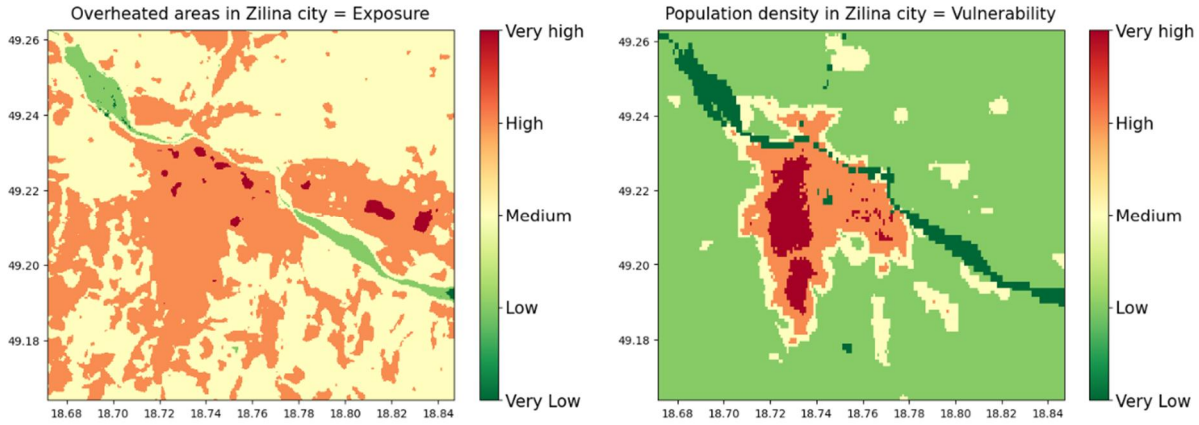

Figure 23. Heatwave exposure (left) and vulnerability (right) maps

Risk visualization

Once assessed, the heatwave risk map is calculated by multiplying the exposure and vulnerability classes and we get a layer with values from 1 to 25. This information is finally visualized in a map as displayed in Figure 24 for historical temperature observations.

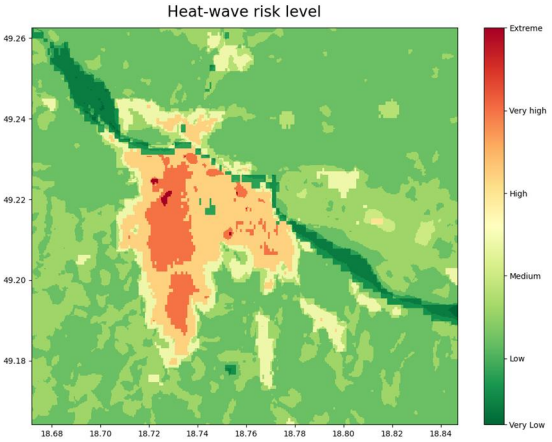

Figure 24. Heatwave risk map for the Zilina CLIMAAX pilot

The same workflow could be used for future temperature data from EURO-CORDEX instead of land surface temperature data (but due to coarse resolution it has limitations, can be used only for whole regions not cities). Based on the risk interpretation map (above), we can identify the places more prone to experience heatwaves (dark red). The same risk workflow can be applied to critical infrastructure rather than vulnerable people. This will provide information on which areas should be prioritized, in case of adaptation or which buildings or squares etc. are most exposed to heatwave.

Funded by the European Union

This project has received funding from the European Union's Horizon Europe research and innovation programme under grant agreement No 101093864. Views and opinions expressed are however those of the author(s) only and do not necessarily reflect those of the European Union or the European Climate, Infrastructure and Environment Executive Agency (CINEA). Neither the European Union nor the granting authority can be held responsible for them.

4.5 Wildfire

4.5.1 Wildfire risk

Risk method

This workflow follows a risk index method approach. Risk estimates are available for both present and future scenarios under two RCPs, namely RCP4.5 and RCP8.5. In the following example, the Catalonia region is used as a reference test area. However, the work can be easily extended to other regions.

Hazard data

The Hazard component is determined using an empirical approach, as described by (Tonini et al., 2020; Trucchia et al., 2022, 2023) which employs a Machine Learning (ML) algorithm. It is important to mention that his workflow also includes the step of building from scratch the likelihood (susceptibility) map, instead of downloading existing products. The susceptibility map represents the propensity of an area to experience fire in the near future provided that climate conditions and land use do not change drastically. This map is generated by a trained ML model, which crosses past fire history and geophysical- climate descriptors. As an assumption, all the descriptors except climate are fixed in time. Changing the climate inputs to the trained ML model can generate different maps which represent different climate scenarios for wildfire susceptibility.

This algorithm utilises topographic data (DEM, Aspect, Slope), land cover information (in this case, Corine land cover is used; Büttner, 2014), historical climate data, and past fire polygons (that can be provided by EFFIS and /or national databases). Regarding climate dataset, the dataset of ECLIPS-2.0, leveraging on a downscaling of EURO-CORDEX, is used as default choice (Chakraborty et al., 2021). This dataset, with a resolution of 30 arcsec, provides to the model 14 variables chosen from the total of 80 available climate variables[15] The trained model was utilised to generate hazard maps for three distinct time periods: the present, the upcoming (2021-2040) and the forthcoming (2041-2060) under two mentioned RCPs. Figure 25 depicts changes present and future hazard maps under the RCP4.5 pathway.

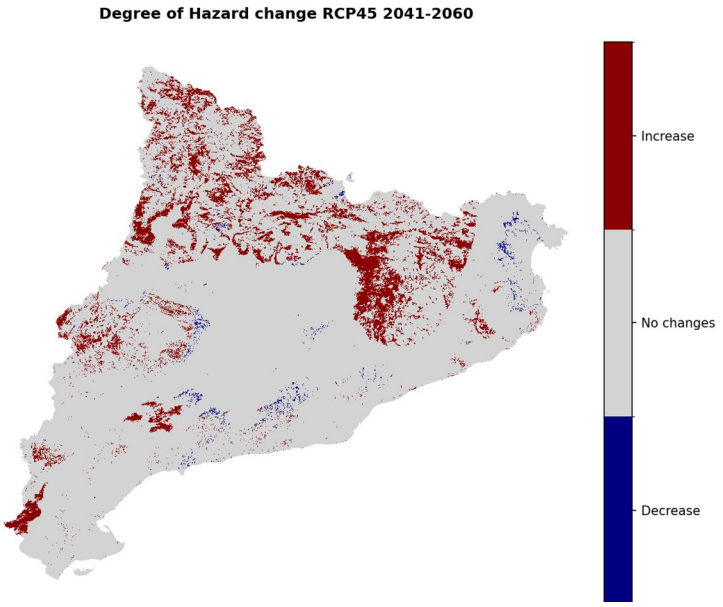

Figure 25. Location with increment-decrement of hazard level in 2041-2060, under RCP45, with respect to present conditions

[15] https://doi.org/10.5281/zenodo.3952159

Funded by the European Union

This project has received funding from the European Union's Horizon Europe research and innovation programme under grant agreement No 101093864. Views and opinions expressed are however those of the author(s) only and do not necessarily reflect those of the European Union or the European Climate, Infrastructure and Environment Executive Agency (CINEA). Neither the European Union nor the granting authority can be held responsible for them.

Exposure and vulnerability data

In this workflow, two categories of exposure and vulnerability are utilised as components of the risk equation. Firstly, a road exposure map sourced from OSM categorises roads into primary, secondary, and tertiary classifications, representing varying levels of vulnerability to potential wildfires. This classification is based on the proximity of roads to wildland areas outside of urban centres, with higher vulnerability attributed to roads closer to such areas.

Additionally, another set of vulnerability maps is derived from the JRC database, encompassing population, ecological, and economic vulnerability. These maps, featuring percentile values, are classified based on predefined thresholds (JRC, 2020) to facilitate their utilisation in the Risk contingency matrix (Figure 26).

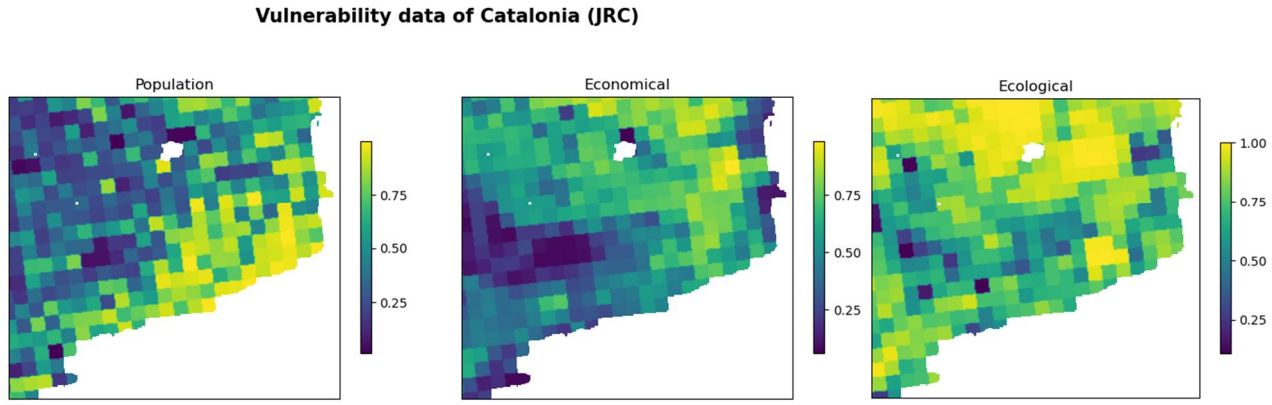

Figure 26. Vulnerability data (Population, Economical, Ecological) from JRC.

Risk visualisation

Four categories of risk maps were generated, encompassing Road, Population, Ecological and Economic risks, for the aforementioned periods.

It's important to note that these risk maps can be aggregated at the NUTS2 level, enhancing user-friendliness and visual clarity for planning purposes such as mitigation strategies and funding allocation in the future. Notably, this framework is adaptable and can be applied to any pilot area within the EU domain, requiring inputs such as DEM, land cover data, fire data (either local data or from large scale databases such as the European Forest Fire Information System[16]), and administrative boundaries (NUTS). In most of the times, when local sources are not available, past fire data can be retrieved from open sources such as the EFFIS dataset.

Figure 27 shows the available risk maps based on this workflow (20 different risk maps). The scheme of output of this workflow is shown in the following table for different scenarios and periods.

[16] https://forest-fire.emergency.copernicus.eu/

Funded by the European Union

This project has received funding from the European Union's Horizon Europe research and innovation programme under grant agreement No 101093864. Views and opinions expressed are however those of the author(s) only and do not necessarily reflect those of the European Union or the European Climate, Infrastructure and Environment Executive Agency (CINEA). Neither the European Union nor the granting authority can be held responsible for them.

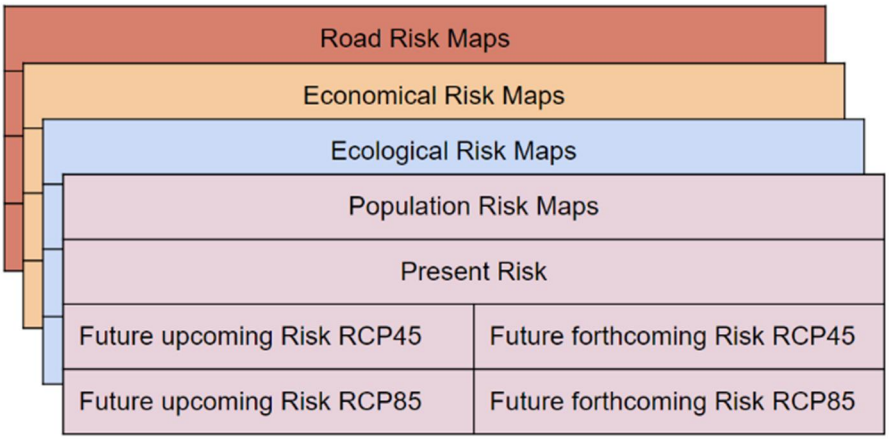

Figure 27. Scheme of all available Risk maps in the present version of the workflow.

4.5.2 Wildfire population exposure

Risk method

This workflow assesses wildfire risk as combination of hazard and exposure data, by overlaying the wildfire hazard data, expressed through the Fire Weather Index (FWI)[17], and population data.

Hazard data

The hazard data is based on the Fire danger indicators for Europe available in the Copernicus Climate Change Service. This dataset provides comprehensive projections of fire danger across Europe based on the Canadian FWI System and is designed to help assess future fire danger conditions under various climate scenarios. The FWI is a meteorologically based index used to estimate fire danger at the large- and/or global-scale. It incorporates daily values of air temperature, relative humidity, wind speed, and 24-hour accumulated precipitation to calculate fire danger levels. The dataset spans from 1970 to 2098, providing daily, seasonal, and annual fire danger indicators. It covers the entire European region with a horizontal resolution of 0.11° x 0.11°. The dataset includes historical simulations (1970-2005) and future projections (near future: 2021-2040; mid-century: 2041-2060; end of century: 2079-2098) based on RCP2.6, 4.5, and 8.5. The projections are derived from multiple global climate models downscaled to regional climate models within the EURO-CORDEX initiative. This multi-model approach helps improve the robustness of the outcomes by providing a range of possible future scenarios.

Exposure and vulnerability data

Similarly to the drought population exposure, exposure is assessed by overlaying the European population density map at 30 arcsec resolution using the Global Human Settlement Population dataset (Pesaresi et al., 2013)

[17] https://cds.climate.copernicus.eu/cdsapp#!/dataset/sis-tourism-fire-danger-indicators?tab=overview

Funded by the European Union

This project has received funding from the European Union's Horizon Europe research and innovation programme under grant agreement No 101093864. Views and opinions expressed are however those of the author(s) only and do not necessarily reflect those of the European Union or the European Climate, Infrastructure and Environment Executive Agency (CINEA). Neither the European Union nor the granting authority can be held responsible for them.

Risk visualization

The main outcome of this workflow is a map overlapping the number of affected populations with the FWI map (Figure 28). In particular, the dataset includes daily, seasonal, and annual FWI values, and threshold-specific indicators such as the number of days with moderate, high, or very high fire danger conditions. These are classified according to the European Forest Fire Information System (EFFIS) thresholds of fire risk:

- Very low: <5.2
- Low: 5.2 - 11.2
- Moderate: 11.2 - 21.3
- High: 21.3 - 38.0
- Very high: 38.0 - 50
- Extreme: >=50.0

Figure 28 represents the average danger over fire season June-September with the fire hazard map averaged over NUTS level 3 regions of Europe.

The dataset is useful for assessing future fire danger conditions, supporting long-term tourism strategies, and reducing the risk of forest fires on nature-based tourism infrastructure. It also aids in forestry, local planning, and disaster risk management.

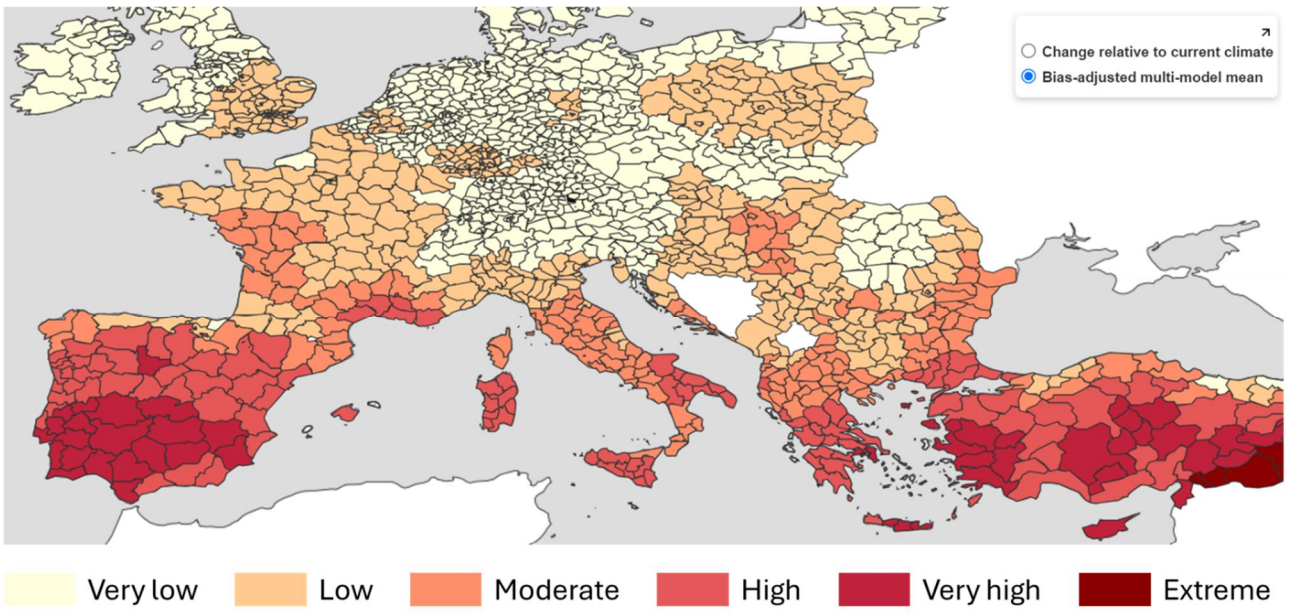

Figure 28. Classes of average danger over fire season (June-September) in case of Mid-century (2041-2060) projection and RCP4.5 scenario.

Funded by the European Union

This project has received funding from the European Union's Horizon Europe research and innovation programme under grant agreement No 101093864. Views and opinions expressed are however those of the author(s) only and do not necessarily reflect those of the European Union or the European Climate, Infrastructure and Environment Executive Agency (CINEA). Neither the European Union nor the granting authority can be held responsible for them.

4.6 Windstorm

Risk method

This event-based windstorm risk workflow allows for assessing the damages to structures due to a storm by combining hazard, exposure and vulnerability. The workflow is a simplified version of the work by Koks & Haer (2020), which is similar to the damage assessment for the river and coastal flood workflow. Damage is assessed based on a vulnerability curve that links hazard intensity with damage based on a specific land use type.

Hazard data

Using the CDS, historical windstorm footprints can be retrieved (CDS, 2022). The CDS also provides plausible yet synthetic storms that are physically realistic. These synthetic storms create a larger than historical overview of possible events that can affect the area in current-day situations. Both datasets give the footprints of the maximum 3-second gust per 72 hours per grid cell. It is worth noting that while the historical windstorm footprint does not allow the user to assess annual damage, the event footprint will provide the damage for that particular event. In this workflow no future projections of windstorms are included since projected changes in maximum windspeeds of storms are small, however, the projected locations of storms could shift northward (Seneviratne et al., 2021). Regions can therefore use historic storm footprints south of their location for potential future impacts.

Exposure and vulnerability data

Exposure to windstorm is assessed using the LUISA dataset as a proxy to assess land value, building density, construction type and in what ratio the construction types are present. Using vulnerability curves from Feuerstein et al. (2011) we classify the building types in six classes ranging from wind resilient to more fragile structures. Their vulnerability curve is a relation between the proportion of the building that is damaged and windspeed. This can be combined with the regional-specific land value that needs to be adjusted by the region to provide valid damage estimations. . In our workflow we give each land use class a different vulnerability curve due to different proportions of the building types in the land use-class (Figure 29).

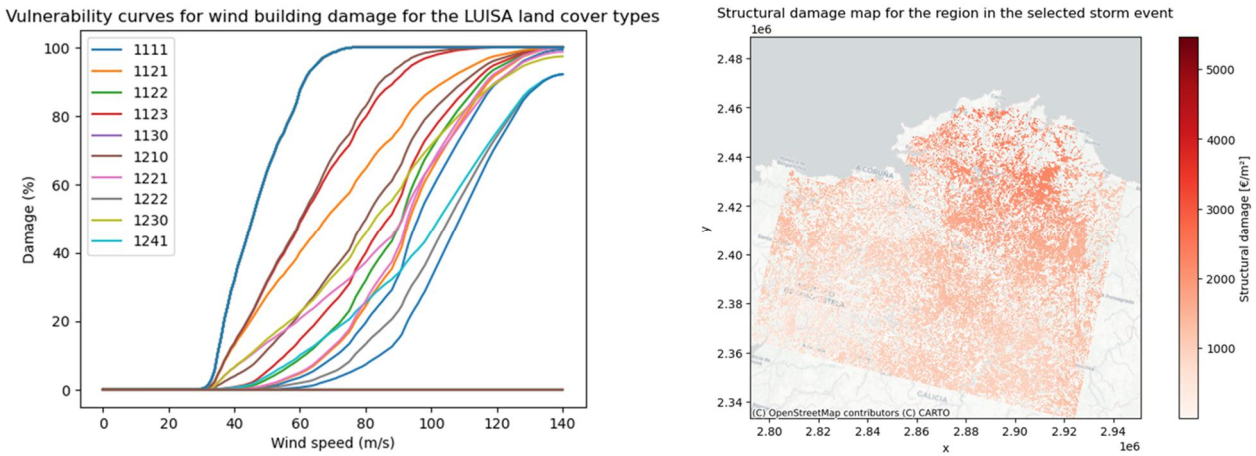

Figure 29. Example of vulnerability curve for 9 different land cover classes (left), and damage map for an European region during a storm event (right)

Funded by the European Union

This project has received funding from the European Union's Horizon Europe research and innovation programme under grant agreement No 101093864. Views and opinions expressed are however those of the author(s) only and do not necessarily reflect those of the European Union or the European Climate, Infrastructure and Environment Executive Agency (CINEA). Neither the European Union nor the granting authority can be held responsible for them.

Risk visualization

The main outputs of this workflow is wind damage, at a grid level and based on historical hazard information, for a specific area as displayed in Figure 29.

4.7 Heavy snow and blizzards

Risk method

In this workflow, risk is expressed as the combination of the probability of occurrence of heavy snow or blizzards, and population density exposure (similarly to the risk workflow for drought exposure). The risk can be assessed for both present and future climate conditions.

Hazard data

Blizzards: A blizzard is a severe storm condition defined by low temperature, sustained wind or frequent wind gust and considerable precipitating or blowing snow. For blizzard conditions we used the following impact indicator (Vajda et al., 2014):

$$Tmean \leq 0\ °C,\ Rs \text{ (snow amount)} \geq 10\ cm \text{ and } Wg \text{ (wind gust)} \geq 17\ m/s.$$

This impact indicator is defined based on an extensive literature review, media reports, surveys conducted with European Critical Infrastructures operators. The impacts and consequences of blizzard on critical infrastructure and transport system are related to i) fallen trees on roads, rails and electricity lines, ii) snowbanks, slippery roads, poor visibility, rail points may get stuck; and iii) accumulated snow on structures and power lines (Groenemeijer et al., 2016; Vajda et al., 2014).

Heavy snow: Heavy snowfall may cause many disruptions and impacts in various sectors; however, the impacts and consequences of this hazard depend on the affected sector, infrastructure, and also preparedness of society which varies over Europe. Similarly to blizzards, the impact indicators for heavy snowfall were defined taking into account the exposure of critical infrastructure, i.e., roads, rails, power lines, and telecommunication to the hazard, and is based on an extensive literature review, media reports, surveys conducted with European CI operators and case studies. The qualitative description of the two-level thresholds (within 24h) are:

- 1st threshold (> 6 cm): Some adverse impacts are expected, their severity depends on the resilience of the system, and transportation is mainly affected.

- 2nd threshold (> 25 cm): The weather phenomena are so severe that is likely that adverse impact will occur, CI system will be seriously impacted. We also offer users the option to define and utilize their own thresholds according to their needs for the snow extreme.

Information regarding temperature, wind gusts, snow depth, and snow density are derived from the ERA5 reanalysis dataset at 0.25 degree spatial resolution and hourly temporal resolution. Daily data are then assessed by means of resampling techniques. The results of six different regional climate models at 50 km spatial resolution produced from EURO-CORDEX (SMHI-RCA4-CanESM2, SMHI-RCA4-NorESM1, SMHI-RCA4-IPSL-CM5A-MR, KNMI-RACMO22E-EC-EARTH, KNMI-RACMO22E-HadGEM2-ES and MPI-CSC-REMO2009-MPI-ESM-LR) are used to represent future emission scenarios (RCP 4.5 and RCP 8.5). Annual probability *P* of occurrence of both heavy snow and

Funded by the European Union

This project has received funding from the European Union's Horizon Europe research and innovation programme under grant agreement No 101093864. Views and opinions expressed are however those of the author(s) only and do not necessarily reflect those of the European Union or the European Climate, Infrastructure and Environment Executive Agency (CINEA). Neither the European Union nor the granting authority can be held responsible for them.

blizzards are then calculated (see Figure 30) as follows: dividing the number of days surpassing the thresholds by the total days in the year, expressed as a percentage.

P = ((variable > threshold) / days in year) X 100

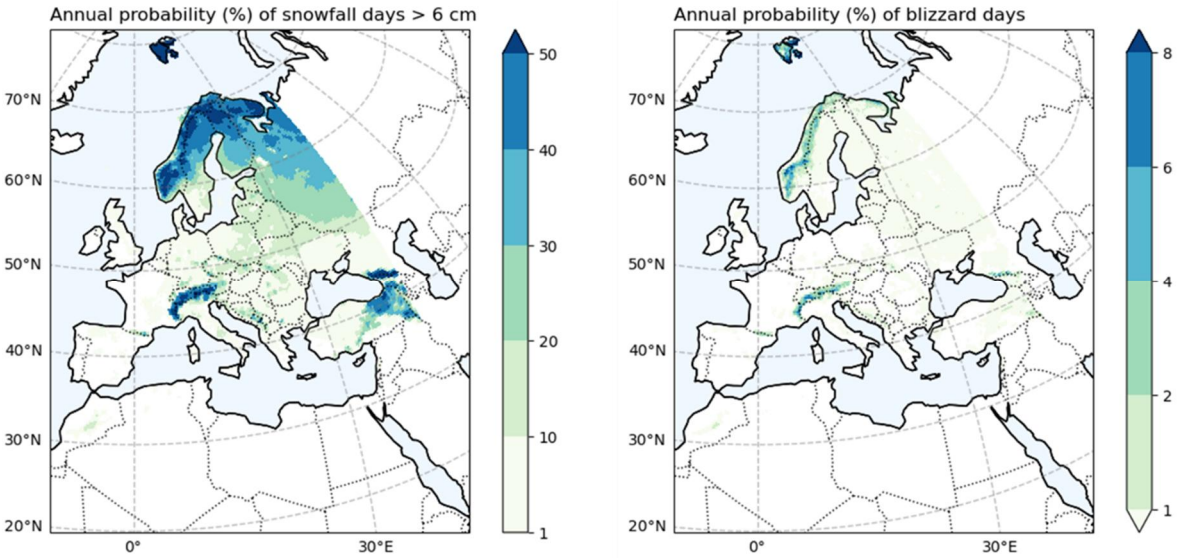

Figure 30. Annual probability of heavy snow (left) and blizzards (right) for the period 1991-2010.

Exposure and vulnerability data

Exposure is assessed by overlaying the European population density map at 30 arcsec resolution using the Global Human Settlement Population dataset (Pesaresi et al., 2013).

Risk visualization

The output of this workflow is a map overlapping population density with the annual probability of occurrence of either heavy snow or blizzards (Figure 31).

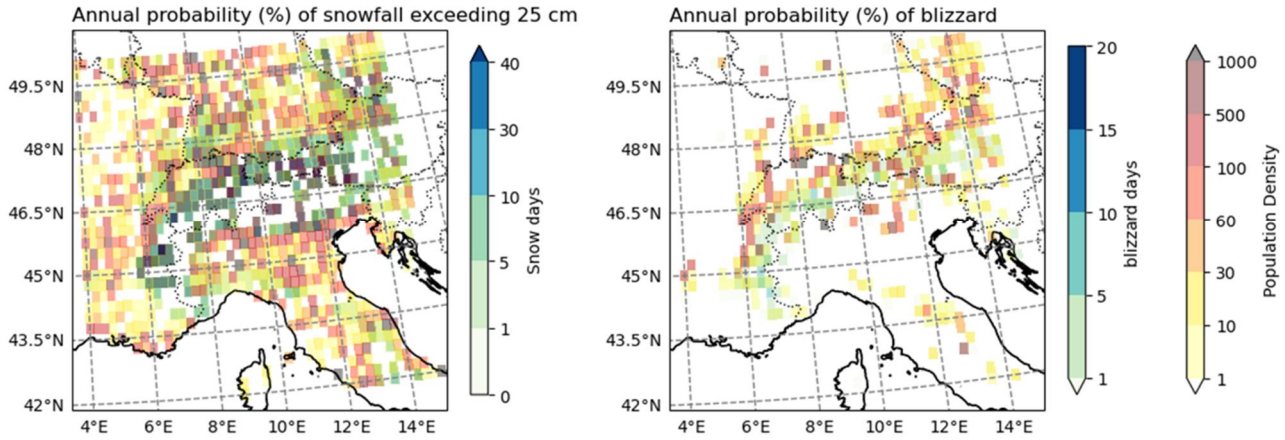

Figure 31. Risk maps of heavy snow (left) and blizzards (right)

Funded by the European Union

This project has received funding from the European Union's Horizon Europe research and innovation programme under grant agreement No 101093864. Views and opinions expressed are however those of the author(s) only and do not necessarily reflect those of the European Union or the European Climate, Infrastructure and Environment Executive Agency (CINEA). Neither the European Union nor the granting authority can be held responsible for them.

4.8 Multi-hazards

Risk method

This risk workflow assess the risk of multi-hazards, i.e. extreme temperature and precipitation, on critical infrastructures such as airports, following the example of De Vivo et al. (2022). In this context the impact of a single hazard (e.g. extreme precipitation, heatwave) can be evaluated on the different assets of infrastructure, for example on the terminal, runway, taxiways, parking areas etc. In this workflow, risk is expressed as a function of hazard, exposure and vulnerability factors and it can be assessed for both present and future climate conditions.

Hazard data

In this workflow two datasets (generic data) will be used, one for the historical part and one for the expected future. We employed one of the most advanced reanalysis data produced in Europe, specifically optimized for the land surface: the UERRA MESCAN-SURFEX. It is a regional reanalysis dataset implemented for Europe within a European FP7 reanalysis preoperational project with the participation of ECMWF. It has a spatial resolution of 5.5 km over Europe, from January 1961 to July 2019. Concerning the climate projections, the EURO-CORDEX high-resolution simulation of the regional climate models (Jacob et al., 2014) were used to assess the potential variation of the hazard indicators. For climate models, RCP 2.6, RCP 4.5, and RCP 8.5 were considered. The use of a set of regional climate models offers the opportunity to evaluate the average (often referred to as “Ensemble mean”), obtained starting from the values of the individual models, as well as the dispersion of the single models around this average value (von Trentini et al., 2019). The dispersion was quantified through the calculation of the standard deviation: a low standard deviation value indicates a high agreement between the climate models of the EURO-CORDEX ensemble, and vice versa (von Trentini et al., 2019). With both datasets a list of hazard data are going to be computed: for extreme precipitation 99, 99.5 and 99.9 percentile of daily precipitation and return periods of 10, 20, 30, 50, 100, 150 years; for heat waves the 95 and 99.9 percentile and number of days where the maximum temperature exceed 35°C, 40°C, 45°C. In the case of projection, the hazard data will be computed as an anomaly with respect to historical period.

Exposure and vulnerability data

When performing a risk assessment, it is important to define which assets are threatened, i.e. the exposed samples. We considered various airport components as exposed samples. From an operational point of view, an airport is generally divided into two main areas of activity: landside and airside activities. In general, the air side components include structures used for the movement of aircraft, such as runways, taxiways, and tower. On the other hand, land side components refer to the public access areas such as offices, terminals, airports access systems and parking areas.

Concerning vulnerability, we selected specific sensitivity and adaptive-capacity indicators. Sensitivity indicators measure how susceptible a system is to climate hazards, influenced by natural, physical, socioeconomic, and morphological factors (Burbidge, 2016; De Vivo et al., 2023). For example, older structures are more vulnerable to extreme weather events, and the percentage of impervious surfaces can increase the risk of flooding or overheating. Social indicators include air

Funded by the European Union

This project has received funding from the European Union's Horizon Europe research and innovation programme under grant agreement No 101093864. Views and opinions expressed are however those of the author(s) only and do not necessarily reflect those of the European Union or the European Climate, Infrastructure and Environment Executive Agency (CINEA). Neither the European Union nor the granting authority can be held responsible for them.

traffic and the number of passengers, which can complicate managing climate impacts at busy airports. It is worth noting that this type of information are available from user local data, no EU level datasets are available.

Concerning adaptive capacity, we selected the indicators which reflect the characteristics of airports that make them more or less able to respond to impacts of climate change (Burbidge, 2016; De Vivo et al., 2023). Adaptation strategies can be physical, social, institutional, technological, and economic. Adaptation options are categorized into grey (technological and engineering solutions), green (ecosystem-based approaches), and soft measures (managerial, legal, and policy measures). Soft measures include improving alert systems, awareness campaigns, emergency management plans, insurance policies for extreme events, and energy consumption optimization initiatives. Grey measures include constructing improved drainage systems to cope with flooding. Green actions involve developing and enhancing green areas around the airport, such as parks, and installing vegetated roofs and walls on existing airport structures to mitigate the effects of extreme temperatures.

Most information relating to exposure and vulnerability data are collected from multiple sources such as online official documents and reports and airport websites.

Risk visualisation

The final risk was obtained by the interaction between hazard, exposure, and vulnerability, properly normalized and aggregated. Figure 32 shows an example of risk due to extreme precipitation. Similar maps can be obtained for temperature and can be then compared between each other as risk indicators are normalized. Quantifying the risk will allow for priorities of intervention in terms of adaptation strategies aimed at making airports more resilient to the changing climate.

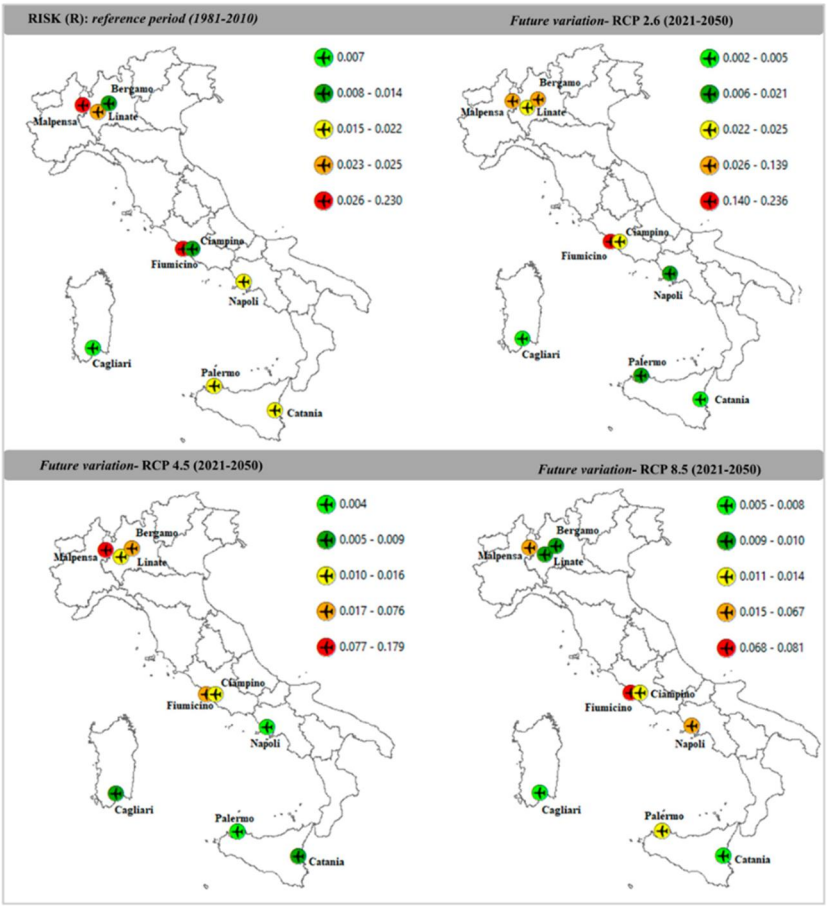

Figure 32. Risk maps related of extreme precipitation events (from De Vivo et al. 2023)

Funded by the European Union

This project has received funding from the European Union's Horizon Europe research and innovation programme under grant agreement No 101093864. Views and opinions expressed are however those of the author(s) only and do not necessarily reflect those of the European Union or the European Climate, Infrastructure and Environment Executive Agency (CINEA). Neither the European Union nor the granting authority can be held responsible for them.

5 Discussion

5.1 Advantages and disadvantages of climate risk assessment

This section describes advantages and disadvantages of the CRA methods implemented within the CLIMAAX toolbox (see Table 4).

Table 4. Summary of the advantages and disadvantages of the different CRA methods

Method	Advantages	Disadvantages
Risk indexing	• Provides a comprehensive risk assessment Allows for the comparison of risks across different regions. • Useful for identifying high-risk areas and prioritizing adaptation measures.	• Relies on data availability and quality, which can be limited in some regions. • Weighting and aggregation of different risk factors can be subjective. • Neglects the complex dynamics between the risk components.
Damage assessment	• Provides a direct measure of the economic impacts of natural hazards. • Can inform cost-benefit analyses and guide resource allocation for adaptation measures. • Helps to raise awareness and support for climate action.	• Requires accurate data of past damages, which can be challenging to obtain. • Does not account for indirect and intangible impacts. • Damage functions that rely on historical data may not adequately capture the effects of changing climate conditions or evolving socioeconomic factors.
Exposed Assets and Population	• Identifies the assets, critical infrastructures, and population at risk from natural hazards. • Supports the development of informed-based targeted adaptation strategies. • Can be combined with other assessment methods to provide a more comprehensive risk profile.	• Focuses primarily on the exposure component of risk, without fully considering vulnerability and adaptive capacity. • Challenges in accurately mapping and quantifying all potentially exposed assets and populations. • Difficulty in projecting future changes in exposure due to complex behaviours of demographic and land-use.

These approaches can be applied at different spatial resolutions, both at local and large scales. For example, large-scale assessments can be performed to explore a broader area, allowing for a more comprehensive understanding of the risks associated with different hazards (Djordjević et al., 2011). Moreover, large-scale assessments can enable stakeholders and policymakers to develop more effective policies for adaptation and mitigation, while facilitating international cooperation (Jones & Mearns, 2005). However, those type of analysis may not capture the physical local-scale characteristics and socio-economic vulnerabilities to different hazards (Padulano et al., 2021). For

Funded by the European Union

This project has received funding from the European Union's Horizon Europe research and innovation programme under grant agreement No 101093864. Views and opinions expressed are however those of the author(s) only and do not necessarily reflect those of the European Union or the European Climate, Infrastructure and Environment Executive Agency (CINEA). Neither the European Union nor the granting authority can be held responsible for them.

example, local cost-effectiveness of measures can be different than the ones assumed at large scale due to site-specific characteristics (Dottori et al., 2023). In addition, large-scale assessments require accurate data and substantial computational resources, which can be a barrier for some organizations or countries.

On the other hand, local-scale CRAs are used for local planning and decision-making at the community or city level. The advantage is to account for local physical characteristics and vulnerabilities more relevant to local communities (Arosio et al., 2021). Moreover, local CRAs can enable decision-makers to develop more effective adaptation and mitigation strategies (Bernardini et al., 2021). By involving local stakeholders and communities, local CRAs foster a sense of ownership and engagement in the risk assessment process (White et al., 2018). However, local CRAs require more detailed data and modelling, and can lead to an incomplete understanding of the broader risk at regional or national context due to the application to a limited area (Kumar et al., 2020). Because of this, combining local- and large-scale CRAs can provide a more robust estimation of the risks associated with different hazards and sectors, allowing for the development of more informed adaptation strategies.

5.2 Risk workflow implementation with local data

As previously mentioned, the CLIMAAX toolbox allows different users to perform CRA either using the pre-calculated hazard and risk maps based on large-scale EU datasets or perform their customized risk assessment based on local and regional data. Therefore, within CLIMAAX, the third-party projects have the possibility to use the large scale CRA workflows in the scoping phase as a first benchmark against CRA from local user data. Later the user could further refine their regional CRAs with additional local data and knowledge. However, the implementation of the risk workflows on local and regional level can be challenging due to the constraints in data and technical capacity.

One of the primary challenges in implementing the CLIMAAX CRA approaches at local and regional scale is the mismatch between the spatial resolution of available climate data (e.g. 5-10km resolution) and the finer scale from the users' local data (1-5km or even finer). This issue can be overcome by downscaling climate data to finer resolutions. However, downscaling approaches can introduce additional uncertainties. Moreover, coarse resolution data (e.g. exposure map at EU level not available at local scale) may not accurately represent local topography and often do not capture the required level of detail to assess the actual climate risk. In addition, using local data with fine resolution for assessing hazard and risk maps in big regions can be computationally expensive and require specific expertise to adapt the CLIMAAX risk workflow to local conditions.

Another challenge is the mismatch between the temporal resolutions of the large scale and local-scale data. Many climate-related risks are associated with extreme events, which may occur at frequencies not well-captured by typical climate model outputs. For example, flood events are often triggered by intense and short-duration rainfall, while climate models typically provide daily rainfall totals, which may not capture the sub-daily intensity crucial for flash flood risk assessment. Moreover, local historical data, crucial for calibrating and validating the CLIMAAX CRA approaches at local level, may be sparse or inconsistent over time.

Funded by the European Union

This project has received funding from the European Union's Horizon Europe research and innovation programme under grant agreement No 101093864. Views and opinions expressed are however those of the author(s) only and do not necessarily reflect those of the European Union or the European Climate, Infrastructure and Environment Executive Agency (CINEA). Neither the European Union nor the granting authority can be held responsible for them.

5.3 Dealing with uncertainty

CRAs is crucial for regional and local authorities to prioritize adaptation activities. Conducing a CRA requires understanding past- and future risk conditions linked to the frequency and intensity of extreme hazards such as floods, droughts, heatwaves, wildfires, storms, and heavy snow, and to the different exposure and vulnerability of society. However, CRAs come with inherent uncertainties due to limitations in our understanding of the physical and social systems, their interplays, data uncertainty, and structural uncertainty of climate models used for CRAs (Harrington et al., 2021).

Uncertainties in data, including measurement errors, missing data, and the representativeness of future climate projections can strongly impact CRAs (Di Baldassarre & Montanari, 2009). For example, uncertain data on past climate extremes can lead to a misleading understanding of current trends and variability. On the other hand, the uncertain scenarios of greenhouse gas emissions can result in inaccurate climate and socioeconomic projections, including population growth, economic development, land use changes, and technological advancements, thus leading to erroneous projection of future risk. Furthermore, climate sensitivity, or the response of the global climate system to an increase in greenhouse gas concentrations, remains uncertain (Rising et al., 2022). Moreover, such future socioeconomic conditions and technological development influence the vulnerability and exposure of communities to climate risks. Uncertainties in projecting these conditions add another layer of complexity to CRAs.

Models used for CRAs (e.g. hydrological and hydraulic models to assess river flow and water availability, or climate models used to project future climate conditions) have inherent limitations and uncertainties. For example, uncertainty in model structure (e.g. representation of physical processes), inherent randomness and unpredictability, initial conditions, and model parameters calibration play a crucial role in propagating uncertainty from input up to the model output (Aronica et al., 2002). Moreover, the variability of the climate system from seasonal to decadal scales is not always well captured by climate models, adding to the uncertainty in CRA (Shen et al., 2018). Finally, CRAs often require downscaling global or regional climate model projections at a regional or local scale. This process introduces additional uncertainties, particularly in areas with complex topography or heterogeneous land cover (Harrington et al., 2021).

Different approaches have been developed over the last years to identify and reduce the influence of those sources of uncertainty in CRAs. Improving the accuracy and resolution of climate models, as well as enhancing the quality and coverage of climate data, can reduce uncertainties in CRA (Shen et al., 2018). Moreover, the use of an ensemble of climate models, rather than relying on a single one, can allow for assessing the range of possible future climate projections, quantify the associated uncertainties, and better understand the robustness of the CRA results (Dawkins et al., 2023). Developing multiple plausible future socioeconomic scenarios and technological pathways into CRA can help address uncertainties related to future vulnerability and exposure (Spinoni et al., 2021). This allows for exploring a wider range of potential climate risk scenarios, allowing for more comprehensive and nuanced assessments for informing decision-making under uncertainty. An example is the adaptation pathways approach by (Haasnoot et al., 2013) who developed a method to test sequences of adaptation measures ('Pathways') under various future scenarios. Furthermore,

Funded by the European Union

This project has received funding from the European Union's Horizon Europe research and innovation programme under grant agreement No 101093864. Views and opinions expressed are however those of the author(s) only and do not necessarily reflect those of the European Union or the European Climate, Infrastructure and Environment Executive Agency (CINEA). Neither the European Union nor the granting authority can be held responsible for them.

robust optimisation approaches can be used in decision-making approaches to identify strategies across a wide range of possible futures rather than optimizing for a single most likely future (Gabrel et al., 2014; Hamarat et al., 2014).

The implementation of sensitivity analyses will further help to unravel the effects of input, model parameters, and model structure on the outcomes of CRA and provide valuable insights into the main sources of uncertainty. Engaging stakeholders, including communities, policymakers, and scientists, in the CRA process can help address uncertainties by incorporating local knowledge and diverse perspectives. Participatory approaches, such as workshops and serious games, can be used. Finally, advanced modelling techniques such as system dynamics or agent-based models can be used to represent the complex climate-water-human system and model the interplays between hazard, exposure, and vulnerability for CRA (Mazzoleni et al., 2021).

6 Conclusions

This deliverable provides an overview of the different approaches used in CRAs and introduces the ones implemented within the CLIMAAX Toolbox. Moreover, we discussed advantages and disadvantages of the different methods and how to deal with uncertainty.

This report highlights the importance of understanding, representing, and quantifying the relation between hazard, exposure, and vulnerability. The methods implemented within the CLIMAAX Toolbox will allow stakeholders to assess climate risk for different hazards at various spatial scales, using either large-scale datasets or local data of hazard, vulnerability, and exposure.

The methods and results of this deliverable will pave the way for a more comprehensive way to assess climate risk within the different CLIMAAX applications, and more in general, within the different European local communities.

Funded by
the European Union

This project has received funding from the European Union's Horizon Europe research and innovation programme under grant agreement No 101093864. Views and opinions expressed are however those of the author(s) only and do not necessarily reflect those of the European Union or the European Climate, Infrastructure and Environment Executive Agency (CINEA). Neither the European Union nor the granting authority can be held responsible for them.

References

Adger, W. N., Brown, I., & Surminski, S. (2018). Advances in risk assessment for climate change adaptation policy. In *Philosophical Transactions of the Royal Society A: Mathematical, Physical and Engineering Sciences* (Vol. 376, Issue 2121, p. 20180106). The Royal Society Publishing.

Aitkenhead, I., Kuleshov, Y., Bhardwaj, J., Chua, Z.-W., Sun, C., & Choy, S. (2023). Validating a tailored drought risk assessment methodology: Drought risk assessment in local Papua New Guinea regions. *Natural Hazards and Earth System Sciences*, *23*(2), 553–586. https://doi.org/10.5194/nhess-23-553-2023

Allen, R. G., Pereira, L. S., Raes, D., & Smith, M. (1998). Crop evapotranspiration-Guidelines for computing crop water requirements-FAO Irrigation and drainage paper 56. *Fao, Rome*, *300*(9), D05109.

Alonso, C., Gouveia, C. M., Russo, A., & Páscoa, P. (2019). Crops' exposure, sensitivity and adaptive capacity to drought occurrence. *Natural Hazards and Earth System Sciences*, *19*(12), 2727–2743. https://doi.org/10.5194/nhess-19-2727-2019

Ara Begum, A., Lempert, R., Ali, E., Benjaminsen, T. A., Bernauer, T., Cramer, W., Cui, X., Mach, K., Nagy, G., Stenseth, N. C., Sukumar, R., & Wester, P. (2022). Point of Departure and Key Concepts. In H.-O. Pörtner, D. C. Roberts, M. Tignor, E. S. Poloczanska, K. Mintenbeck, A. Alegría, & M. Craig (Eds.), *Climate Change 2022: Impacts, Adaptation and Vulnerability. Contribution of Working Group II to the Sixth Assessment Report of the Intergovernmental Panel on Climate Change* (pp. 121–196). Cambridge University Press.

Aronica, G., Bates, P. D., & Horritt, M. S. (2002). Assessing the uncertainty in distributed model predictions using observed binary pattern information within GLUE. *Hydrological Processes*, *16*(10), 2001–2016.

Aznar-Siguan, G., & Bresch, D. N. (2019). CLIMADA v1: A global weather and climate risk assessment platform. *Geoscientific Model Development*, *12*(7), 3085–3097. https://doi.org/10.5194/gmd-12-3085-2019

Batke, S. P., Jocque, M., & Kelly, D. L. (2014). Modelling Hurricane Exposure and Wind Speed on a Mesoclimate Scale: A Case Study from Cusuco NP, Honduras. *PLOS ONE*, *9*(3), e91306. https://doi.org/10.1371/journal.pone.0091306

Baugh, C., Colonese, J., D'Angelo, C., Dottori, F., Neal, J., Prudhomme, C., & Salamon, P. (2024). *River flood hazard maps for Europe and the Mediterranean Basin region*. https://doi.org/10.2905/1D128B6C-A4EE-4858-9E34-6210707F3C81

Boettle, M., Rybski, D., & Kropp, J. P. (2016). Quantifying the effect of sea level rise and flood defence – a point process perspective on coastal flood damage. *Natural Hazards and Earth System Sciences*, *16*(2), 559–576. https://doi.org/10.5194/nhess-16-559-2016

Burbidge, R. (2016). Adapting European Airports to a Changing Climate. *Transportation Research Procedia*, *14*, 14–23. https://doi.org/10.1016/j.trpro.2016.05.036

Büttner, G. (2014). CORINE land cover and land cover change products. In *Land use and land cover mapping in Europe: Practices & trends* (pp. 55–74). Springer.

Cardona, O. D., Van Aalst, M. K., Birkmann, J., Fordham, M., Mc Gregor, G., Rosa, P., Pulwarty, R. S., Schipper, E. L. F., Sinh, B. T., & Décamps, H. (2012). Determinants of risk: Exposure and vulnerability. In *Managing the risks of extreme events and disasters to advance climate change adaptation: Special report of the intergovernmental panel on climate change* (pp. 65–108). Cambridge University Press.

Carrão, H., Naumann, G., & Barbosa, P. (2016). Mapping global patterns of drought risk: An empirical framework based on sub-national estimates of hazard, exposure and vulnerability. *Global Environmental Change*, *39*, 108–124. https://doi.org/10.1016/j.gloenvcha.2016.04.012

Chakraborty, D., Dobor, L., Zolles, A., Hlásny, T., & Schueler, S. (2021). High-resolution gridded climate data for Europe based on bias-corrected EURO-CORDEX: The ECLIPS dataset. *Geoscience Data Journal*, *8*(2), 121–131.

Funded by the European Union

This project has received funding from the European Union's Horizon Europe research and innovation programme under grant agreement No 101093864. Views and opinions expressed are however those of the author(s) only and do not necessarily reflect those of the European Union or the European Climate, Infrastructure and Environment Executive Agency (CINEA). Neither the European Union nor the granting authority can be held responsible for them.

Chambers, J. (2020). Global and cross-country analysis of exposure of vulnerable populations to heatwaves from 1980 to 2018. *Climatic Change*, *163*(1), 539–558. https://doi.org/10.1007/s10584-020-02884-2

Chuvieco, E., Yebra, M., Martino, S., Thonicke, K., Gómez-Giménez, M., San-Miguel, J., Oom, D., Velea, R., Mouillot, F., Molina, J. R., Miranda, A. I., Lopes, D., Salis, M., Bugaric, M., Sofiev, M., Kadantsev, E., Gitas, I. Z., Stavrakoudis, D., Eftychidis, G., … Viegas, D. (2023). Towards an Integrated Approach to Wildfire Risk Assessment: When, Where, What and How May the Landscapes Burn. *Fire*, *6*(5), Article 5. https://doi.org/10.3390/fire6050215

CIESIN, C. for I. E. S. I. N.-C.-C. U. (2016). *Gridded Population of the World, Version 4 (GPWv4): Population Density*. https://sedac.ciesin.columbia.edu/data/collection/gpw-v4

Copernicus Climate Change Service, Climate Data Store. (2022). *Winter windstorm indicators for Europe from 1979 to 2021 derived from reanalysis. . DOI: (Accessed on DD-MMM-YYYY)* [dataset]. Copernicus Climate Change Service (C3S) Climate Data Store (CDS). https://doi.org/10.24381/cds.9b4ea013

CRED. (2019). *EM-DAT: The CRED/OFDA International Disaster Database*. Université Catholique de Louvain. https://www.emdat.be/

Cui, Y., Jiang, S., Jin, J., Ning, S., & Feng, P. (2019). Quantitative assessment of soybean drought loss sensitivity at different growth stages based on S-shaped damage curve. *Agricultural Water Management*, *213*, 821–832.

Das, J., Das, S., & Umamahesh, N. V. (2023). Population exposure to drought severities under shared socioeconomic pathways scenarios in India. *Science of The Total Environment*, *867*, 161566. https://doi.org/10.1016/j.scitotenv.2023.161566

Dawkins, L. C., Bernie, D. J., Lowe, J. A., & Economou, T. (2023). Assessing climate risk using ensembles: A novel framework for applying and extending open-source climate risk assessment platforms. *Climate Risk Management*, *40*, 100510. https://doi.org/10.1016/j.crm.2023.100510

Dawson, R. J., Thompson, D., Johns, D., Wood, R., Darch, G., Chapman, L., Hughes, P. N., Watson, G. V. R., Paulson, K., Bell, S., Gosling, S. N., Powrie, W., & Hall, J. W. (2018). A systems framework for national assessment of climate risks to infrastructure. *Philosophical Transactions of the Royal Society A: Mathematical, Physical and Engineering Sciences*, *376*(2121), 20170298. https://doi.org/10.1098/rsta.2017.0298

de Brito, M. M., Sodoge, J., Fekete, A., Hagenlocher, M., Koks, E., Kuhlicke, C., Messori, G., de Ruiter, M., Schweizer, P.-J., & Ward, P. J. (2024). Uncovering the Dynamics of Multi-Sector Impacts of Hydrological Extremes: A Methods Overview. *Earth's Future*, *12*(1), e2023EF003906.

de Moel, H., van Vliet, M., & Aerts, J. C. J. H. (2014). Evaluating the effect of flood damage-reducing measures: A case study of the unembanked area of Rotterdam, the Netherlands. *Regional Environmental Change*, *14*(3), 895–908. Scopus. https://doi.org/10.1007/s10113-013-0420-z

De Vivo, C., Barbato, G., Ellena, M., Capozzi, V., Budillon, G., & Mercogliano, P. (2023). Application of climate risk assessment framework for selected Italian airports: A focus on extreme temperature events. *Climate Services*, *30*, 100390. https://doi.org/10.1016/j.cliser.2023.100390

De Vivo, C., Ellena, M., Capozzi, V., Budillon, G., & Mercogliano, P. (2022). Risk assessment framework for Mediterranean airports: A focus on extreme temperatures and precipitations and sea level rise. *Natural Hazards*, *111*(1), 547–566. https://doi.org/10.1007/s11069-021-05066-0

Di Baldassarre, G., & Montanari, A. (2009). Uncertainty in river discharge observations: A quantitative analysis. *Hydrology and Earth System Sciences*, *13*(6), 913–921. https://doi.org/10.5194/hess-13-913-2009

Di Baldassarre, G., Viglione, A., Carr, G., Kuil, L., Salinas, J. L., & Blöschl, G. (2013). Socio-hydrology: Conceptualising human-flood interactions. *Hydrology and Earth System Sciences*, *17*(8), 3295–3303. https://doi.org/10.5194/hess-17-3295-2013

Funded by the European Union

This project has received funding from the European Union's Horizon Europe research and innovation programme under grant agreement No 101093864. Views and opinions expressed are however those of the author(s) only and do not necessarily reflect those of the European Union or the European Climate, Infrastructure and Environment Executive Agency (CINEA). Neither the European Union nor the granting authority can be held responsible for them.

Dilley, M. (2005). *Natural disaster hotspots: A global risk analysis* (Vol. 5). World Bank Publications.

Djordjević, S., Butler, D., Gourbesville, P., Mark, O., & Pasche, E. (2011). New policies to deal with climate change and other drivers impacting on resilience to flooding in urban areas: The CORFU approach. *Environmental Science & Policy*, *14*(7), 864–873. https://doi.org/10.1016/j.envsci.2011.05.008

Doorenbos, J., & Kassam, A. H. (1979). Yield response to water. *Irrigation and Drainage Paper*, *33*, 257.

Dottori, F., Mentaschi, L., Bianchi, A., Alfieri, L., & Feyen, L. (2023). Cost-effective adaptation strategies to rising river flood risk in Europe. *Nature Climate Change*, *13*(2), Article 2. https://doi.org/10.1038/s41558-022-01540-0

Duo, E., Fernández-Montblanc, T., & Armaroli, C. (2020). Semi-probabilistic coastal flood impact analysis: From deterministic hazards to multi-damage model impacts. *Environment International*, *143*, 105884. https://doi.org/10.1016/j.envint.2020.105884

Eberenz, S., Stocker, D., Röösli, T., & Bresch, D. N. (2020). Asset exposure data for global physical risk assessment. *Earth System Science Data*, *12*(2), 817–833. https://doi.org/10.5194/essd-12-817-2020

Edwards, D. C., & McKee, T. B. (1997). *Characteristics of 20th Century Drought in the United States at Multiple Time Scales* (97–2; Climatology Report). Colorado State University.

Egbinola, C. N., Olaniran, H. D., & Amanambu, A. C. (2017). Flood management in cities of developing countries: The example of Ibadan, Nigeria. *Journal of Flood Risk Management*, *10*(4), 546–554.

El Meouche, R., Abunemeh, M., Hijazi, I., Mebarki, A., Fatayer, F., & Issa, A. (2020). Probabilistic Fire Risk Framework for Optimizing Construction Site Layout. *Sustainability*, *12*(10), Article 10. https://doi.org/10.3390/su12104065

Endendijk, T., Botzen, W. J. W., de Moel, H., Aerts, J. C. J. H., Slager, K., & Kok, M. (2023). Flood Vulnerability Models and Household Flood Damage Mitigation Measures: An Econometric Analysis of Survey Data. *Water Resources Research*, *59*(8), e2022WR034192. https://doi.org/10.1029/2022WR034192

Englhardt, J., de Moel, H., Huyck, C. K., de Ruiter, M. C., Aerts, J. C. J. H., & Ward, P. J. (2019). Enhancement of large-scale flood risk assessments using building-material-based vulnerability curves for an object-based approach in urban and rural areas. *Natural Hazards and Earth System Sciences*, *19*(8), 1703–1722. https://doi.org/10.5194/nhess-19-1703-2019

European Environment Agency. (2024). *European climate risk assessment: Executive summary* (EEA Report 01/2024).

Fader, M., Shi, S., von Bloh, W., Bondeau, A., & Cramer, W. (2016). Mediterranean irrigation under climate change: More efficient irrigation needed to compensate for increases in irrigation water requirements. *Hydrology and Earth System Sciences*, *20*(2), 953–973. https://doi.org/10.5194/hess-20-953-2016

Feuerstein, B., Groenemeijer, P., Dirksen, E., Hubrig, M., Holzer, A. M., & Dotzek, N. (2011). Towards an improved wind speed scale and damage description adapted for Central Europe. *Atmospheric Research*, *100*(4), 547–564.

Gabrel, V., Murat, C., & Thiele, A. (2014). Recent advances in robust optimization: An overview. *European Journal of Operational Research*, *235*(3), 471–483. https://doi.org/10.1016/j.ejor.2013.09.036

Gardiner, B., Byrne, K., Hale, S., Kamimura, K., Mitchell, S. J., Peltola, H., & Ruel, J.-C. (2008). A review of mechanistic modelling of wind damage risk to forests. *Forestry: An International Journal of Forest Research*, *81*(3), 447–463. https://doi.org/10.1093/forestry/cpn022

Garschagen, M., Doshi, D., Reith, J., & Hagenlocher, M. (2021). Global patterns of disaster and climate risk—An analysis of the consistency of leading index-based assessments and their results. *Climatic Change*, *169*(1), 11. https://doi.org/10.1007/s10584-021-03209-7

Funded by the European Union

This project has received funding from the European Union's Horizon Europe research and innovation programme under grant agreement No 101093864. Views and opinions expressed are however those of the author(s) only and do not necessarily reflect those of the European Union or the European Climate, Infrastructure and Environment Executive Agency (CINEA). Neither the European Union nor the granting authority can be held responsible for them.

Gill, J. C., & Malamud, B. D. (2016). Hazard interactions and interaction networks (cascades) within multi-hazard methodologies. *Earth System Dynamics*, *7*(3), 659–679. https://doi.org/10.5194/esd-7-659-2016

Gobron, N., Pinty, B., Mélin, F., Taberner, M., Verstraete, M. M., Belward, A., Lavergne, T., & Widlowski, J. -L. (2005). The state of vegetation in Europe following the 2003 drought. *International Journal of Remote Sensing*, *26*(9), 2013–2020. https://doi.org/10.1080/01431160412331330293

Gonçalves, A., Oliveira, S., & Zêzere, J. L. (2024). Assessing wildfire exposure and social vulnerability at the local scale using a GIS-based approach. *MethodsX*, *12*, 102650. https://doi.org/10.1016/j.mex.2024.102650

Groenemeijer, P., Vajda, A., Lehtonen, I., Kämäräinen, M., Venäläinen, A., Gregow, H., Becker, N., Nissen, K., Ulbrich, U., Berlin, F., Nápoles, O. M., & Paprotny, D. (2016). *Present and future probability of meteorological and hydrological hazards in Europe*.

Grusson, Y., Wesström, I., & Joel, A. (2021). Impact of climate change on Swedish agriculture: Growing season rain deficit and irrigation need. *Agricultural Water Management*, *251*, 106858. https://doi.org/10.1016/j.agwat.2021.106858

Gu, L., Chen, J., Yin, J., Sullivan, S. C., Wang, H.-M., Guo, S., Zhang, L., & Kim, J.-S. (2020). Projected increases in magnitude and socioeconomic exposure of global droughts in 1.5 and 2 °C warmer climates. *Hydrology and Earth System Sciences*, *24*(1), 451–472. https://doi.org/10.5194/hess-24-451-2020

Haasnoot, M., Kwakkel, J. H., Walker, W. E., & ter Maat, J. (2013). Dynamic adaptive policy pathways: A method for crafting robust decisions for a deeply uncertain world. *Global Environmental Change*, *23*(2), 485–498. https://doi.org/10.1016/j.gloenvcha.2012.12.006

Hagenlocher, M., Meza, I., Anderson, C. C., Min, A., Renaud, F. G., Walz, Y., Siebert, S., & Sebesvari, Z. (2019). Drought vulnerability and risk assessments: State of the art, persistent gaps, and research agenda. *Environmental Research Letters*, *14*(8), 083002. https://doi.org/10.1088/1748-9326/ab225d

Hamarat, C., Kwakkel, J. H., Pruyt, E., & Loonen, E. T. (2014). An exploratory approach for adaptive policymaking by using multi-objective robust optimization. *Simulation Modelling Practice and Theory*, *46*, 25–39. https://doi.org/10.1016/j.simpat.2014.02.008

Harrington, L. J., Schleussner, C.-F., & Otto, F. E. L. (2021). Quantifying uncertainty in aggregated climate change risk assessments. *Nature Communications*, *12*(1), 7140. https://doi.org/10.1038/s41467-021-27491-2

Heneka, P., & Ruck, B. (2008). A damage model for the assessment of storm damage to buildings. *Engineering Structures*, *30*(12), 3603–3609. https://doi.org/10.1016/j.engstruct.2008.06.005

Hinkel, J., Lincke, D., Vafeidis, A. T., Perrette, M., Nicholls, R. J., Tol, R. S. J., Marzeion, B., Fettweis, X., Ionescu, C., & Levermann, A. (2014). Coastal flood damage and adaptation costs under 21st century sea-level rise. *Proceedings of the National Academy of Sciences*, *111*(9), 3292–3297. https://doi.org/10.1073/pnas.1222469111

Hirabayashi, Y., Mahendran, R., Koirala, S., Konoshima, L., Yamazaki, D., Watanabe, S., Kim, H., & Kanae, S. (2013). Global flood risk under climate change. *Nature Climate Change*, *3*(9), 816–821. https://doi.org/10.1038/nclimate1911

Hong, S. B., & Yun, H. S. (2024). Predicting black ice-related accidents with probabilistic modeling using GIS-based Monte Carlo simulation. *PLOS ONE*, *19*(5), e0303605. https://doi.org/10.1371/journal.pone.0303605

Huizinga, J., De Moel, H., & Szewczyk, W. (2017). *Global flood depth-damage functions: Methodology and the database with guidelines*. Joint Research Centre (Seville site).

Funded by the European Union

This project has received funding from the European Union's Horizon Europe research and innovation programme under grant agreement No 101093864. Views and opinions expressed are however those of the author(s) only and do not necessarily reflect those of the European Union or the European Climate, Infrastructure and Environment Executive Agency (CINEA). Neither the European Union nor the granting authority can be held responsible for them.

Jacob, D., Petersen, J., Eggert, B., Alias, A., Christensen, O. B., Bouwer, L. M., Braun, A., Colette, A., Déqué, M., Georgievski, G., Georgopoulou, E., Gobiet, A., Menut, L., Nikulin, G., Haensler, A., Hempelmann, N., Jones, C., Keuler, K., Kovats, S., … Yiou, P. (2014). EURO-CORDEX: New high-resolution climate change projections for European impact research. *Regional Environmental Change*, *14*(2), 563–578. https://doi.org/10.1007/s10113-013-0499-2

Joint Research Centre (European Commission), Costa, H., De Rigo, D., Libertà, G., Houston Durrant, T., & San-Miguel-Ayanz, J. (2020). *European wildfire danger and vulnerability in a changing climate: Towards integrating risk dimensions : JRC PESETA IV project : Task 9 forest fires*. Publications Office of the European Union. https://data.europa.eu/doi/10.2760/46951

Jones, R., & Mearns, L. O. (2005). Assessing future climate risks. *Adaptation Policy Frameworks for Climate Change: Developing Strategies, Policies and Measures*, 119–143.

Joo, H., Choi, C., Kim, J., Kim, D., Kim, S., & Kim, H. S. (2019). A Bayesian Network-Based Integrated for Flood Risk Assessment (InFRA). *Sustainability*, *11*(13), Article 13. https://doi.org/10.3390/su11133733

Jung, C., & Schindler, D. (2024). Introducing a new hazard and exposure atlas for European winter storms. *Science of The Total Environment*, *929*, 172566. https://doi.org/10.1016/j.scitotenv.2024.172566

Jurgilevich, A., Räsänen, A., Groundstroem, F., & Juhola, S. (2017). A systematic review of dynamics in climate risk and vulnerability assessments. *Environmental Research Letters*, *12*(1), 013002. https://doi.org/10.1088/1748-9326/aa5508

Kelly, M., Schwarz, I., Ziegelaar, M., Watkins, A. B., & Kuleshov, Y. (2023). Flood Risk Assessment and Mapping: A Case Study from Australia's Hawkesbury-Nepean Catchment. *Hydrology*, *10*(2), Article 2. https://doi.org/10.3390/hydrology10020026

Kettner, A. J., Brakenridge, G. R., Schumann, G. J.-P., & Shen, X. (2021). Chapter 7—DFO—Flood Observatory. In G. J.-P. Schumann (Ed.), *Earth Observation for Flood Applications* (pp. 147–164). Elsevier. https://doi.org/10.1016/B978-0-12-819412-6.00007-9

Koks, E. E., & Haer, T. (2020). A high-resolution wind damage model for Europe. *Scientific Reports*, *10*(1), 6866. https://doi.org/10.1038/s41598-020-63580-w

Koks, E. E., & Haer., T. (2020). A high-resolution wind damage model for Europe. *Scientific Reports*, *10*(1), Article 1. https://doi.org/10.1038/s41598-020-63580-w

Koks, E. E., Jongman, B., Husby, T. G., & Botzen, W. J. W. (2015). Combining hazard, exposure and social vulnerability to provide lessons for flood risk management. *Environmental Science & Policy*, *47*, 42–52. https://doi.org/10.1016/j.envsci.2014.10.013

Laguardia, G., & Niemeyer, S. (2008). On the comparison between the LISFLOOD modelled and the ERS/SCAT derived soil moisture estimates. *Hydrology and Earth System Sciences*, *12*(6), 1339–1351. https://doi.org/10.5194/hess-12-1339-2008

Lee, H., Calvin, K., Dasgupta, D., Krinner, G., Mukherji, A., Thorne, P., Trisos, C., Romero, J., Aldunce, P., & Barrett, K. (2023). *Climate change 2023: Synthesis report. Contribution of working groups I, II and III to the sixth assessment report of the intergovernmental panel on climate change*. The Australian National University.

Lüthi, S., Aznar-Siguan, G., Fairless, C., & Bresch, D. N. (2021). Globally consistent assessment of economic impacts of wildfires in CLIMADA v2.2. *Geoscientific Model Development*, *14*(11), 7175–7187. https://doi.org/10.5194/gmd-14-7175-2021

Marin-Ferrer, M., Vernaccini, L., & Poljansek, K. (2017). INFORM index for risk management. *Concept and Methodology Version*.

Mazzoleni, M., Odongo, V. O., Mondino, E., & Di Baldassarre, G. (2021). Water management, hydrological extremes, and society: Modeling interactions and phenomena. *Ecology & Society*, *26*(4).

McKee, T. B., Doesken, N. J., & Kleist, J. (n.d.). *The relationship of drought frequency and duration to time scale*.

Funded by the European Union

This project has received funding from the European Union's Horizon Europe research and innovation programme under grant agreement No 101093864. Views and opinions expressed are however those of the author(s) only and do not necessarily reflect those of the European Union or the European Climate, Infrastructure and Environment Executive Agency (CINEA). Neither the European Union nor the granting authority can be held responsible for them.

Meléndez-Landaverde, E. R., & Sempere-Torres, D. (2022). Design and evaluation of a community and impact-based site-specific early warning system (SS-EWS): The SS-EWS framework. *Journal of Flood Risk Management*, *n/a*, e12860. https://doi.org/10.1111/jfr3.12860

Mishra, V., Mukherjee, S., Kumar, R., & Stone, D. A. (2017). Heat wave exposure in India in current, 1.5 °C, and 2.0 °C worlds. *Environmental Research Letters*, *12*(12), 124012. https://doi.org/10.1088/1748-9326/aa9388

Monteleone, B., Borzí, I., Bonaccorso, B., & Martina, M. (2022). Developing stage-specific drought vulnerability curves for maize: The case study of the Po River basin. *Agricultural Water Management*, *269*, 107713. https://doi.org/10.1016/j.agwat.2022.107713

Mora, C., Dousset, B., Caldwell, I. R., Powell, F. E., Geronimo, R. C., Bielecki, C. R., Counsell, C. W. W., Dietrich, B. S., Johnston, E. T., Louis, L. V., Lucas, M. P., McKenzie, M. M., Shea, A. G., Tseng, H., Giambelluca, T. W., Leon, L. R., Hawkins, E., & Trauernicht, C. (2017). Global risk of deadly heat. *Nature Climate Change*, *7*(7), 501–506. https://doi.org/10.1038/nclimate3322

Muis, S., Apecechea, M. I., Dullaart, J., de Lima Rego, J., Madsen, K. S., Su, J., Yan, K., & Verlaan, M. (2020). A High-Resolution Global Dataset of Extreme Sea Levels, Tides, and Storm Surges, Including Future Projections. *Frontiers in Marine Science*, *7*. https://doi.org/10.3389/fmars.2020.00263

Muis, S., Güneralp, B., Jongman, B., Aerts, J. C. J. H., & Ward, P. J. (2015). Flood risk and adaptation strategies under climate change and urban expansion: A probabilistic analysis using global data. *The Science of the Total Environment*, *538*, 445–457. https://doi.org/10.1016/j.scitotenv.2015.08.068

Naumann, G., Spinoni, J., Vogt, J. V., & Barbosa, P. (2015). Assessment of drought damages and their uncertainties in Europe. *Environmental Research Letters*, *10*(12), 124013. https://doi.org/10.1088/1748-9326/10/12/124013

Nishant, N., Ji, F., Guo, Y., Herold, N., Green, D., Virgilio, G. D., Beyer, K., Riley, M. L., & Perkins-Kirkpatrick, S. (2022). Future population exposure to Australian heatwaves. *Environmental Research Letters*, *17*(6), 064030. https://doi.org/10.1088/1748-9326/ac6dfa

Oppenheimer, M., Campos, M., Warren, R., Birkmann, J., Luber, G., O'Neill, B., Takahashi, K., Brklacich, M., Semenov, S., & Licker, R. (2015). Emergent risks and key vulnerabilities. In *Climate change 2014 impacts, adaptation and vulnerability: Part a: Global and sectoral aspects* (pp. 1039–1100). Cambridge University Press.

Ortner, G., Bründl, M., Kropf, C. M., Röösli, T., Bühler, Y., & Bresch, D. N. (2023). Large-scale risk assessment on snow avalanche hazard in alpine regions. *Natural Hazards and Earth System Sciences*, *23*(6), 2089–2110. https://doi.org/10.5194/nhess-23-2089-2023

Pachauri, R. K., Allen, M. R., Barros, V. R., Broome, J., Cramer, W., Christ, R., Church, J. A., Clarke, L., Dahe, Q., & Dasgupta, P. (2014). *Climate change 2014: Synthesis report. Contribution of Working Groups I, II and III to the fifth assessment report of the Intergovernmental Panel on Climate Change*. Ipcc.

Padulano, R., Rianna, G., Costabile, P., Costanzo, C., Del Giudice, G., & Mercogliano, P. (2021). Propagation of variability in climate projections within urban flood modelling: A multi-purpose impact analysis. *Journal of Hydrology*, *602*, 126756. https://doi.org/10.1016/j.jhydrol.2021.126756

Parodi, M. U., Giardino, A., van Dongeren, A., Pearson, S. G., Bricker, J. D., & Reniers, A. J. H. M. (2020). Uncertainties in coastal flood risk assessments in small island developing states. *Natural Hazards and Earth System Sciences*, *20*(9), 2397–2414. https://doi.org/10.5194/nhess-20-2397-2020

Peltonen-Sainio, P., Juvonen, J., Korhonen, N., Parkkila, P., Sorvali, J., & Gregow, H. (2021). Climate change, precipitation shifts and early summer drought: An irrigation tipping point for Finnish farmers? *Climate Risk Management*, *33*, 100334. https://doi.org/10.1016/j.crm.2021.100334

Pesaresi, M., Huadong, G., Blaes, X., Ehrlich, D., Ferri, S., Gueguen, L., Halkia, M., Kauffmann, M., Kemper, T., Lu, L., Marin-Herrera, M. A., Ouzounis, G. K., Scavazzon, M., Soille, P., Syrris, V., & Zanchetta, L. (2013). A

Funded by the European Union

This project has received funding from the European Union's Horizon Europe research and innovation programme under grant agreement No 101093864. Views and opinions expressed are however those of the author(s) only and do not necessarily reflect those of the European Union or the European Climate, Infrastructure and Environment Executive Agency (CINEA). Neither the European Union nor the granting authority can be held responsible for them.

Global Human Settlement Layer From Optical HR/VHR RS Data: Concept and First Results. *IEEE Journal of Selected Topics in Applied Earth Observations and Remote Sensing*, *6*(5), 2102–2131. https://doi.org/10.1109/JSTARS.2013.2271445

Petrova, E. (2011). Critical infrastructure in Russia: Geographical analysis of accidents triggered by natural hazards. *Environmental Engineering & Management Journal (EEMJ)*, *10*(1).

Prahl, B. F., Boettle, M., Costa, L., Kropp, J. P., & Rybski, D. (2018). Damage and protection cost curves for coastal floods within the 600 largest European cities. *Scientific Data*, *5*(1), 180034. https://doi.org/10.1038/sdata.2018.34

Prahl, B. F., Rybski, D., Boettle, M., & Kropp, J. P. (2016). Damage functions for climate-related hazards: Unification and uncertainty analysis. *Natural Hazards and Earth System Sciences*, *16*(5), 1189–1203. https://doi.org/10.5194/nhess-16-1189-2016

Reig, P., Shiao, T., & Gassert, F. (2013). *Aqueduct water risk framework*. WRI Working Paper, Washington DC: World Resources Institute, forthcoming.

Reisinger, A., Howden, M., Vera, C., Garschagen, M., Hurlbert, M., Kreibiehl, S., Mach, K. J., Mintenbeck, K., O'Neill, B., & Pathak, M. (2020). The concept of risk in the IPCC Sixth Assessment Report: A summary of cross-working group discussions. *Intergovernmental Panel on Climate Change*, *15*.

Riddell, G. A., van Delden, H., Maier, H. R., & Zecchin, A. C. (2019). Exploratory scenario analysis for disaster risk reduction: Considering alternative pathways in disaster risk assessment. *International Journal of Disaster Risk Reduction*, *39*, 101230.

Rising, J., Tedesco, M., Piontek, F., & Stainforth, D. A. (2022). The missing risks of climate change. *Nature*, *610*(7933), 643–651. https://doi.org/10.1038/s41586-022-05243-6

Romali, N. S., Sulaiman, M. @ S. A. K., Yusop, Z., & Ismail, Z. (2015). Flood Damage Assessment: A Review of Flood Stage–Damage Function Curve. In S. H. Abu Bakar, W. Tahir, M. Ab. Wahid, S. R. Mohd Nasir, & R. Hassan (Eds.), *ISFRAM 2014* (pp. 147–159). Springer. https://doi.org/10.1007/978-981-287-365-1_13

Salis, M., Arca, B., Del Giudice, L., Palaiologou, P., Alcasena-Urdiroz, F., Ager, A., Fiori, M., Pellizzaro, G., Scarpa, C., Schirru, M., Ventura, A., Casula, M., & Duce, P. (2021). Application of simulation modeling for wildfire exposure and transmission assessment in Sardinia, Italy. *International Journal of Disaster Risk Reduction*, *58*, 102189. https://doi.org/10.1016/j.ijdrr.2021.102189

Savelli, E., Mazzoleni, M., Di Baldassarre, G., Cloke, H., & Rusca, M. (2023). Urban water crises driven by elites' unsustainable consumption. *Nature Sustainability*, 1–12. https://doi.org/10.1038/s41893-023-01100-0

Seneviratne, S. I., Zhang, X., Adnan, M., Badi, W., Derecynski, C., Di Luca, A., Ghosh, S., Iskandar, I., Kossin, J., & Lewis, S. (2021). Weather and Climate Extreme Events in a Changing Climate. In V. Masson-, P. Zhai, A. Pirani, S. L. Connors, C. Péan, S. Berger, N. Caud, Y. Chen, L. Goldfarb, & M. I. Gomis (Eds.), *Climate Change 2021 – The Physical Science Basis: Working Group I Contribution to the Sixth Assessment Report of the Intergovernmental Panel on Climate Change* (1st ed., pp. 1513–1766). Cambridge University Press. https://doi.org/10.1017/9781009157896

Sepulcre-Canto, G., Horion, S., Singleton, A., Carrao, H., & Vogt, J. (2012). Development of a Combined Drought Indicator to detect agricultural drought in Europe. *Natural Hazards and Earth System Sciences*, *12*(11), 3519–3531. https://doi.org/10.5194/nhess-12-3519-2012

Shen, M., Chen, J., Zhuan, M., Chen, H., Xu, C.-Y., & Xiong, L. (2018). Estimating uncertainty and its temporal variation related to global climate models in quantifying climate change impacts on hydrology. *Journal of Hydrology*, *556*, 10–24.

Shu, E. G., Porter, J. R., Hauer, M. E., Sandoval Olascoaga, S., Gourevitch, J., Wilson, B., Pope, M., Melecio-Vazquez, D., & Kearns, E. (2023). Integrating climate change induced flood risk into future population projections. *Nature Communications*, *14*(1), 7870. https://doi.org/10.1038/s41467-023-43493-8

Funded by the European Union

This project has received funding from the European Union's Horizon Europe research and innovation programme under grant agreement No 101093864. Views and opinions expressed are however those of the author(s) only and do not necessarily reflect those of the European Union or the European Climate, Infrastructure and Environment Executive Agency (CINEA). Neither the European Union nor the granting authority can be held responsible for them.

Spinoni, J., Barbosa, P., Bucchignani, E., Cassano, J., Cavazos, T., Cescatti, A., Christensen, J. H., Christensen, O. B., Coppola, E., Evans, J. P., Forzieri, G., Geyer, B., Giorgi, F., Jacob, D., Katzfey, J., Koenigk, T., Laprise, R., Lennard, C. J., Kurnaz, M. L., … Dosio, A. (2021). Global exposure of population and land-use to meteorological droughts under different warming levels and SSPs: A CORDEX-based study. *International Journal of Climatology*, *41*(15), 6825–6853. https://doi.org/10.1002/joc.7302

Tilloy, A., Malamud, B. D., Winter, H., & Joly-Laugel, A. (2019). A review of quantification methodologies for multi-hazard interrelationships. *Earth-Science Reviews*, *196*, 102881. https://doi.org/10.1016/j.earscirev.2019.102881

Tonini, M., D'Andrea, M., Biondi, G., Degli Esposti, S., Trucchia, A., & Fiorucci, P. (2020). A machine learning-based approach for wildfire susceptibility mapping. The case study of the Liguria region in Italy. *Geosciences*, *10*(3), 105.

Trucchia, A., Meschi, G., Fiorucci, P., Gollini, A., & Negro, D. (2022). Defining Wildfire Susceptibility Maps in Italy for Understanding Seasonal Wildfire Regimes at the National Level. *Fire*, *5*(1), Article 1. https://doi.org/10.3390/fire5010030

Trucchia, A., Meschi, G., Fiorucci, P., Provenzale, A., Tonini, M., & Pernice, U. (2023). Wildfire hazard mapping in the eastern Mediterranean landscape. *International Journal of Wildland Fire*, *32*(3), 417–434. https://doi.org/10.1071/WF22138

Ullah, S., You, Q., Chen, D., Sachindra, D. A., AghaKouchak, A., Kang, S., Li, M., Zhai, P., & Ullah, W. (2022). Future Population Exposure to Daytime and Nighttime Heat Waves in South Asia. *Earth's Future*, *10*(5), e2021EF002511. https://doi.org/10.1029/2021EF002511

Usman, T., Fu, L., & Miranda-Moreno, L. F. (2011). Accident prediction models for winter road safety: Does temporal aggregation of data matter? *Transportation Research Record*, *2237*(1), 144–151.

Vajda, A., Tuomenvirta, H., Juga, I., Nurmi, P., Jokinen, P., & Rauhala, J. (2014). Severe weather affecting European transport systems: The identification, classification and frequencies of events. *Natural Hazards*, *72*(1), 169–188. https://doi.org/10.1007/s11069-013-0895-4

von Trentini, F., Leduc, M., & Ludwig, R. (2019). Assessing natural variability in RCM signals: Comparison of a multi model EURO-CORDEX ensemble with a 50-member single model large ensemble. *Climate Dynamics*, *53*(3), 1963–1979. https://doi.org/10.1007/s00382-019-04755-8

Wang, T., & Sun, F. (2022). Global gridded GDP data set consistent with the shared socioeconomic pathways. *Scientific Data*, *9*(1), 221. https://doi.org/10.1038/s41597-022-01300-x

Ward, P. J., Winsemius, H. C., Kuzma, S., Bierkens, M. F., Bouwman, A., De Moel, H., Loaiza, A. D., Eilander, D., Englhardt, J., & Erkens, G. (2020). Aqueduct floods methodology. *World Resources Institute*, 1–28.

Wei, Y., Jin, J., Li, H., Zhou, Y., Cui, Y., Commey, N. A., Zhang, Y., & Jiang, S. (2023). Assessment of Agricultural Drought Vulnerability Based on Crop Growth Stages: A Case Study of Huaibei Plain, China. *International Journal of Disaster Risk Science*, *14*(2), 209–222. https://doi.org/10.1007/s13753-023-00479-w

Welker, C., Röösli, T., & Bresch, D. N. (2021). Comparing an insurer's perspective on building damages with modelled damages from pan-European winter windstorm event sets: A case study from Zurich, Switzerland. *Natural Hazards and Earth System Sciences*, *21*(1), 279–299. https://doi.org/10.5194/nhess-21-279-2021

Wetzel, M., Schudel, L., Almoradie, A., Komi, K., Adounkpè, J., Walz, Y., & Hagenlocher, M. (2022). Assessing Flood Risk Dynamics in Data-Scarce Environments—Experiences From Combining Impact Chains With Bayesian Network Analysis in the Lower Mono River Basin, Benin. *Frontiers in Water*, *4*. https://doi.org/10.3389/frwa.2022.837688

Wilson, C., Guivarch, C., Kriegler, E., van Ruijven, B., van Vuuren, D. P., Krey, V., Schwanitz, V. J., & Thompson, E. L. (2021). Evaluating process-based integrated assessment models of climate change mitigation. *Climatic Change*, *166*(1), 3. https://doi.org/10.1007/s10584-021-03099-9

Funded by the European Union

This project has received funding from the European Union's Horizon Europe research and innovation programme under grant agreement No 101093864. Views and opinions expressed are however those of the author(s) only and do not necessarily reflect those of the European Union or the European Climate, Infrastructure and Environment Executive Agency (CINEA). Neither the European Union nor the granting authority can be held responsible for them.

Winsemius, H. C., Van Beek, L. P. H., Jongman, B., Ward, P. J., & Bouwman, A. (2013). A framework for global river flood risk assessments. *Hydrology and Earth System Sciences*, *17*(5), 1871–1892.

Wouters, L., Couasnon, A., de Ruiter, M. C., van den Homberg, M. J. C., Teklesadik, A., & de Moel, H. (2021). Improving flood damage assessments in data-scarce areas by retrieval of building characteristics through UAV image segmentation and machine learning – a case study of the 2019 floods in southern Malawi. *Natural Hazards and Earth System Sciences*, *21*(10), 3199–3218. https://doi.org/10.5194/nhess-21-3199-2021

Zhang, T., Cheng, C., & Wu, X. (2023). Mapping the spatial heterogeneity of global land use and land cover from 2020 to 2100 at a 1 km resolution. *Scientific Data*, *10*(1), 748. https://doi.org/10.1038/s41597-023-02637-7

Zscheischler, J., Westra, S., van den Hurk, B. J. J. M., Seneviratne, S. I., Ward, P. J., Pitman, A., AghaKouchak, A., Bresch, D. N., Leonard, M., Wahl, T., & Zhang, X. (2018). Future climate risk from compound events. *Nature Climate Change*, *8*(6), Article 6. https://doi.org/10.1038/s41558-018-0156-3

Zubkov, P., Gardiner, B., Nygaard, B. E., Guttu, S., Solberg, S., & Eid, T. (2024). Predicting snow damage in conifer forests using a mechanistic snow damage model and high-resolution snow accumulation data. *Scandinavian Journal of Forest Research*, *39*(1), 59–75. https://doi.org/10.1080/02827581.2023.2289660

Funded by the European Union

This project has received funding from the European Union's Horizon Europe research and innovation programme under grant agreement No 101093864. Views and opinions expressed are however those of the author(s) only and do not necessarily reflect those of the European Union or the European Climate, Infrastructure and Environment Executive Agency (CINEA). Neither the European Union nor the granting authority can be held responsible for them.